Serum Albumin as a Carrier of Immunostimulatory Oligodeoxynucleotides for Cancer Therapy

Patrick C. Guley

A dissertation submitted to the faculty of the University of North Carolina at Chapel Hill in partial fulfillment of the requirements for the degree of Doctor of Philosophy in the School of Pharmacy.

Chapel Hill
2013

Approved by:

Moo J. Cho, Ph.D.

Michael Jay, Ph.D.

Geoff Hird, Ph.D.

Leaf Huang, Ph.D.

Michael Jarstfer, Ph.D.

ABSTRACT

PATRICK C. GULEY: Serum Albumin as a Carrier of Immunostimulatory Oligonucleotides for Cancer Therapy
(Under the direction of Moo J. Cho, Ph.D.)

Toll-like receptor 9 (TLR9) is an endosomal receptor expressed on immune cells. The receptor recognizes microbial DNA, which contains a higher frequency of unmethylated CpG sequences than host DNA. Oligodeoxynucleotides containing such CpG motifs (CpG) are potent activators of TLR9, causing release of inflammatory cytokines and initiating both the innate and adaptive immune response. CpG has been successfully used to treat solid tumors, but its use is limited by its unfavorable pharmacokinetics. In preclinical studies, CpG was effective only when injected peritumorally; i.e., ineffective when administered systemically. In an attempt to overcome this limitation, CpG was derivatized with a maleimide moiety to allow a chemical reaction with free thiols. The derivative is referred to as CpG-mal throughout this dissertation.

Albumin, the most abundant serum protein, contains one free thiol, Cys_{34}, which comprises greater than 80% of the serum thiol content. Consequently, upon intravenous injection, the CpG-mal will react with circulating albumin to form a 1:1 conjugate in a predictable manner. Serum pharmacokinetics and biodistribution of phosphodiester CpG-mal was investigated in tumor-bearing mice using a PET/CT imaging procedure. For this series of studies, a novel tyrosine-containing crosslinker was synthesized to facilitate radioiodination of the CpG with ^{124}I in high yields. Imaging studies revealed the reaction

between the CpG-mal and albumin was fast enough to outcompete the high renal clearance of CpG, with the reaction complete within minutes. The new CpG-albumin conjugate displayed a similar distribution pattern and plasma half-life as albumin; half-life was increased 70-fold and tumor accumulation was increased 30-fold over control CpG.

In vitro plasma stability studies showed that albumin conjugation lead to a 1.5-fold reduction in the rate of enzymatic degradation of phosphodiester CpG. An *in vitro* macrophage activation assay indicated that phosphodiester CpG-albumin conjugates were weak agonists of TLR9. However, phosphorothioate CpG-albumin adducts were able to interact with TLR9 to initiate cytokine release from J774 macrophage cells, although this activity was reduced compared to control phosphorothioate CpG. The activation was independent of crosslinker length, and introducing a reducible disulfide crosslinkage did not enhance the activity. Pharmacokinetics and biodistribution of phosphorothioate CpG were measured using [^{3}H]-labeled CpG. The [^{3}H]-CpG-mal had a longer plasma half-life than control CpG, however, the liver accumulation was significantly increased. This liver uptake led to a less striking increase in tumor accumulation of CpG-mal than control CpG.

In vivo tumor growth inhibition studies using a CT26 colon carcinoma model showed both the CpG-mal and control CpG were equally efficacious and caused complete tumor regression in 6/10 mice. On the other hand, in the 4T1 model no tumor regression was observed presumably due to lack of tumor-associated antigens from the 4T1 cells.

To the pursuit of Truth

ACKNOWLEDGEMENTS

No man is an island; and none of this would have been possible without a considerable amount of direct and indirect assistance by many people. Obviously, my advisor Dr. Cho has had a huge impact on my training and development as a scientist and an intellectual (I use the word liberally). He gave me the freedom to experiment which often times lead to failure but he was always offering encouragement and challenging me to do better. My only hope is that the time spent was not a one-way street.

I would like to thank the members of my committee for providing insight and assistance with designing experiments. Additionally, I want to thank all the professors in the School of Pharmacy for teaching me diverse knowledge in the field of pharmaceutics. The staff and administrative assistants (Kathryn, Kim, Jubina, Ning, Rod, Amber, and Ain) deserve praise for making the bureaucratic red tape manageable and enabling quick ordering of supplies.

Additional acknowledgment goes to members of core facilities at UNC who provided valuable technical assistance: Arlene Bridges for mass spectrometry assistance; Karl Koshlap for NMR assistance; Nick Shalosky at Tissue Culture Facility for cell lines; Hong Yuan, Kevin Guley, and Carla Johnson at Biomedical Research Imaging Center for help with imaging experiments; Charlene Santos at Animal Study Core for help with animal experiments.

I would like to thank the other graduate students and research scientists in the School of Pharmacy for the many discussions and friendships we've had. I would like to thank Feng Liu for letting me use his cell hood and Yang Liu for helping me on short notice with some final experiments. I especially want to thank former Cho lab members: Kevin Han, Kayla Knilans, Roland Cheung, John An, Brad Gustafson, and June Lee. Tip of the hat to Shyam Joolakankti for teaching me tips and tricks of chemical synthesis. I particularly want to acknowledge my friendship with Michael Hackett, we've had plenty of deep scientific and philosophical conversations in addition to the many memories outside of lab.

I would like to thank my parents for their support during the many trials and tribulations I encountered during the past few years and most importantly for providing the many educational opportunities that led me here.

I am indebted to my wife, Natalie, whom I met during my first year of graduate school. She is the constant balancing force in my life and has provided unconditional positive support. I can't wait for the birth of our first daughter in the coming weeks.

Lastly, I want to reiterate that this work is based on other damn good scientist's previous discoveries; many of which are now taken for granted but without them I would have been utterly clueless. Here goes nothing…(inhale)...

TABLE OF CONTENTS

LIST OF TABLES

LIST OF FIGURES

LIST OF ABBREVIATIONS AND SYMBOLS

ACN	Acetonitrile
AcOH	Acetic Acid
APC	Antigen presenting cell
BD	Biodistribution
BSA	Bovine Serum albumin
CpG	Cytidine-phosphate-Guanosine
CT	Computer assisted tomography
DCC	*N,N'*-Dicyclohexylcarbodiimide
DCM	Dichloromethane
DIEA	*N*,*N*-Diisopropylethylamine
DNP	2,4 Dinitrophenol
EDC	*N*-(3-Dimethylaminopropyl)-*N′*-ethylcarbodiimide
EDTA	Ethylenediaminetetraacetic acid
ELISA	Enzyme Linked Immunosorbent Assay
EMCS	N-(ε-Maleimidocaproyloxy)succinimide
EtOAc	Ethyl acetate
EtOH	Ethanol
g	Gravitational constant
HPLC	High Performance Liquid Chromatography
HSA	Human Serum Albumin
IL-6	Interleukin 6

IL-12	Interleukin 12
iv	intravenous
LPS	Lipopolysaccharide
mal	maleimide
MeOH	methanol
MSA	Mouse Serum albumin
NEM	N-ethylmaleimide
NHS	*N*-hydroxysuccinimide
NK	Natural Killer cell
ODN	Oligodeoxynucleotide
PAMP	Pathogen-associated molecular pattern
PBS	Phosphate Buffered Saline
PD	Pharmacodynamics
PET	Positron Emission Tomography
PK	Pharmacokinetics
PO	Phosphodiester
PS	Phosphorothioate
sc	subcutaneous
TEA	Triethylamine
TEAA	Triethylammonium acetate
TFA	Trifluroacetic acid
THF	Tetrahydrofuran
TLC	Thin Layer Chromatography

TLR9	Toll-like receptor 9
TMS	Tetramethyl silane
Tyr	tyrosine

CHAPTER I: INTRODUCTION

For every minute of 2013, it is predicted that one United States citizen will succumb to cancer.(Siegel, Naishadham et al., 2013) The total direct and indirect economic impact of cancer-related healthcare in the United States for 2008 totaled $200 billion and will undoubtedly rise in the future.(Society, 2013) Society needs better treatments for cancer, especially for younger patients. Ideally, these treatments should be as cost effective as possible. One potential way to reduce the cost of therapy and increase the effectiveness is to utilize existing natural defense mechanisms to our advantage.

1.1 Cancer and Immunotherapy

Current medical understanding of the pathophysiology of cancer suggests we are constantly under assault from cancer causing agents, be they ultraviolent rays from the sun, chemical carcinogens, radiation exposure, reactive oxygen species, or viral and bacterial infections. Any of these agents can cause the genetic mutations that transform normal cells into cancer cells. However, as these mutations occur, the human body is not constantly developing clinical tumors. This implicates the existence of a controlling mechanism. The cancer-controlling mechanism largely consists of two components: an intracellular and an extracellular mechanism.

Cell growth is normally regulated tightly by many tumor suppressor genes and contact inhibition; furthermore, significant aberrant mutations lead to apoptosis.(Norbury and

Hickson, 2001) The majority of transformed cells are thought to be repaired or eliminated by these intracellular mechanisms. Some cells can accumulate mutations in these controlling genes and are rendered neoplastic.

The extracellular phase is known as immunosurveillance and, more recently, immunoediting(Dunn, Old et al., 2004); the immune system is able to differentiate and destroy these abnormal cells before they develop into a tumor. A number of experimental studies using genetically-engineered knockout mice with incomplete immune systems have an increase in tumor incidence. (Shankaran, Ikeda et al., 2001; Enzler, Gillessen et al., 2003; Street, Hayakawa et al., 2004) Additionally, it is known that humans with immunodeficiencies have a greater chance of developing tumors.(Rabkin, Biggar et al., 1991; Grulich, van Leeuwen et al., 2007) In some instances, abnormal cells are able to escape this control mechanism and their unchecked growth leads to cancer pathology. The exact nature of how some cells escape the immunoediting mechanism is not currently well understood. One school of thought involves a selective proliferation of non-immunogenic cells lacking specific tumor antigens. The consensus view of tumor immunobiology is that the lack of immune response is not merely due to an absence of immune cells in the vicinity of the tumor. In fact, most tumors contain large amounts of immune cells.(Lin and Pollard, 2004) Rather, the issue appears to be that the cells have been anergized and no longer function as active immune cells. They have been regulated by a sub population of T cells commonly known as Treg and other immunosurpessive cells that tell them that the tumor is not a threat.(Wolf, Wolf et al., 2003)

There is a growing interest in using the immune system to detect and cure cancer, but the concept is not new. Some of the earliest clinical uses of immunotherapy were performed

in the late 1890s by Dr. William Coley, who recognized that patients who suffered from bacterial infections showed a regression in tumor size. He hypothesized that bacteria was the cause of tumors, and could be treated by injection of bacterial extracts. His extracts contained two strains of bacteria and were injected in or around the tumor. As a result, the patients would become febrile and develop flu-like symptoms. In cases that responded positively, the tumors would quickly undergo liquefactive necrosis and begin to dissipate. Repeated injections over the span of multiple months provided complete remission for his patients who initially had a positive response. In patients that did not respond to the initial treatment, subsequent treatments were also ineffective, and these patients were given different therapies.

Cancer vaccines are another type of heavily investigated- and thus heavily invested- immunotherapy. This approach appears flawed because, by their very nature, cancers are heterogeneous and thus do not express the same antigens across the population. The second issue with cancer vaccines is that clinicians have no way of knowing which antigens are present without a biopsy. Additionally, tumors contain a heterogeneous population of cells. A single cancer vaccine can target a single antigen, but will not affect the tumors cells which do not express the specific antigen. This would require a multi-vaccine approach, which further increases cost and feasibility issues. Finally, from a philosophical standpoint, it is questionable whether researchers can select an appropriate set of antigens *in vitro* against tumors better than the patient's own immune system *in vivo*.

In spite of these conceptual flaws, from a cost-benefit perspective, immunotherapies are attractive mainly because they have the ability to exert an effect after the treatment has cleared the body. This should translate to reduced treatment frequency and associated costs.

1.2 Biological Response Modifiers

Humans have evolved in intimate contact with bacteria. Our immune systems have thus developed methods to detect and limit the threat bacteria pose to our survival. A consequence of this natural progression is a system to detect the conserved components of bacteria that renders virtually any type of bacteria to be identifiable by the immune system. These conserved components are called pathogen-associated molecular patterns, or PAMPs. They include components from gram negative cell walls such as lipopolysaccharides (LPS), DNA and RNA, also flagella and other membrane-associated proteins.(Kawai and Akira, 2010) Some of the receptors that are responsible for detecting these are the Toll-like receptor (TLR) family. When these PAMPs are detected by a TLR, the immune system becomes activated and primed for further activity.

Bacterial DNA serves as a PAMP because it expresses higher levels of unmethylated cytidine-phosphate-guanosine (CpG) dinucleotide sequences. In higher animals such as mammals, CpG sequences occur at a quarter of the frequency.(Bird, 1986) The CpG regions are usually flanked by residues that potentiate the immune response,(Krieg, Wu et al., 1998) and most importantly the cytosine is highly methylated at the 5 position, which abolishes the immune-stimulating activity.(Krieg, Yi et al., 1995) Due to these differences in unmethylated CpG expression, our immune system has a way to discriminate between our own self DNA and foreign bacterial DNA. Mammalian mitochondrial DNA also contains high amounts of unmethylated CpG DNA. Thus, when released during blunt tissue trauma, it can activate the immune system independently of exogenous bacteria.(Zhang, Itagaki et al., 2010)

Unmethylated CpG is recognized by toll-like receptor 9 (TLR9). It is an intracellular membrane receptor expressed almost exclusively on immune cells. TLR9 is thought to exist as a homodimer, and the majority is found in the endoplasmic reticulum.(Latz, Verma et al., 2007) When cells are exposed to CpG, TLR9 is localized to the endosomal membranes by a currently unknown mechanism,(Latz, Schoenemeyer et al., 2004) whereby proteolytic cleavage coverts the TLR9 into its active form.(Park, Brinkmann et al., 2008) Upon CpG binding, the active form undergoes a conformational change and transmembrane binding of MyD88 occurs.(Latz, Verma et al., 2007) MyD88 signaling eventually leads to activation of NF-κB and release of inflammatory cytokines. These cytokines are able to initiate an innate immune response by activating macrophages and natural killer (NK) cells and also an adaptive response by dendritic cell activation of CD8+ T cells and activation of B cells (**Figure 1.1**).(Krieg, 2003)

Biological response modifiers (BRMs) are attractive drug candidates for cancer therapy because they are able to overcome some of the issues associated with tumor vaccines. Since BRM are immune adjuvants, they are capable of activating the immune system and potentiating targeting of tumor antigens by immune cells. This also means that a poly-antigen response can be initiated, decreasing the chance that tumor cells will be able to escape by altering their antigen expression. BRM can be used to either activate or potentiate the immune system.(Williams, Ha et al., 1999) In addition to their use in cancer immunotherapy, they can be also be used in various clinical pathologies such as allergies or autoimmune disorders.(Gupta and Agrawal, 2010)

1.3 CpG Oligodeoxynucleotides

CpG oligodeoxynucleotides (ODN) are short 6-23 nucleotide DNA molecules that bind to TLR9 and can mimic the effects of bacterial DNA.(Krieg, Yi et al., 1995) Random screening showed the immune response to CpG ODN was sensitive to sequences flanking the CpG: the optimal sequence found for mice was GACGTT, whereas for larger animals, including humans and primates, the optimal sequence was GTCGTT.(Rankin, Pontarollo et al., 2001)

Our bodies are not accustomed to having DNA exist outside the cells and have mechanisms to remove this potential danger. Extracellular nucleases can rapidly cleave DNA into nucleotides; 5'- or 3'-exonucleases cleave DNA at the terminal ends while endonucleases can cleave anywhere along the strand. The majority of nucleases present extracellularly and in plasma are 3'-exonucleases and to a lesser extent endonucleases and 5'-exonucleases. ODN that have a natural phosphodiester (PO) backbone are rapidly metabolized by these nucleases and have poor pharmacokinetics (PK). This instability limits their therapeutic potential.

Several strategies have emerged to increase the resistance of ODN to nucleases.(Crooke, 1992) The most common has been to replace one of the oxygens in the phosphate group with a sulfur atom; this modification is called phosphorothioate (PS). The PS backbone prevents cleavage of the ODN by nucleases and the ODN remain intact to be therapeutically active. However, this modification also alters the physicochemical properties of the ODN and increases the hydrophobicity. PS ODN have extensive non-specific binding to cell surfaces and proteins; they are known to bind to serum proteins and weakly bind to

albumin with a k_d ~ 50-300 μM.(Srinivasan, Tewary et al., 1995) This binding is not very tight as evidenced by the rapid distribution of ODN when injected into mice.(Sands, Gorey-Feret et al., 1994) In the physiological setting, PS ODN have affinities to other targets which seem to be collectively greater than that of albumin.

CpG monotherapy has been used in the preclinical setting to treat solid tumors. The general consensus is that the CpG must be injected near the site of the tumor to elicit a response.(Heckelsmiller, Rall et al., 2002; Nierkens, den Brok et al., 2009) If it is injected systemically, the response is not sufficient enough to have clinical effects. This is no doubt a consequence of the poor PK of ODN. When they are injected systemically, only a small percentage of the dose arrives at the tumor, whereas if the dose is injected near the tumor, a higher amount of the drug is in the tumor vicinity before it diffuses out. This suggests delivery to the tumor is a limiting step in the therapeutic potential of systemically-injected ODN.

Our lab has previously shown that IgG antibodies can be used as a carrier for CpG to increase its systemic effectiveness.(Palma and Cho, 2007) CpG was derivatized with a 2,4-Dintriophenol (DNP) hapten and were injected into mice that had been previously immunized against DNP and therefore expressed a high anti-DNP IgG titer in their circulation. The anti-DNP IgG were able to form monomeric immune conjugates with the DNP-CpG and increase the plasma half-life and tumor accumulation. Consequently, the DNP-CpG was considerably more efficacious than underivatized CpG in tumor suppression.

While this approach showed promise, it has limitations. The biggest issue is the amount of specific IgG carrier. The effectiveness of the therapy is directly proportional to

the amount of IgG present.(Cheung and Cho, 2010) The average concentration of IgG in normal adults is 12 mg/ml. This corresponds to the total amount of IgG for all antigens, but only a small fraction of the IgG will be specific for a single antigen. This could be overcome by creating an active immune response prior to CpG-hapten therapy, but that would require extra time and more procedures. Because of these limitations, we decided to investigate the potential of using a different endogenous carrier for CpG ODN that would be abundant and accessible.

1.4 Serum Albumin

The most abundant protein in our blood is serum albumin. It has a molecular weight of 67 kDa and bears a net -19 charge at physiological pH. In humans, the plasma concentration is approximately 40 mg/ml and the interstitial concentration is approximately 20 mg/ml. This concentration difference gives rise to oncotic pressure which balances blood pressure and potentiates osmotic pressure. Albumin has several other functions in the body: it acts as a carrier for fatty acids, bilirubin, and numerous other endogenous ligands.(Peters, 1996) It also provides binding sites for numerous insoluble therapeutic agents. The amount of albumin in the average human is approximately 350 g, and its half-life in healthy individuals is estimated to be approximately 20 days.

At normal homeostasis albumin is thought to exist at steady state, where the rate of production is equal to the rate of catabolism. The only site of albumin synthesis that has been discovered is the liver.(Peters, 1996) The sites of catabolism have not been exclusively established because of the widespread distribution of albumin, but it is thought the skin and muscle account for the majority of albumin catabolism. In order to conserve energy by

preventing unwarranted catabolism, a recycling receptor, FcRn, is expressed on endothelial cells and other phagocytic cells.(Akilesh, Christianson et al., 2007) FcRn has a higher affinity for albumin at low pH, such as that found in the endosome, and lower affinity at neutral pH. This pH-dependent binding is related to protonation of His residues of FcRn.(Andersen, Dee Qian et al., 2006; Andersen and Sandlie, 2009) This allows the albumin to be recovered from the endosome and recycled back to the surface of the cell, and is responsible for the longer half-life that albumin and IgG have compared to other serum proteins.(Chaudhury, Mehnaz et al., 2003)

There are several other receptors involved in the transport of albumin. Albondin, or gp60, is an endothelial surface protein that can transcytose albumin into the extravascular space.(Schnitzer and Oh, 1994) Other scavenger receptors, gp30 and gp18, have a higher affinity for modified or degraded albumin and lead to degradation, primarily in the liver, rather than transcytosis.(Schnitzer, Sung et al., 1992)

The half-life and distribution of albumin scales with species weight: in mice, the halflife is 1.2 d, rat 2.5 d, rabbits 5.7 d, dogs 8 d, and humans 20 d.(Allison, 1960) Albumin plasma profiles, when introduced via bolus injection, exhibit biphasic behavior. They are indicative of an initial distribution to tissues followed by a slower clearance phase. In humans, this distribution phase takes approximately 3 days to complete and the concentration drops to approximately 40% of the initial value.(Peters, 1996)

The endothelial cells that constitute continuous capillaries have gaps between them which allow plasma carrying nutrients to flow out of the arterial capillaries and into the interstitium according to Starlings equation. Interestingly, these gaps are approximately 4

nm, which approximates the size of albumin and as a result, normal vasculature can restrict the transport of albumin out of the vessels via hydrodynamic sieving.(Rippe, Rosengren et al., 2002) The restriction is not a complete barrier to albumin escape but is sufficient to generate and maintain an albumin concentration gradient across the vessel wall. It is not clearly established if the intercellular leakage implied by Starlings equation is, in fact, the albondin-mediated transcytosis which has since been discovered.

Albumin has 35 Cys residues; 34 of these are engaged in disulfides leaving one free thiol, Cys_{34}. Cys_{34}, albeit located within a hydrophobic cleft of the albumin molecule, is accessible to the surrounding solvent and accounts for up to 85% of the total free thiol content of blood.(Kratz, Warnecke et al., 2002) Approximately 25% of Cys_{34} exists as a disulfide with small molecular weight thiols such as cysteine or glutathione attached. Despite being located on a large molecule, Cys_{34} is quite reactive because its pKa~5-6 is much lower than the pKa~8 for most thiols. It thus exists as thiolate anion at physiological pH,(Kratz, Warnecke et al., 2002) much more nucleophilic than a neutral free thiol group.

Since albumin contains only one Cys_{34}, it can be utilized as a specific handle to reproducibly derivatize albumin to form a 1:1 conjugate. Several of the most common thiol-specific chemistries are maleimide, haloacetyl, and pyridyl disulfide. Maleimide groups undergo Michael addition with thiols to create a stable thioether. Haloacetyls, commonly iodoacetyl or bromoacetyl, undergo substitution reaction to form stable thioethers. In contrast, pyridyl disulfides undergo substitution to form a disulfide bond that can be reversibly reduced. Of these, the maleimide is probably the most frequently used and currently researched, partly because the reaction is fast and no side products are generated.

Several studies have investigated the potential of using albumin as a carrier by modifying drugs with maleimide groups.(Elsadek and Kratz, 2012) When the maleimide-containing drugs are injected into animals they react covalently with Cys_{34} within minutes.(Kratz, Warnecke et al., 2002) Due to this fast rate, it has been possible to inject maleimide-modified drugs and have them react with circulating albumin without appreciable loss. While a 1:1 conjugate may seem like a poor loading capacity, it avoids the polyvalenancy which is known provoke an immune response and generate antibodies.(Singh, Kaur et al., 2004) This may be even more important when using an immune-activating drug. Additionally, the more that albumin is modified, the more it is recognized as non-native and is subject to rapid clearance.(Stehle, Sinn et al., 1997)

1.5 Albumin and Cancer

Cancer cells are constantly dividing and thus require a high amount of nutrients to sustain their growth. The need for sustenance requires the formation of new blood vessels, which leads to a high rate of angiogenesis.(Folkman, 1990) Histological examinations suggest that the blood vessels surrounding tumors are different than normal vessels- having unusually large gaps between adjacent endothelial cells.(Hashizume, Baluk et al., 2000) Indeed, the scientific rationale of many nanoparticle drug therapies is exploiting this difference.(Jain and Stylianopoulos, 2010) In order to clear out an area for new growth of tumor cells and neovascularization, tumors release various enzymes to degrade the adjacent extracellular matrix. All of these biochemical phenomena induce an increase in permeability for macromolecules, including albumin, at the tumor vicinity.(Matsumura and Maeda, 1986; Yuan, Dellian et al., 1995) Many cancer patients develop cachexia, a state of severe malnourishment, in part due to the tumor consuming a large amount of serum proteins and

nutrients to sustain its growth.(Stehle, Sinn et al., 1997) This leads to a loss of body weight and low concentration of serum proteins.

1.6 Proposed Studies

Collectively, those facts and findings introduced above indicate that serum albumin could be used as a carrier of CpG ODN. The proposed sequence of events that may happen in order to lead to a response can be described as follows: (i) upon intravenous injection, the majority of maleimide-modified CpG ODN will covalently bind to albumin thereby limiting their rapid clearance and distribution; (ii) the CpG-albumin conjugate will behave similarly to albumin and will have increased circulation half-life; (iii) the CpG-albumin will extravasate from the tumor endothelium near the tumor periphery to a higher extent due to local increased permeability; (iv) the CpG-albumin will be taken up by highly phagocytic cells, such as macrophages and dendritic cells, in the tumor vicinity; (v) CpG-albumin will bind to TLR9 and cause upregulation of cytokine release, NK cell activation, and silencing of immunosuppressive Treg cells; (vi) antigen-presenting cells (APCs) will sample tumor antigen and become activated, (vii) APCs will travel to lymph nodes to initiate clonal expansion of CD8+ T cells; (viii) CD8+ T cells will infiltrate the tumor and begin to destroy the tumor cells; and (ix) any distant metastases can be identified by the lasting immune response. This scenario appears to be wholly consistent with the scientific knowledge well established thus far and represents the scope of this dissertation.

Based on the aforementioned timeline several specific hypothesis can be stated and experimentally tested. First, albumin conjugation of maleimide-CpG will increase the blood half live compared to unconjugated CpG. Second, tumor exposure of maleimide-CpG will

be greater than unconjugated CpG. Lastly, the therapeutic efficacy of maleimide-CpG will be increased compared to unconjugated CpG. Experiments contained within this dissertation have been designed to test these stated hypotheses.

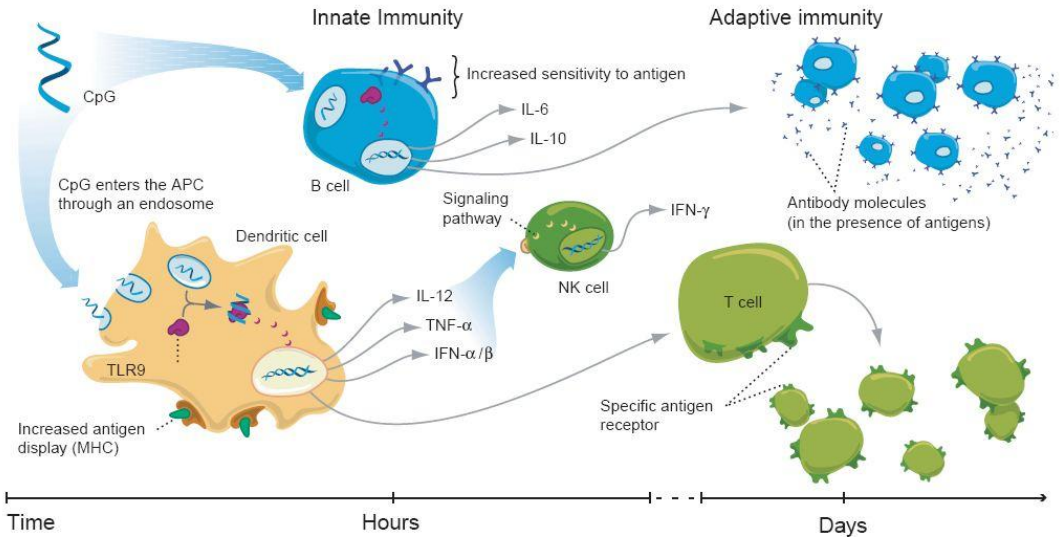

Figure 1.1. The cellular mechanisms of immune activation by CpG ODN. Image from Krieg, A.M. (2003) Nat Med, 9(7), 831-5.

REFERENCES

Akilesh, S., G. J. Christianson, D. C. Roopenian and A. S. Shaw (2007). "Neonatal FcR expression in bone marrow-derived cells functions to protect serum IgG from catabolism." J Immunol **179**(7): 4580-4588.

Allison, A. C. (1960). "Turnovers of erythrocytes and plasma proteins in mammals." Nature **188**: 37-40.

Andersen, J. T., J. Dee Qian and I. Sandlie (2006). "The conserved histidine 166 residue of the human neonatal Fc receptor heavy chain is critical for the pH-dependent binding to albumin." Eur J Immunol **36**(11): 3044-3051.

Andersen, J. T. and I. Sandlie (2009). "The versatile MHC class I-related FcRn protects IgG and albumin from degradation: implications for development of new diagnostics and therapeutics." Drug Metab Pharmacokinet **24**(4): 318-332.

Bird, A. P. (1986). "CpG-rich islands and the function of DNA methylation." Nature **321**(6067): 209-213.

Chaudhury, C., S. Mehnaz, J. M. Robinson, W. L. Hayton, D. K. Pearl, D. C. Roopenian and C. L. Anderson (2003). "The major histocompatibility complex-related Fc receptor for IgG (FcRn) binds albumin and prolongs its lifespan." J Exp Med **197**(3): 315-322.

Cheung, R. and M. Cho (2010). "Importance of avidity for an endogenous drug carrier: an antibody carrier for CpG oligonucleotides." Mol Pharm **7**(4): 1338-1341.

Crooke, S. T. (1992). "therapeutic applications of oligonucleotides."

Dunn, G. P., L. J. Old and R. D. Schreiber (2004). "The three Es of cancer immunoediting." Annu Rev Immunol **22**: 329-360.

Elsadek, B. and F. Kratz (2012). "Impact of albumin on drug delivery - New applications on the horizon." J Control Release **157**(1): 4-28.

Enzler, T., S. Gillessen, J. P. Manis, D. Ferguson, J. Fleming, F. W. Alt, M. Mihm and G. Dranoff (2003). "Deficiencies of GM-CSF and interferon gamma link inflammation and cancer." J Exp Med **197**(9): 1213-1219.

Folkman, J. (1990). "What is the evidence that tumors are angiogenesis dependent?" J Natl Cancer Inst **82**(1): 4-6.

Grulich, A. E., M. T. van Leeuwen, M. O. Falster and C. M. Vajdic (2007). "Incidence of cancers in people with HIV/AIDS compared with immunosuppressed transplant recipients: a meta-analysis." The Lancet **370**(9581): 59-67.

Gupta, G. K. and D. K. Agrawal (2010). "CpG oligodeoxynucleotides as TLR9 agonists: therapeutic application in allergy and asthma." BioDrugs **24**(4): 225-235.

Hashizume, H., P. Baluk, S. Morikawa, J. W. McLean, G. Thurston, S. Roberge, R. K. Jain and D. M. McDonald (2000). "Openings between defective endothelial cells explain tumor vessel leakiness." Am J Pathol **156**(4): 1363-1380.

Heckelsmiller, K., K. Rall, S. Beck, A. Schlamp, J. Seiderer, B. Jahrsdorfer, A. Krug, S. Rothenfusser, S. Endres and G. Hartmann (2002). "Peritumoral CpG DNA elicits a coordinated response of CD8 T cells and innate effectors to cure established tumors in a murine colon carcinoma model." J Immunol **169**(7): 3892-3899.

Jain, R. K. and T. Stylianopoulos (2010). "Delivering nanomedicine to solid tumors." Nat Rev Clin Oncol **7**(11): 653-664.

Kawai, T. and S. Akira (2010). "The role of pattern-recognition receptors in innate immunity: update on Toll-like receptors." Nat Immunol **11**(5): 373-384.

Kratz, F., A. Warnecke, K. Scheuermann, C. Stockmar, J. Schwab, P. Lazar, P. Druckes, N. Esser, J. Drevs, D. Rognan, C. Bissantz, C. Hinderling, G. Folkers, I. Fichtner and C. Unger (2002). "Probing the cysteine-34 position of endogenous serum albumin with thiol-binding doxorubicin derivatives. Improved efficacy of an acid-sensitive doxorubicin derivative with specific albumin-binding properties compared to that of the parent compound." J Med Chem **45**(25): 5523-5533.

Krieg, A. M. (2003). "CpG motifs: the active ingredient in bacterial extracts?" Nat Med **9**(7): 831-835.

Krieg, A. M., T. Wu, R. Weeratna, S. M. Efler, L. Love-Homan, L. Yang, A. K. Yi, D. Short and H. L. Davis (1998). "Sequence motifs in adenoviral DNA block immune activation by stimulatory CpG motifs." Proc Natl Acad Sci U S A **95**(21): 12631-12636.

Krieg, A. M., A. K. Yi, S. Matson, T. J. Waldschmidt, G. A. Bishop, R. Teasdale, G. A. Koretzky and D. M. Klinman (1995). "CpG motifs in bacterial DNA trigger direct B-cell activation." Nature **374**(6522): 546-549.

Latz, E., A. Schoenemeyer, A. Visintin, K. A. Fitzgerald, B. G. Monks, C. F. Knetter, E. Lien, N. J. Nilsen, T. Espevik and D. T. Golenbock (2004). "TLR9 signals after translocating from the ER to CpG DNA in the lysosome." Nat Immunol **5**(2): 190-198.

Latz, E., A. Verma, A. Visintin, M. Gong, C. M. Sirois, D. C. Klein, B. G. Monks, C. J. McKnight, M. S. Lamphier, W. P. Duprex, T. Espevik and D. T. Golenbock (2007).

"Ligand-induced conformational changes allosterically activate Toll-like receptor 9." Nat Immunol **8**(7): 772-779.

Lin, E. Y. and J. W. Pollard (2004). "Role of infiltrated leucocytes in tumour growth and spread." Br J Cancer **90**(11): 2053-2058.

Matsumura, Y. and H. Maeda (1986). "A new concept for macromolecular therapeutics in cancer chemotherapy: mechanism of tumoritropic accumulation of proteins and the antitumor agent smancs." Cancer Res **46**(12 Pt 1): 6387-6392.

Nierkens, S., M. H. den Brok, T. Roelofsen, J. A. Wagenaars, C. G. Figdor, T. J. Ruers and G. J. Adema (2009). "Route of administration of the TLR9 agonist CpG critically determines the efficacy of cancer immunotherapy in mice." PLoS One **4**(12): e8368.

Norbury, C. J. and I. D. Hickson (2001). "Cellular responses to DNA damage." Annu Rev Pharmacol Toxicol **41**: 367-401.

Palma, E. and M. J. Cho (2007). "Improved systemic pharmacokinetics, biodistribution, and antitumor activity of CpG oligodeoxynucleotides complexed to endogenous antibodies in vivo." J Control Release **120**(1-2): 95-103.

Park, B., M. M. Brinkmann, E. Spooner, C. C. Lee, Y. M. Kim and H. L. Ploegh (2008). "Proteolytic cleavage in an endolysosomal compartment is required for activation of Toll-like receptor 9." Nat Immunol **9**(12): 1407-1414.

Peters, T. (1996). All about albumin : biochemistry, genetics, and medical applications. San Diego, Academic Press.

Rabkin, C. S., R. J. Biggar and J. W. Horm (1991). "Increasing incidence of cancers associated with the human immunodeficiency virus epidemic." Int J Cancer **47**(5): 692-696.

Rankin, R., R. Pontarollo, X. Ioannou, A. M. Krieg, R. Hecker, L. A. Babiuk, S. van Drunen and L. V. van den Hurk (2001). "CpG motif identification for veterinary and laboratory species demonstrates that sequence recognition is highly conserved." Antisense Nucleic Acid Drug Dev **11**(5): 333-340.

Rippe, B., B. I. Rosengren, O. Carlsson and D. Venturoli (2002). "Transendothelial transport: the vesicle controversy." J Vasc Res **39**(5): 375-390.

Sands, H., L. J. Gorey-Feret, A. J. Cocuzza, F. W. Hobbs, D. Chidester and G. L. Trainor (1994). "Biodistribution and metabolism of internally 3H-labeled oligonucleotides. I. Comparison of a phosphodiester and a phosphorothioate." Mol Pharmacol **45**(5): 932-943.

Schnitzer, J. E. and P. Oh (1994). "Albondin-mediated capillary permeability to albumin. Differential role of receptors in endothelial transcytosis and endocytosis of native and modified albumins." J Biol Chem **269**(8): 6072-6082.

Schnitzer, J. E., A. Sung, R. Horvat and J. Bravo (1992). "Preferential interaction of albumin-binding proteins, gp30 and gp18, with conformationally modified albumins. Presence in many cells and tissues with a possible role in catabolism." J Biol Chem **267**(34): 24544-24553.

Shankaran, V., H. Ikeda, A. T. Bruce, J. M. White, P. E. Swanson, L. J. Old and R. D. Schreiber (2001). "IFNgamma and lymphocytes prevent primary tumour development and shape tumour immunogenicity." Nature **410**(6832): 1107-1111.

Siegel, R., D. Naishadham and A. Jemal (2013). "Cancer statistics, 2013." CA Cancer J Clin **63**(1): 11-30.

Singh, K. V., J. Kaur, G. C. Varshney, M. Raje and C. R. Suri (2004). "Synthesis and characterization of hapten-protein conjugates for antibody production against small molecules." Bioconjug Chem **15**(1): 168-173.

Society, A. C. (2013). "Cancer Facts & Figures 2013." Atlanta: American Cancer Society.

Srinivasan, S. K., H. K. Tewary and P. L. Iversen (1995). "Characterization of binding sites, extent of binding, and drug interactions of oligonucleotides with albumin." Antisense Res Dev **5**(2): 131-139.

Stehle, G., H. Sinn, A. Wunder, H. H. Schrenk, S. Schutt, W. Maier-Borst and D. L. Heene (1997). "The loading rate determines tumor targeting properties of methotrexate-albumin conjugates in rats." Anticancer Drugs **8**(7): 677-685.

Stehle, G., H. Sinn, A. Wunder, H. H. Schrenk, J. C. M. Stewart, G. Hartung, W. MaierBorst and D. L. Heene (1997). "Plasma protein (albumin) catabolism by the tumor itself - implications for tumor metabolism and the genesis of cachexia." Critical Reviews in Oncology/Hematology **26**(2): 77-100.

Street, S. E., Y. Hayakawa, Y. Zhan, A. M. Lew, D. MacGregor, A. M. Jamieson, A. Diefenbach, H. Yagita, D. I. Godfrey and M. J. Smyth (2004). "Innate immune surveillance of spontaneous B cell lymphomas by natural killer cells and gammadelta T cells." J Exp Med **199**(6): 879-884.

Williams, D. L., T. Ha, C. Li, J. H. Kalbfleisch, J. J. Laffan and D. A. Ferguson (1999). "Inhibiting early activation of tissue nuclear factor-κB and nuclear factor interleukin 6 with (1→ 3)-β-d-glucan increases long-term survival in polymicrobial sepsis." Surgery **126**(1): 54-65.

Wolf, A. M., D. Wolf, M. Steurer, G. Gastl, E. Gunsilius and B. Grubeck-Loebenstein (2003). "Increase of regulatory T cells in the peripheral blood of cancer patients." Clin Cancer Res **9**(2): 606-612.

Yuan, F., M. Dellian, D. Fukumura, M. Leunig, D. A. Berk, V. P. Torchilin and R. K. Jain (1995). "Vascular permeability in a human tumor xenograft: molecular size dependence and cutoff size." Cancer Res **55**(17): 3752-3756.

Zhang, Q., K. Itagaki and C. J. Hauser (2010). "Mitochondrial DNA is released by shock and activates neutrophils via p38 map kinase." Shock **34**(1): 55-59.

CHAPTER II: SYNTHESIS AND APPLICATION OF A HETEROTRIFUNCTIONAL CROSSLINKER FOR ^{124}I-BASED PET IMAGING

2.1 Overview

An efficient method for radioiodinating drug-carrier conjugates where the site of iodination is contained within the crosslinker has been developed. A heterotrifunctional crosslinker was synthesized with terminal maleimide and *N*-hydroxysuccinimide ester groups for conjugation to cargo and a centrally incorporated Tyr residue to allow facile labeling with ^{124}I. The crosslinker was applied to amino-modified oligodeoxynucleotides (ODN) in order to measure *in vivo* conjugation to Cys_{34} of circulating serum albumin. It was found the *in situ* reaction was complete within minutes and proceeded quickly enough to dramatically alter the clearance and distribution of the ODN. This labeling strategy could be used as a way to introduce any isotope of radioiodine to various drug-carrier combinations bearing the requisite functional groups.

2.2 Introduction

The ability to non-invasively measure the pharmacokinetics and biodistribution (PK/BD) of experimental therapeutics is a promising tool for the pharmaceutical scientist for a number of reasons. Primarily, it enables longitudinal studies involving small animals where multiple blood/organ samplings are not experimentally feasible.(Rygh, Qin et al.,

2011) Additionally, since each animal can provide information at multiple time points, there is a net reduction in the total number of experimental animals needed to obtain an equivalent amount of information. Finally, non-invasive imaging can be translated to a clinical setting. However, current imaging systems require a radioisotope as a label for detection. Incorporation of the desired label into the therapeutic may not be trivial, as often there is not an accessible labeling functionality.

Considerable research is being performed using macromolecular carriers and nanoparticles to enhance the therapeutic potential of drugs, particularly for targeting drugs to solid tumors.(Bae and Park, 2011) In many cases this involves crosslinking drug molecules to larger carrier molecules. In this study, a labeling moiety is incorporated into the crosslinker itself, rendering radiolabeling of the conjugate independent of the drug or carrier. The purpose of these experiments was to investigate the potential of using serum albumin as carrier of ODN. Other groups have shown that modifying therapeutics with a maleimide functional group allows them to covalently react with the Cys_{34} of circulating albumin.(Elsadek and Kratz, 2012) This approach has been extensively applied to small molecule anticancer drugs(Chung and Kratz, 2006; Kratz, 2007) and various peptides(Leger, Thibaudeau et al., 2004; Thibaudeau, Leger et al., 2005; Xie, Yao et al., 2010). The present work was designed to test whether this approach would also work for ODN and to specifically address whether the *in situ* reaction was fast enough to prevent the ODN from rapid distribution and excretion.(Lau, Graham et al., 2012)

Positron emission tomography (PET) was chosen as the method to measure the PK/BD of modified ODN due to its resolution and quantification. Normally, the preferred isotope for PET imaging is ^{18}F ($t_{1/2}$ = 110 min; β^+ = 98%) but its short radiological $t_{1/2}$ is not

applicable for measuring PK/BD at longer biological $t_{1/2}$. Iodine has several radioactive isotopes and the ^{124}I isotope ($t_{1/2}$ = 4.2 d; β^+ = 22%) can be used for PET imaging. In spite of some limitations(Pentlow, Graham et al., 1996), ^{124}I is successfully quantified.

2.3 Experimental Procedures

All chemicals, except where noted, were purchased from EMD Sciences or Sigma Aldrich and were ACS reagent grade or higher.

2.3.1 Crosslinker Synthesis (Scheme 2.1)

1. Mal-Tyr(tBu)-OtBu

To a 25-mL round bottom flask was added 115 mg (0.54 mmol) of N-ε-maleimidocaproic acid, 120 mg (0.62 mmol) of N-(3-Dimethylaminopropyl)-N′-ethylcarbodiimide hydrochloride (EDC·HCl), 75 mg (0.65 mmol) of N-hydroxysuccinimide (NHS), and 3 mL of dichloromethane (DCM). After 15 min 200 mg (0.61 mmol) of H-Tyr(tBu)-OtBu·HCl was added in 2 mL of DCM followed by 400 µL (2.9 mmol) of triethylamine. After 4 h at 25°C the reaction mixture was evaporated and the residue was dissolved in 15 mL of ethyl acetate and extracted twice with 10 mL of 1N HCl and 10 mL of saturated brine. The organic layer was dried over MgSO4 and dried in vacuo. The residue was purified on silica gel using 1:1 ethyl acetate:petroleum ether to give 160 mg (60%) of a slight yellow oil. 1H NMR (400 MHz, CD3OD): δ 1.22 (m, 2H, –CH2CH2CH2–), 1.30 (s, 9H, –OC(CH3)3), 1.38 (s, 9H, –OC(CH3)3), 1.5-1.6 (m, 4H, –CH2CH2CH2–), 2.18 (t, 2H, –CH2C=O), 2.9-3.05 (m, 2H, CHCH2–), 3.44 (t, 2H, NCH2–), 4.56 (t, 1H, CHCH2–), 6.79 (s, 2H, –CH=CH–), 6.9 (d, 2H, Ar–H,m), 7.1 (d, 2H, Ar–H,o). 13C NMR (100 MHz, CD3OD):

δ 174.4, 171.2, 154.2, 134.9, 134.2, 133.5, 132.2, 130.2, 129.3, 124.7, 124.2, 123.3, 37.2, 35.3, 28.1, 27.2, 27.1, 26.1, 25.2.

2. Mal-Tyr

To a 25-mL round bottom flask was added 650 mg of 1 and 8 mL of 50% trifluoroacetic acid in DCM. After 10 h at 25°C, the solvent was evaporated under a stream of N2 and the product was recrystallized from acetone/DCM to give 425 mg (86%) of slight yellow crystals. mp: 161-163°C. 1H NMR (400 MHz, (CD3)2CO): δ 1.25 (m, 2H, –CH2CH2CH2–), 1.5-1.6 (m, 4H, –CH2CH2CH2–), 2.2 (t, 2H, –CH2C=O), 2.9-3.1 (m, 2H, CHCH2–), 3.44 (t, 2H, NCH2–), 4.7 (q, 1H, CHCH2–), 6.7 (d, 2H, Ar–H,m), 6.81 (s, 2H, –CH=CH–), 7.08 (d, 2H, Ar–H,o), 7.32 (d, 1H, CONH–). 13C NMR (100 MHz, CD3OD): δ 174.6, 173.8, 171.4, 156.1, 134.8, 134.0, 133.4, 130.4, 129.6, 127.9, 115.6, 115.2, 114.8, 114.4, 37.2, 35.3, 28.0, 25.9, 25.1. ESI-MS (neg, MeOH): m/z 373.1 [M – H]-

3. Mal-Tyr-TEG-COOH

To a 25-mL round bottom flask was added 400 mg (1.1 mmol) of 2, 250 mg (2.2 mmol) of NHS, and 5 mL of freshly distilled tetrahydrofuran (THF). The reaction mixture was placed in an ice bath and 220 mg (1.1 mmol) of *N,N'*-Dicyclohexylcarbodiimide was added in 5 mL THF. After 10 h the reaction mixture was filtered and dried in vacuo. The residue was dissolved in 5 mL DCM, placed in an ice bath, and 350 mg (1.3 mmol) of carboxy-PEG4-amine was added followed by 250 µL (1.4 mmol) of *N,N*-Diisopropylethylamine. After 1 h the reaction mixture was diluted with 20 mL DCM and washed twice with 20 mL of 1N HCl and 20 mL of saturated brine. The DCM layer was dried over MgSO4 and dried in vacuo. The residue was purified on silica gel using 1% acetic

acid in 1:9 methanol:DCM to give 465 mg (70%) of a yellow oil. 1H NMR (400 MHz, CDCl3): δ 1.2 (m, 2H, –CH2CH2CH2–), 1.5-1.6 (m, 4H, –CH2CH2CH2–), 2.2 (t, 2H, –CH2C=O), 2.6 (t, 2H, –CH2CH2CO–), 2.9 (m, 2H, CHCH2–), 3.2-3.7 (m, 18H, –CH2CH2O–), 3.79 (t, 2H, NCH2–), 4.68 (q, 1H, CHCH2–), 6.71 (s, 2H, –CH=CH–), 6.76 (d, 2H, Ar–H,m), 7.01 (d, 2H, Ar–H,o), 7.06 (d, 1H, –CONHCH–) 7.38 (t, 1H, –CONHCH2–). 13C NMR (100 MHz, CDCl3): δ 174.8, 173.5, 172.0, 171.1, 155.8, 134.4, 134.1, 130.6, 130.2, 127.6, 115.8, 115.6, 70.5 70.1, 66.8, 37.8, 36.2, 35.4, 28.5, 26.4, 25.2. ESI-MS (neg, MeOH): m/z 620.2 [M – H]-

4. Mal-Tyr-TEG-NHS

To a 25-mL round bottom flask was added 200 mg (0.3 mmol) of 3, 115 mg (1 mmol) of NHS, 80 mg (0.4 mmol) of EDC·HCl and 7 mL of DCM. The reaction was carried out at 4°C for 10 h. The reaction mixture was diluted with 20 mL of DCM and washed twice with 20 mL 1N HCl, 20 mL of saturated bicarbonate, and 20 mL saturated brine. The DCM layer was dried using MgSO4 and was concentrated in vacuo to give 150 mg (65%) of a slight yellow oil. 1H NMR (400 MHz, CDCl3): δ 1.2 (m, 2H, –CH2CH2CH2–), 1.5-1.6 (m, 4H, –CH2CH2CH2–), 2.2 (t, 2H, –CH2C=O), 2.8-2.9 (m, 6H, C=OCH2CH2C=O, –CH2CH2CO–), 2.9-3.0 (m, 2H, CHCH2–), 3.2-3.7 (m, 18H, –CH2CH2O–), 3.82 (t, 2H, NCH2–), 4.55 (q, 1H, CHCH2–), 6.28 (t, 1H, –CONHCH2–), 6.45 (d, 1H, –CONHCH–), 6.69 (s, 2H, –CH=CH–), 6.76 (d, 2H, Ar–H,m), 7.04 (d, 2H, Ar–H,o), 7.45 (s, 1H, COH). 13C NMR (100 MHz, CDCl3): δ 172.7, 171.1, 169.4, 167.0, 155.8, 134.4, 134.1, 130.7, 128.0, 116.0, 70.8, 70.6, 70.3, 65.9, 37.8, 36.4, 32.2, 28.4, 26.4, 25.8, 25.2. ESI-MS (pos, MeOH): m/z 741.5 [M + Na]+

2.3.2 ODN Chemistry

The ODN used in all experiments was a 20mer purchased from either Integrated DNA Technologies (Coralville, IA) or from Girindus America, Inc. (Cincinnati, OH) with a phosphodiester backbone, unless specifically stated. They were supplied as the Na^+ salt form. The sequence was TCCATGACGTTCCTGACGTT and contained a commercially available 3'-amino modification.

HPLC Conditions

All HPLC analysis and purification was performed using Shimadzu SCL-10A system controller with two Shimadzu LC-8A pumps connected to a Rainin Dynamax UV-C detector and a Shimadzu C-R6A Chromatopac recorder. Solvent **A** was 5% acetonitrile in 10 mM triethylammonium acetate buffer; solvent **B** was 100% acetonitrile. For analytical work an Agilent Zorbax 300SB-C18 4.6 x 150mm analytical column with 5 µm particle size and a total flow rate of 1.0 mL/min was used with the following gradient: t = 0-5 min, %**B** = 0; t = 5-30 min, %**B** = 0-25; t = 30-33 min, %**B** = 25-100. For purification work the same gradient protocol was used with an Agilent Zorbax 300SB-C18 9.4 x 250mm semi-preparative column and a total flow rate of 4 mL/min. All detection was performed at λ = 260 nm.

ODN-mal

To a 3-dram glass vial containing 13 mg (2.1 µmol) of ODN-NH_2 in 2 mL of 0.1M sodium phosphate buffer, pH = 7.4 was added 20 mg (28 µmol) of **4** in 850 µL of acetonitrile. The reaction progress was judged complete after 1.5 h at 25°C by analytical HPLC. The acetonitrile was evaporated under a stream of N_2 and the reaction mixture was purified using semi-preparative HPLC. The product peak was manually collected and

evaporated *in vacuo* after addition of excess 3 M sodium acetate to acidify the pH to 5.2. The ODN was then ethanol precipitated from 0.3M sodium acetate at -20°C to give 7 mg (56%) of ODN-mal as a Na^+ salt. ESI-MS (neg, H_2O) 7194.4 [M], 7211.8 [M + NH_4].

ODN-COOH

To a microcentrifuge tube containing 900 µg of ODN-mal was added 200 µL of 50 mM NaOH. After 4 h at 37ºC the ODN was ethanol precipitated from 0.3 M sodium acetate to give 840 µg (93%) of ODN-COOH as a Na^+ salt.

Murine Mercaptalbumin

Mouse serum albumin (MSA) Fraction V was purchased from MP Biomedicals (Solon, OH). Reaction with Ellman's reagent indicated that the free thiol content of this albumin ranged from 0.2-0.3 mol of thiol per mol of MSA.(Janatova, Fuller et al., 1968) Mercaptalbumin was generated by the addition of 3 molar equivalents of DL-Dithiothreitol and incubation for 5 min at 25°C.(Funk, Li et al., 2010) The unquenched reaction was directly applied to a Sephadex® G-25 size exclusion column equilibrated with phosphate buffered saline (PBS). The unretained fractions containing MSA, as measured by UV, were pooled and Ellman's test indicated the thiol content was 0.9-1.0 mol of thiol per mol of MSA. The MSA was further purified by mini-Q strong anion exchange spin columns (Pierce, Rockford, IL) and eluted with PBS to generate mercaptalbumin in a manner similar to methods previously reported.(Janatova, Fuller et al., 1968)

ODN-MSA

Radiolabeled ODN-mal was added to 8 equivalents of mercaptalbumin in PBS for 2 h at 25°C. The reaction mixture was loaded onto Q strong anion exchange spin columns and eluted with increasing stepwise NaCl gradient in 20 mM phosphate buffer, pH = 7.4. Unreacted MSA was eluted with 300 mM NaCl and the conjugate was eluted with 400 mM NaCl. The buffer was exchanged to PBS by repetitive ultracentrifugation using 30 kDa molecular weight cut off (MWCO) filters.

2.3.3 Pharmacokinetic Experiments

Iodination of ODN and MSA

The ODN were iodinated using pre-coated Iodogen® tubes (Pierce, Rockford, IL). $Na^{124}I$ was purchased from IBA Molecular (Richmond, VA). The $Na^{124}I$ needed to be regenerated to in order obtain reliable yields. The regeneration process consisted of calculated addition of stock solution containing 1 mg/mL of NaI and 1 mg/mL of $NaIO_3$ in 1 mM NaOH.(Verel, Visser et al., 2004) The general procedure was as follows: The ODN to be labeled was dissolved in 100 µL of 100 mM sodium phosphate buffer at pH 7.4. To a pre-rinsed iodination tube, added were $Na^{124}I$ and a calculated amount of regeneration stock containing 0.9 mol equivalent of total iodine relative to ODN. After 1 min the ODN was added to the tube and the reaction was allowed to progress for 6 min with periodic gentle shaking. The unquenched reaction was directly applied to a Sephadex® G-25 size exclusion column equilibrated with PBS. The fractions containing ODN, as measured by UV, were pooled and concentrated using ultracentrifugation with 3 kDa MWCO filters. MSA was labeled using a similar procedure.

Mice and Tumor Model

All animals were handled in accordance with an approved protocol by UNC Institutional Animal Care and Use Committee. 4T1 cells were purchased from ATCC (Manassas, VA) and grown according to ATCC recommendations. Eight female Balb/c mice, 18-20 g, were orthotopically inoculated with 1 x 10^5 4T1 cells in 50 µL PBS by subcutaneous injection into the mammary fad pad. The mice were randomly divided into four groups and imaging experiments began 15 days after tumor inoculation.

PET Image Acquisition

One day prior and throughout the imaging experiments mice were supplied *ad libitum* drinking water supplemented with 0.1% KI to block thyroid uptake of labeled ^{124}I.(Verel, Visser et al., 2004) All animals were anesthetized using isoflurane and catheterized via tail vein. For each scan, two mice were placed on a cardboard platform on the scanning bed of a GE VISTA eXplore scanner and secured with surgical tape. A heart and breathing rate probe was used to monitor vitals while scanning. The mice were first imaged with a CT scan and then were dynamically imaged with PET for 1 h. The animals were injected with 0.2-0.3 mCi of ^{124}I labeled material corresponding to 100 µg of ODN in 100 µL of sterile 0.22 µm filtered PBS and the catheters were flushed with a minimal volume of normal saline. The amount of activity remaining in the catheter and syringe was measured using a calibrated dose calorimeter (Capintec CRC®-25R, Ramsey, NJ) and subtracted from the initial amount to quantify the amount of injected activity.

Image Processing

The raw data was rebinned according to the following scheme: 0-10 minutes, 1-min intervals; 10-30 minutes, 2-min intervals; and 30-60 minutes, 3-minute intervals. Images

were reconstructed using an attenuation correction, scatter correction, and 2D OSEM projection using the supplied manufacturer software (MMWKS Image Software, Laboratorio de Imagen HGUGM, Spain). The images were then loaded into AMIDE for analysis.(Loening and Gambhir, 2003) The images were aligned using fiducial markers placed below the scanning bed. Three-dimensional regions of interest (ROI) were manually drawn around the heart and bladder using the CT images. The amount of PET signal contained within a ROI was calculated and converted to percent of injected dose per mL (%ID/mL) using appropriate conversions to correct for time decay and a cylindrical phantom of known activity.

2.4 Results

2.4.1 Crosslinker Synthesis

The crosslinker used throughout this investigation was synthesized using carbodiimide chemistry from the amino acid Tyr according to **Scheme 2.1**. A maleimide group was first conjugated to the $–NH_2$ terminus of di-*t*-butyl protected Tyr using EDC. After subsequent *t*-butyl deprotection, the –COOH terminus was converted to an NHS ester using DCC. Conjugation of this intermediate to the ODN-NH_2 was attempted but no reaction was observed. The failure was attributed to low aqueous solubility and stearic hindrance. Subsequently, a tetra(ethylene glycol) spacer was added to the crosslinker, which successfully enabled conjugation to ODN-NH_2. The final crosslinker was synthesized in overall yield of 25% over 4 steps.

2.4.2 ODN Preparation and Iodination

The crosslinker **4** was conjugated to ODN-NH_2 using standard conditions.(Hermanson, 1996) Non-thiol reactive control ODN-COOH was synthesized from ODN-mal by hydrolysis of the maleimide group under basic conditions.(El-Sagheer, Cheong et al., 2011) The structures of the ODN are shown in **Figure 2.2.** Thiol reactivity was monitored using a mercaptohexanol HPLC shift assay; ODN-mal underwent a reaction as evidenced by an increase in peak retention time, whereas ODN-COOH showed no change in peak retention time when treated with mercaptohexanol.

Conjugation with the crosslinker enabled the ODN to be iodinated with ^{124}I using commercially available pre-coated Iodogen® tubes in yields ranging from 80-90%. In a control experiment, ODN-NH_2 was modified with a crosslinker which did not contain a Tyr residue. These ODN were not iodinated with the same iodination protocol; yields <0.5%. This result suggests the labeling was specific to the Tyr and not due to non-specific labeling of the ODN bases which can occur at elevated temperatures and extended labeling times.(Piatyszek, Jarmolowski et al., 1988)

2.4.3 Image Analysis

PET/CT whole body images, **Figure 2.3**, show this difference in initial distribution of the different treatments. MSA and MSA-ODN are restricted to the vasculature volume and show high heart signal, whereas the ODN-COOH is rapidly cleared and distributed showing low heart signal. ODN-mal shows a combination of these two patterns.

Time-dependent radioactivity curves of blood and urine were generated by integrating the total PET signal contained within an ROI outlining the heart and bladder (**Figure 2.4**).

The heart is classically assumed to be highly perfused with blood; therefore blood concentration was approximated by total heart concentration.(Bading, Horling et al., 2008) The concentrations were dose-normalized and expressed as %ID/mL.

ODN typically have a PK profile that can be characterized by rapid elimination from the plasma(Sands, Gorey-Feret et al., 1994), which is similar to the profile of ODN-COOH in **Figure 2.4.** On the other hand, ODN-mal shows a different plasma profile. Initially there is a steep drop, similar to ODN-COOH, which then transitions to a much slower plasma clearance. The transition appears to be complete after approximately 8 min. To confirm Cys_{34} of albumin is the major reaction product, ODN-mal was preconjugated to MSA *ex vivo* prior to injection. This curve did not display a rapid plasma clearance indicating there was no significant free ODN contamination. However, there was a delayed disappearance from the plasma and into the bladder. MSA was used as a control in order to determine if there was a difference between the ODN-MSA conjugates and native albumin. Both the MSA and ODN-MSA appear to be restricted to vascular space and do not undergo a rapid distribution.

2.5 Discussion

The crosslinker synthesized for this study was specifically designed to accommodate the following three functionalities: (i) a maleimide group for conjugation to -SH groups; (ii) an activated ester for conjugation to $-NH_2$ groups; and (iii) a phenol group for ^{124}I PET label incorporation. Therefore, the tertiary nature of the Tyr was utilized as the scaffold for the crosslinker. The crosslinker was conjugated to ODN-NH_2 and enabled specific radiolabeling of the Tyr. An attempt was made to iodinate ODN-mal with a phosphorothioate backbone; however, yields were substantially lower. The phosphorothioate groups appear to interfere

with the oxidation.(Xie, Liang et al., 2012) This observation shows the crosslinker requires compatibility with the drug or carrier and cannot be used indiscriminately. In this case, no attempt was made to iodinate the crosslinker prior to conjugation with the phosphorothioate ODN-NH_2.

The cutoff for kidney filtration is approximately 40 kDa and continuous capillary endothelial gaps are approximately 4 nm (Rippe, Rosengren et al., 2002), therefore, there is no *a priori* reason to suspect any difference in renal clearance and distribution between ODN-COOH and ODN-mal. Immediately upon injection and prior to any thiol reaction, these two ODN should have similar disposition. However, the ODN-mal is able to undergo thiol addition which has the potential to alter disposition. The ODN-mal blood curve should follow the ODN-COOH curve at early timepoints and begin to transition to a new curve as the thiol addition reaction occurs. The majority of free thiol content in the blood is due to Cys_{34} of albumin(Kratz, Warnecke et al., 2002), therefore, this new curve should behave similar to albumin. The expected biphasic nature of the ODN-mal blood curve is clearly observed in **Figure 2.4**.

It appears that albumin is indeed the major reaction product based on the similar dispositions of preconjugated ODN-MSA to that of ODN-mal. Interestingly, there was a delayed clearance of ODN-MSA and we speculate this is may be due to an impurity in the formulation, most likely dimer/multimer aggregates being recognized by scavenger receptors and degraded.(Schnitzer and Bravo, 1993) It does not appear that monomeric ODN-MSA adduct is overtly recognized by scavenger receptors because no delayed degradation was observed in the ODN-mal curve and the plasma $t_{1/2}$ is similar to MSA.

The blood and urine were not directly analyzed for stability of the label or integrity of the conjugate. In preliminary experiments where the mice were not given KI-supplemented drinking water to block thyroid uptake, the amount of thyroid uptake was greater for labeled MSA compared to the ODN-mal (data not shown). Additionally, labeled MSA was excreted predominantly through the urine, whereas all other treatments containing the radiolabeled crosslinker were excreted in the both urine and feces. Taken together these suggest the crosslinker iodination has greater *in vivo* dehalogenation stability than labeled protein tyrosines, which is in agreement with other reports of prosthetic iodinations.(Vaidyanathan and Zalutsky, 1990)

In summary, we were able to develop a strategy of labeling drug-carrier conjugates by incorporating a Tyr residue into the crosslinker to allow direct iodination. Placing the radiolabel within the crosslinker should not interfere with the drug or the carrier. This should leave their biological functions intact. Maleimide-modified ODN were able to covalently react with Cys_{34} of circulating albumin and the reaction was complete within minutes which was fast enough to outcompete the rapid plasma clearance of the ODN. The conjugation to albumin has a dramatic effect on the PK/BD of ODN. Regardless of the radioisotope of iodine employed, the crosslinker is a promising tool due to its modular nature and could be used to study a variety of different drug-carrier combinations in numerous experimental settings.

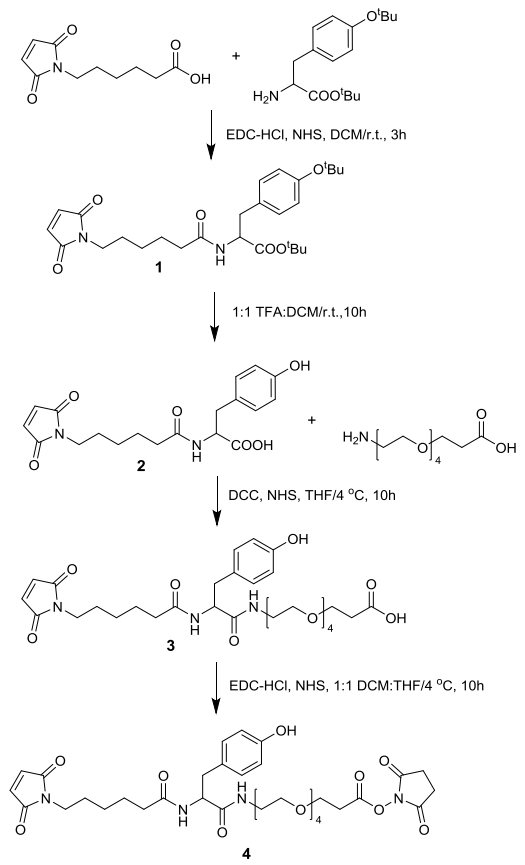

Scheme 2.1. Synthetic scheme for the synthesis of the heterotrifunctional crosslinker used throughout this study.

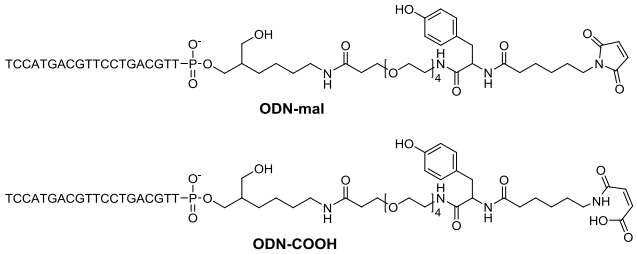

Figure 2.2. Chemical structures of the modified ODN synthesized for the study. The site of ^{124}I labeling is ortho to the tyrosine phenolic hydroxyl, both mono- and di-iodinated ODN were observed.

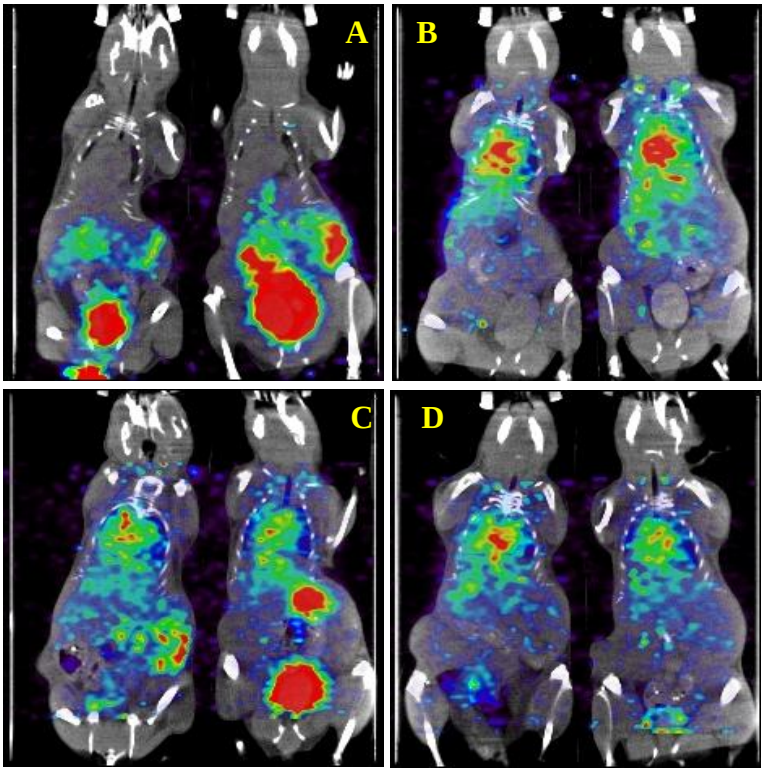

Figure 2.3. Normalized whole body PET/CT images of biodistribution of the ^{124}I radiolabeled treatments after 20 min post injection. Each panel shows a coronal slice through the heart of two mice that were simultaneously imaged. Panel A: ODN-COOH, B: MSA, C: ODN-mal, D: ODN-MSA. All images were normalized by scaling the maximum color threshold with average injected dose.

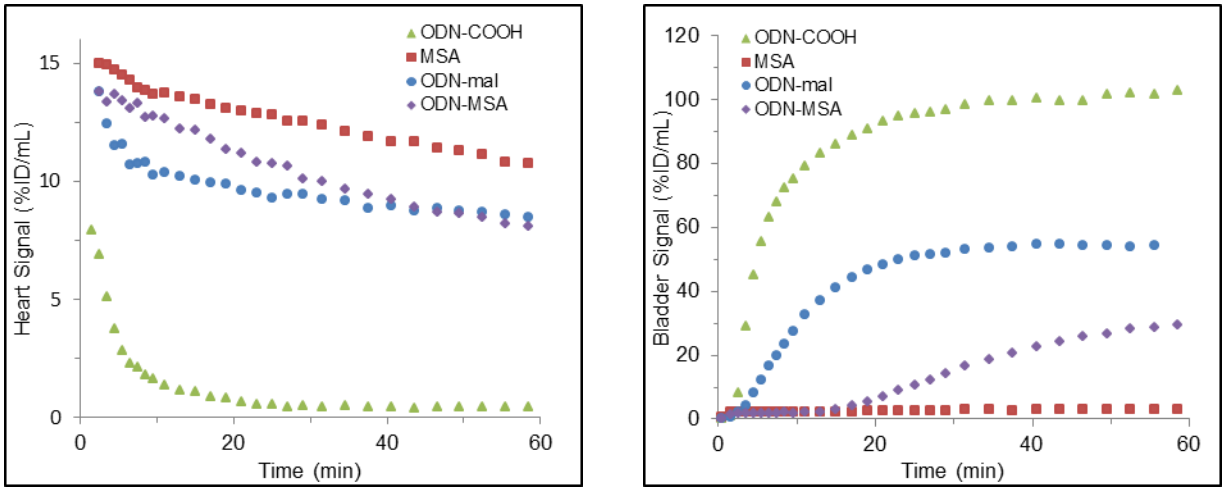

Figure 2.4. Time activity curves for the blood and urine during 1 h post injection. Rapid clearance from the blood and into the urine is observed for the control ODN-COOH. Reduced blood clearance and urine excretion is observed for ODN-mal, ODN-MSA, and MSA. Each point represents the average of 2 mice imaged simultaneously.

REFERENCES

Bading, J. R., M. Horling, L. E. Williams, D. Colcher, A. Raubitschek and S. E. Strand (2008). "Quantitative serial imaging of an 124I anti-CEA monoclonal antibody in tumor-bearing mice." Cancer Biother Radiopharm **23**(4): 399-409.

Bae, Y. H. and K. Park (2011). "Targeted drug delivery to tumors: myths, reality and possibility." J Control Release **153**(3): 198-205.

Chung, D. E. and F. Kratz (2006). "Development of a novel albumin-binding prodrug that is cleaved by urokinase-type-plasminogen activator (uPA)." Bioorg Med Chem Lett **16**(19): 5157-5163.

El-Sagheer, A. H., V. V. Cheong and T. Brown (2011). "Rapid chemical ligation of oligonucleotides by the Diels-Alder reaction." Org Biomol Chem **9**(1): 232-235.

Elsadek, B. and F. Kratz (2012). "Impact of albumin on drug delivery - New applications on the horizon." J Control Release **157**(1): 4-28.

Funk, W. E., H. Li, A. T. Iavarone, E. R. Williams, J. Riby and S. M. Rappaport (2010). "Enrichment of cysteinyl adducts of human serum albumin." Anal Biochem **400**(1): 61-68.

Hermanson, G. T. (1996). Bioconjugate techniques. San Diego, Academic Press.

Janatova, J., J. K. Fuller and M. J. Hunter (1968). "The heterogeneity of bovine albumin with respect to sulfhydryl and dimer content." J Biol Chem **243**(13): 3612-3622.

Kratz, F. (2007). "DOXO-EMCH (INNO-206): the first albumin-binding prodrug of doxorubicin to enter clinical trials." Expert Opin Investig Drugs **16**(6): 855-866.

Kratz, F., A. Warnecke, K. Scheuermann, C. Stockmar, J. Schwab, P. Lazar, P. Druckes, N. Esser, J. Drevs, D. Rognan, C. Bissantz, C. Hinderling, G. Folkers, I. Fichtner and C. Unger (2002). "Probing the cysteine-34 position of endogenous serum albumin with thiol-binding doxorubicin derivatives. Improved efficacy of an acid-sensitive doxorubicin derivative with specific albumin-binding properties compared to that of the parent compound." J Med Chem **45**(25): 5523-5533.

Lau, S., B. Graham, N. Cao, B. J. Boyd, C. W. Pouton and P. J. White (2012). "Enhanced extravasation, stability and in vivo cardiac gene silencing via in situ siRNA-albumin conjugation." Mol Pharm **9**(1): 71-80.

Leger, R., K. Thibaudeau, M. Robitaille, O. Quraishi, P. van Wyk, N. Bousquet-Gagnon, J. Carette, J. P. Castaigne and D. P. Bridon (2004). "Identification of CJC-1131-albumin bioconjugate as a stable and bioactive GLP-1(7-36) analog." Bioorg Med Chem Lett **14**(17): 4395-4398.

Loening, A. M. and S. S. Gambhir (2003). "AMIDE: a free software tool for multimodality medical image analysis." Mol Imaging **2**(3): 131-137.

Pentlow, K. S., M. C. Graham, R. M. Lambrecht, F. Daghighian, S. L. Bacharach, B. Bendriem, R. D. Finn, K. Jordan, H. Kalaigian, J. S. Karp, W. R. Robeson and S. M. Larson (1996). "Quantitative imaging of iodine-124 with PET." J Nucl Med **37**(9): 1557-1562.

Piatyszek, M. A., A. Jarmolowski and J. Augustyniak (1988). "Iodo-Gen-mediated radioiodination of nucleic acids." Anal Biochem **172**(2): 356-359.

Rippe, B., B. I. Rosengren, O. Carlsson and D. Venturoli (2002). "Transendothelial transport: the vesicle controversy." J Vasc Res **39**(5): 375-390.

Rygh, C. B., S. Qin, J. W. Seo, L. M. Mahakian, H. Zhang, R. Adamson, J. Q. Chen, A. D. Borowsky, R. D. Cardiff, R. K. Reed, F. R. Curry and K. W. Ferrara (2011). "Longitudinal investigation of permeability and distribution of macromolecules in mouse malignant transformation using PET." Clin Cancer Res **17**(3): 550-559.

Sands, H., L. J. Gorey-Feret, A. J. Cocuzza, F. W. Hobbs, D. Chidester and G. L. Trainor (1994). "Biodistribution and metabolism of internally 3H-labeled oligonucleotides. I. Comparison of a phosphodiester and a phosphorothioate." Mol Pharmacol **45**(5): 932-943.

Schnitzer, J. E. and J. Bravo (1993). "High affinity binding, endocytosis, and degradation of conformationally modified albumins. Potential role of gp30 and gp18 as novel scavenger receptors." J Biol Chem **268**(10): 7562-7570.

Thibaudeau, K., R. Leger, X. Huang, M. Robitaille, O. Quraishi, C. Soucy, N. Bousquet-Gagnon, P. van Wyk, V. Paradis, J. P. Castaigne and D. Bridon (2005). "Synthesis and evaluation of insulin-human serum albumin conjugates." Bioconjug Chem **16**(4): 1000-1008.

Vaidyanathan, G. and M. R. Zalutsky (1990). "Protein radiohalogenation: observations on the design of N-succinimidyl ester acylation agents." Bioconjug Chem **1**(4): 269-273.

Verel, I., G. W. Visser, M. J. Vosjan, R. Finn, R. Boellaard and G. A. van Dongen (2004). "High-quality 124I-labelled monoclonal antibodies for use as PET scouting agents prior to 131I-radioimmunotherapy." Eur J Nucl Med Mol Imaging **31**(12): 1645-1652.

Xie, D., C. Yao, L. Wang, W. Min, J. Xu, J. Xiao, M. Huang, B. Chen, B. Liu, X. Li and H. Jiang (2010). "An albumin-conjugated peptide exhibits potent anti-HIV activity and long in vivo half-life." Antimicrob Agents Chemother **54**(1): 191-196.

Xie, X., J. Liang, T. Pu, F. Xu, F. Yao, Y. Yang, Y. L. Zhao, D. You, X. Zhou, Z. Deng and Z. Wang (2012). "Phosphorothioate DNA as an antioxidant in bacteria." Nucleic Acids Res **40**(18): 9115-9124.

CHAPTER III: PHARMACOKINETICS/BIODISTRIBUTION AND PHARMACODYNAMICS OF MALEMIDE DERIVATIZED OLIGODEOXYNUCLEOTIDES WITH PHOSPHODIESTER BACKBONE IN TUMOR BEARING MICE

3.1 Overview

A 20-mer CpG oligodeoxynucleotide (ODN) with a phosphodiester backbone was derivatized with maleimide (CpG-mal) at 3'-end to promote their reaction with Cys_{34} of serum albumin. *In vitro* plasma stability indicated albumin conjugation could partially protect the CpG from nuclease degradation. Pharmacokinetics (PK) and biodistribution (BD) were measured by PET/CT imaging of [^{124}I]-labeled CpG-mal. Plasma and tumor exposure of CpG-mal was increased 70- and 30-fold, respectively, compared to control CpG. *In vivo* efficacy was measured in an orthotopic 4T1 murine breast carcinoma model. No difference was observed in tumor growth, post-resection survival, or number of lung metastasis for any treatments compared to negative control. *In vitro* macrophage activation was assessed by IL-6 and IL-12 production in J774 cells. The lack of antitumor response is explained by the weak agonist properties of CpG with phosphodiester backbone.

3.2 Introduction

Cancer immunotherapy is a promising field of cancer research that has yet to live up to its potential. Systemic CpG monotherapy as a cancer treatment is presumably limited by

the low uptake by dendritic cells and macrophages in the tumor vicinity due to the poor plasma PK and tumor accumulation of CpG. A method of increasing the plasma halflife of systemically-administered CpG should allow more opportunity for the CpG to interact with the tumor tissue and increase the tumor exposure, thereby improving efficacy.(Palma and Cho, 2007) Using serum albumin as a carrier of anticancer drugs is an attractive way to increase the plasma half-life and tumor exposure.(Elsadek and Kratz, 2012) Derivatizing therapeutics with maleimide groups to allow them to covalently react with Cys_{34} of serum albumin.(Kratz, Warnecke et al., 2002) Maleimide-modified ODN were able to covalently bind with circulating albumin within minutes which dramatically reduced the initial distribution of the ODN compared to control ODN which was otherwise rapidly cleared from the blood (**Figure 2.4**). Importantly, the study showed that albumin could be accessed by CpG-mal quickly enough to outcompete the rapid clearance of free CpG-mal so that *ex vivo* albumin conjugation was unnecessary.

The purpose of this study is to determine the PK and BD of CpG-mal and to test the efficacy in tumor-bearing mice. A rationale for exploring CpG immunotherapies lies in the premise that they can lead to both an innate and an adaptive immune response that causes primary tumor regression, prevent tumor reoccurrence, and treat distant metastases.(Kawarada, Ganss et al., 2001; Kunikata, Sano et al., 2004) Advances in surgery have led to a good prognosis for non-metastatic primary tumors; however, prognosis is considerably worse after the presence of metastases. Therefore treatment of metastasis is of paramount clinical importance.

The interaction between tissue stroma and cancer cells has an effect on the development of solid tumors.(Tlsty and Coussens, 2006; Ma, Dahiya et al., 2009) The use of

xenograph models may not sufficiently replicate this delicate balance. For these reasons we have chosen to use a most aggressive orthotopic breast cancer model that is capable of metastasis in order to test the efficacy of the CpG therapy.

3.3 Experimental Procedures

All chemicals, except where noted, were purchased from EMD Sciences or Sigma Aldrich and were ACS reagent grade or higher.

3.3.1 CpG ODN Chemistry

Unless specifically stated, the CpG used in all experiments were purchased from either Integrated DNA Technologies (Coralville, IA) or from Girindus America, Inc. (Cincinnati, OH) with a phosphodiester backbone. They are supplied as the Na^+ salt form. The CpG-NH_2 sequence was CpG1826: TCCATGACGTTCCTGACGTT and contained a commercially available 3'-amino modification; non-stimulatory GpC-NH_2 sequence CpG1982: TCCAGGACTTCTCTCAGGTT was also purchased with a commercially available 3'-amino modification. Unmodified CpG1826 (CpG) was also purchased.

HPLC Conditions

All HPLC analysis and purification was performed using Shimadzu SCL-10A system controller with two Shimadzu LC-8A pumps connected to a Rainin Dynamax UV-C detector and a Shimadzu C-R6A Chromatopac recorder. Solvent A was 5% acetonitrile in 10 mM triethylammonium acetate buffer; solvent B was 100% acetonitrile. For analytical work an Agilent Zorbax 300SB-C18 4.6 x 150 mm analytical column with 5 µm particle size was used with a total flow rate of 1 mL/min using the following gradient: t = 0-5 min, %B = 0; t =

5-30 min, %B = 0-25; and t = 30-33 min, %B = 25-100. For purification work the same gradient protocol was used but with an Agilent Zorbax 300SB-C18 9.4 x 250 mm semi-preparative column and a total flow rate of 4 mL/min. All detection was performed at λ = 260 nm.

CpG-mal

To a microcentrifuge tube containing CpG-NH_2 in 100 mM sodium phosphate buffer at pH = 7.4 was added 20 equivalents of *N*-(ε-Maeimidocaproyloxy)succinimide ester (EMCS) (Pierce, Rockford, IL) in acetonitrile. After 90 min at 25°C the reaction was judged complete by analytical HPLC. The mixture was concentrated under a stream of N_2 and purified using semi-preparative HPLC. The desired peak was manually collected and concentrated *in vacuo* after acidification to pH = 5.2 by the addition of excess 3M sodium acetate buffer. The CpG-mal was ethanol precipitated from 0.3 M sodium acetate to give the Na^+ salt; yields: 55-70%. ESI-MS (neg, H_2O) 6461.2 [M]

CpG-COOH

To a microcentrifuge tube containing CpG-mal was added 50 mM NaOH. After 2h at 37°C the reaction was judged complete by analytical HPLC. The CpG-COOH was ethanol precipitated from 0.3 M sodium acetate at -20°C to give the Na^+ salt; yield: 97%.

CpG-MSA Conjugation

Mouse serum albumin (MSA) Fraction V was purchased from MP Biomedicals (Solon, OH). Conjugation of CpG-mal to MSA was performed according to a previously described procedure in **Section 2.3.2**. Briefly, MSA was reacted with 3 equivalents of DTT

for 5 min at 25°C to generate mercaptalbumin and separated on a Sephadex® G-25 size exclusion column equilibrated with phosphate buffered saline (PBS). The void fractions containing MSA were pooled and loaded onto a mini-Q strong anion exchange column (Pierce, Rockford, IL) and eluted with PBS. The MSA was added in 8-fold excess to CpG-mal in PBS. After 2 h at 25°C the reaction mixture was loaded onto a mini-Q strong anion exchange column and eluted with increasing stepwise NaCl gradient in 20 mM sodium phosphate buffer pH = 7.4. Unreacted MSA was eluted with 300 mM NaCl, CpG-albumin conjugate was eluted with 400 mM NaCl, and unreacted CpG-mal was eluted with 500 mM NaCl. When phosphorothioate CpG-mal was used a stronger gradient was needed: 500 mM to elute unreacted MSA, 1 M NaCl to elute CpG-MSA, and 2 M NaCl to elute unreacted CpG-mal. Buffer exchange to PBS was performed using 30 kDa molecular weight cut off (MWCO) ultracentrifugation (Millipore, Billerica, MA); yield: 50-70%.

3.3.2 Pharmacokinetics and Biodistribution

[^{124}I] Radiolabeling

$Na^{124}I$ was purchased from IBA Molecular (Richmond, VA) two days prior to iodination. CpG-mal and CpG-COOH were radiolabeled with ^{124}I according to a previous procedure described in **Section 2.3.3**. Briefly, CpG-NH_2 was conjugated to a maleimide crosslinker that contains a tyrosine residue and was radiolabelled with ^{124}I using Iodogen® precoated tubes (Pierce, Rockford, IL). The iodination protocol was as follows: CpG to be labeled was dissolved in 100 µL of 100 mM sodium phosphate buffer at pH 7.4. To a pre-rinsed iodination tube, added were $Na^{124}I$ and a calculated amount of 1 mg/mL of NaI and 1 mg/mL of $NaIO_3$ in 1 mM NaOH containing 0.9 mol equivalent of total iodine relative to

CpG. After 1 min the CpG was added to the tube and the reaction was allowed to progress for 6 min at 25°C with periodic gentle shaking. The unquenched reaction was directly applied to a Sephadex® G-25 size exclusion column equilibrated with PBS. The fractions containing CpG ODN, as measured by UV, were pooled and concentrated using ultracentrifugation with 3 kDa MWCO filters. MSA was labeled using a similar procedure. *Ex vivo* conjugated CpG-MSA was prepared by using ^{124}I labeled CpG-mal in the same manner as previously described.

PET Image Acquisition

One day prior and throughout the imaging experiments mice were supplied *ad libitum* drinking water supplemented with 0.1% KI to block thyroid uptake of labeled ^{124}I.(Verel, Visser et al., 2004) All animals were anesthetized using isoflurane and catheterized via tail vein. For each scan, two mice were placed on a cardboard platform on the scanning bed of a GE VISTA eXplore scanner and secured with surgical tape. A heart and breathing rate probe was used to monitor vitals while scanning. The mice were first imaged with a CT scan and then were dynamically imaged with PET for 1 h and statically imaged at 4, 8, 16, 24, 36 hr for 5 minutes. The animals were injected with 0.2-0.3 mCi of ^{124}I labeled material corresponding to 100 µg of ODN in 100 µL of sterile 0.22 µm filtered PBS and the catheters were flushed with a minimal volume of normal saline. The amount of activity remaining in the catheter and syringe was measured using a calibrated dose calorimeter (Capintec CRC®-25R, Ramsey, NJ) and subtracted from the initial amount to quantify the amount of injected activity.

Immediately after the final image acquisition the mice were sacrificed by exsanguination by cardiac puncture under isoflurane anesthesia. In order to remove any residual organ blood, each mouse was perfused for 4 min with fetal bovine serum containing 100 IU/mL of heparin sodium using a peristaltic pump (Rainin Rabbit Plus, Woburn MA) at a flow rate of 1.5 mL/min by inserting and clamping a blunt needle into the left ventricle and cutting the vena cava. The heart, lungs, liver, kidneys, spleen, and tumor were harvested, rinsed in PBS, blotted dry and inserted into preweighed microfuge vials. The organs were stored at -20°C until the radioactivity was measured using a well gamma counter (PerkinElmer 2470 WIZARD^2, Waltham, MA).

Image Processing

The raw data for the dynamic scan was rebinned according to the following scheme: 0-10 minutes, 1-min intervals; 10-30 minutes, 2-min intervals; and 30-60 minutes, 3-minute intervals. Images were reconstructed using an attenuation correction, scatter correction, and 2D OSEM projection using the supplied manufacturer software (MMWKS Image Software, Laboratorio de Imagen HGUGM, Spain). The images were then loaded into AMIDE for analysis.(Loening and Gambhir, 2003) The images were aligned using fiducial markers placed below the scanning bed. Three dimensional regions of interest (ROI) were manually drawn on the heart, tumor, lungs, liver, kidneys, and intestines using the CT images. The amount of PET signal contained within a ROI was calculated and converted to percent of injected dose per mL (%ID/mL) using appropriate conversions to correct for time decay and a cylindrical phantom of known activity. Non-compartmental and PK analysis were performed using MATLAB 2012b (The MathWorks, Inc., Natick, MA).

3.3.3 *In Vitro* Plasma Stability

[^{3}H] Radiolabeling

CpG-NH_2 was radiolabelled using the procedure of Graham et al.(Graham, Freier et al., 1993) Briefly, 2 mg of CpG-NH_2 was lyophilized from 200 µL of 0.1 M sodium phosphate buffer, pH = 7.8, containing 0.2 mM EDTA in microfuge tube. To the dry powder was added 200 µL of T_2O (5 Ci/g, Moravek Biochemicals; Brea, CA) and 8.3 µL of β-mercaptoethanol. After 6h at 90℃ the reaction mixture was subjected to repeated ultracentrifugation using 5kDa MWCO filters to remove the bulk of excess T_2O. Exchangeable tritium was removed by several rounds of suspension in 1 mL H_2O, incubation at 25°C for 1 h, and lyophilization. The [^{3}H]-CpG-NH_2 (1.5 mg; 75% yield) was stored as a dry power at -20℃ until use. Analytical HPLC indicated no degradation had occurred during the procedure and the [^{3}H]-CpG-NH_2 was processed with EMCS as above.

Plasma Incubation

Whole blood was collected from female Balb/c mice via cardiac puncture into heparinized tubes and was spun at 2,000 x *g* for 10 min at 25°C. The supernatant was collected and filtered through 0.22 µm PVDF filters and stored at 4°C until use. To a microfuge tube containing 200 µL of plasma at 37°C was added 25 µg of [^{3}H]-CpG ODN in 25 µL PBS. At specified timepoints, a 25 µL aliquot was removed for size exclusion analysis. For the [^{3}H]-CpG-COOH sample an additional 5 µL aliquot was removed for gel electrophoresis and was added to 25 µL of urea gel loading buffer and stored at 4°C until use. A control experiment where 25 µg of CpG-mal was incubated in 225 µL of PBS at 37°C was also performed.

A 1 x 30 cm column was packed with Sephadex® G-50 and equilibrated with PBS containing 5 mM EDTA. The plasma aliquot was diluted with 25 µL of the column running buffer prior to column loading. Fractions were collected using a Bio-Rad model 2110 fraction collector set to 30 drops per fraction. From each fraction 550 µL was removed and transferred to a 20 ml scintillation vial followed by the addition of 3 mL of Ultima Gold XR scintillation cocktail fluid. The radioactivity in each vial was measured using a Packard Tri-Carb 2900TR liquid scintillation analyzer and reported in DPM.

The amount of radioactivity in each fraction was plotted versus fraction number. Since all fractions were of equal size, the area under the curve (AUC) was calculated by the summing the radioactivity over an empirically determined range of fractions corresponding to the column void and retention volumes. The amount of degradation was calculated according to the following equation:

$$fraction\ degraded = \frac{\left[AUC_{retained}^{t=i}\right] - \left[AUC_{retained}^{t=0}\right]}{\left[AUC_{total}^{t=i}\right]}$$

The fraction degraded was plotted versus time and the data was fit using a least-squares linear regression algorithm.

Gel electrophoresis

Gel electrophoresis was performed using 15% Mini-PROTEAN® TBE-Urea Precast Gels (Bio-Rad, Hercules, CA) and run at 200V for 40 min. The gels were stained with SYBR® Gold (Molecular Probes, Eugene, OR) and imaged using AlphaImager (Alpha Innotech, San Leandro, CA) equipped with a SYBR photographic filter.

4T1 Tumor Growth Study

Fifty female Balb/c mice, age 6-8 weeks, were orthotopically inoculated with 1 x 10^5 syngeneic 4T1 cells in 50 µL PBS into the mammary fat pad. Once the tumors were established reached a diameter of 5 mm, as measured by calipers, the mice were randomly divided into groups of 8 and experimental treatments were initiated. A total of five tail vein injections were given every other day consisting of 100 µg equivalents of CpG in 100 µL PBS. All treatments were sterile filtered using 0.22 µm PVDF membrane filters prior to injection. The experiment treatment arms were as follows: group A received 100 µg of CpG-mal, group B received 100 µg of GpC-mal, group C received 100 µg CpG-COOH, group D received 100 µl of PBS, group E received 100 µg of CpG. The tumors were allowed to grow to a maximum diameter of 12 mm at which point they were surgically resected and flash-frozen in liquid N_2. The mice were allowed to continue to survive until either of the humane endpoints of 20% loss of total body weight loss or body condition score ≤ 2 were reached. The mice were sacrificed by cervical dislocation after CO_2 asphyxiation and the lungs and livers were harvested in formalin. Tumor volumes were calculated as $V = \frac{1}{2}ab^2$, where *a* is longest diameter and *b* is the length of the perpendicular diameter in mm. Metastatic nodules in the lungs were counted by gross visual inspection of the organ.

3.3.4 *In Vitro* Macrophage Activation

J774 cells were obtained from the UNC Tissue Culture Facility, with provenance from ATTC (Manassas, VA), and were cultured with Dubelco modified essential media supplemented with 10% bovine calf serum in 5% CO_2 atmosphere at 37°C. The cells were grown in T150 flasks and harvested by scraping when 80% confluence was reached. All experiments were performed with cells with a passage number less than twenty. For experiments, the entire contents of a T-150 flask would be transferred to a 24 well plate (ca.

7 x 10^5 cells/well by hemocytometer count) in 1 mL/well of media. After 4 h, the media was removed, and replaced with 900 µL of fresh media and 100 µL of PBS containing the desired treatment. All treatments were sterile filtered using 0.22 µm PVDF membrane filters prior to dilution and addition to the cells. After 20 h, the media was removed and spun at 1000 x *g* for 5 min at 25°C. The supernatant was carefully removed and assayed within 1 h or frozen on dry ice and stored at -20°C until ELISA analysis.

IL-6 and IL-12 (p40) ELISA kits and appropriate buffer sets were purchased from BD Biosciences (San Jose, CA). The assays were performed in accordance to manufacturer's instructions. When dilutions were necessary the cell culture supernatant was diluted with assay diluent. The absorbance was read at 450 nm and was corrected with 570 nm subtraction using a Hidex Plate Chameleon™V (Turku, Finland) plate reader. The concentration of cytokine was then back calculated using the appropriate standard curve and dilution factors. The results were assayed in duplicate and are expressed as the average.

3.4 Results

3.4.1 *In Vitro* Plasma Stability

The stability of radiolabeled [^{3}H]-CpG-COOH and [^{3}H]-CpG-mal in undiluted mouse plasma was measured at various time points by size exclusion chromatography and gel electrophoresis. A plot of the fraction degraded versus time is shown in **Figure 3.1** and the slope indicates the [^{3}H]-CpG-COOH and [^{3}H]-CpG-mal were degraded in murine plasma at a rate of 2.3 and 1.5 % per hr, respectively, compared to a rate of 0.15 % per hr in PBS for [^{3}H]-CpG-mal. Gel electrophoresis of the [^{3}H]-CpG-COOH showed the majority of the material corresponds to intact [^{3}H]-CpG-COOH with a slow appears of smaller sequences.

3.4.2 Plasma Pharmacokinetics

There was a dramatic difference in the plasma concentration profile of the [^{124}I]-CpG-mal versus [^{124}I]-CpG-COOH, which can be seen in **Figure 3.2**. The [^{124}I]-CpG-COOH rapidly falls below the limit of the detection within 7 h, whereas, the [^{124}I]-CpG-mal has a higher concentration and longer half-life and never reaches background levels during the course of the experiment. When the data are fit to a two-compartment model the half-lives for [^{124}I]-CpG-COOH and [^{124}I]-CpG-mal were 0.3 h and 10 hr respectively. The half-life of precomplexed [^{124}I]-CpG-MSA was 7 hr which is similar to [^{124}I]-CpG-mal and half-life of [^{124}I]-MSA was 13 hr, which was longer than both of the CpG-albumin conjugates.

3.4.3 Biodistribution and Tumor Accumulation

The tumor accumulation of the different CpG ODN is shown in **Figure 3.3**. [^{124}I]-CpG-COOH reached a maximal tumor accumulation of ~2 %ID/mL approximately 30 min after injection and begins to quickly drop thereafter. On the other hand, [^{124}I]-CpG-mal reached a maximum of ~3 %ID/mL approximately 4 h after injection and slowly decreases which is similar to ex vivo complexed [^{124}I]-CpG-MSA. [^{124}I]-MSA had a tumor accumulation of ~5%ID/mL approximately 4 h after injection. The tumor exposure was increased 30 fold for [^{124}I]-CpG-mal compared to [^{124}I]-CpG-COOH.

The [^{124}I]-CpG-COOH is rapidly excreted by the kidneys into the urine and no other organs appear to accumulate the drug. On the other hand, [^{124}I]-CpG-mal, [^{124}I]-CpG-MSA, and [^{124}I]-MSA show widespread distribution to all organs. Post-sacrifice organ distribution, **Figure 3.4**, showed the majority of ^{124}I radiolabel to be contained within the blood and the tumor had the next highest concentration. The predominate mode of clearance was by the

kidneys and also by elimination in the feces. [^{124}I]-MSA appeared to be exclusively eliminated by the kidneys.

3.4.4 4T1 Tumor Growth Study

There was no difference in initial tumor growth rate prior to surgical resection between any of the study groups. All of the groups showed a steady increase in tumor volume during treatment and the tumors were resected one week after the first treatment. Due to the aggressive nature of the 4T1 cells infiltrating adjacent muscle and skin tissue, complete surgical resection without major surgical intervention was not possible, but a drastic reduction in primary tumor burden was achieved. Skin ulcerations which were attributed to complications from the surgery were prevalent and necessitated euthanasia. No difference in the survival time post-surgery was observed across the study groups, as shown in **Figure 3.5**.

3.4.5 *In Vitro* Cytokine Release

The purpose of the *in vitro* activation study was to test CpG-albumin conjugates are active to antigen presenting cells in the absence of any physiological barriers limiting access to these cells. The murine macrophage cell line J774 was incubated with various concentrations of different CpG treatments and ELISA against IL-6 and IL-12 was performed on the cell supernatants to determine the extent of activation. It can be seen from the results in **Figure 3.6** that the activation was reduced for CpG-albumin compared to CpG. It is also clear from the results that phosphodiester CpG are not able to activate the macrophages as well as the phosphorothioate CpG.

3.5 Discussion

It is possible that albumin conjugation may affect the interaction between CpG ODN and enzymatic nucleases and serve to protect them from degradation. The CpG-COOH and CpG-mal were both moderately stable when incubated with mouse plasma *in vitro* and the CpG-mal was approximately 1.5 times more stable. Since the 3'-end was modified these CpG were not subject to rapid degradation by 3'-exonucleases that are prevalent and responsible for the majority of degradation in plasma.(Eder, DeVine et al., 1991) Other studies indicated that *in vitro* stability does not correlate to *in vivo* stability due to higher levels of cellular endonucleases.(Kang, Boado et al., 1995) In this study the ^{124}I radiolabel is located on the crosslinker linking the CpG to albumin. The measured ^{124}I radioactivity gives no information whether the CpG is still intact. Therefore the results represent the upper limit of how long the CpG could remain assuming that degradation of the CpG does not influence the disposition.

The 30-fold increase in tumor accumulation of [^{124}I]-ODN-mal compared to [^{124}I]-ODN-COOH is attributed to the increased plasma $t_{1/2}$ and increased vascular permeability in the tumor vicinity.(Matsumura and Maeda, 1986) The extended retention of [^{124}I]-ODN-mal compared to [^{124}I]-ODN-COOH by the tumor is consistent with impaired lymphatics and reduced diffusion of the macromolecular conjugate versus the smaller ODN (74 kDa vs 7 kDa) in the tumor microenvironment.(Matsumura and Maeda, 1986) Although, the tumor has higher accumulation, it never appreciably exceeded the plasma concentration in our study.

Albumin has historically been used as a predictor of plasma volume because it does not readily extravasate and its distribution upon injection is limited to the intravascular volume. The initial signals for the blood concentration are lower than would be expected and this may be related to using the heart ROI as an approximation of the blood concentration. The total heart ROI signal is composed of both the blood and heart tissue signals. **Figure 3.4** shows the concentration of ^{124}I in the blood was consistently greater than heart tissue so the majority of the heart signal comes from the blood. This should lead to two signal distribtutions, a higher one for the blood volume and a lower one for the heart tissue. Interestingly, a histogram of the ROI signal did not reveal these two distinction signal distributions (data not shown).

The lack of an efficacious response despite a difference in tumor accumulation prompted us to investigate whether albumin conjugation possibly interfered with TLR9 signaling. We found that phosphodiester CpG was not a very potent agonist of TLR9 which is in agreement with other studies and attribute this to nuclease instability.(Krieg, MATSON et al., 1996) Replacing the CpG phosphodiester backbone with phosphorothioate significantly increases the activation of TLR9. Modification of the 3'-end of CpG was not expected to alter the activation,(Kandimalla, Bhagat et al., 2002) but we noticed a distinct difference which must related to the difference in nature of modification. Conjugation of albumin further reduced the activation but did not totally abolish the activity. It is concluded based on the results of the *in vitro* activation assay that the lack of *in vivo* efficacy was related to the PO CpG not being a potent TLR9 agonist.

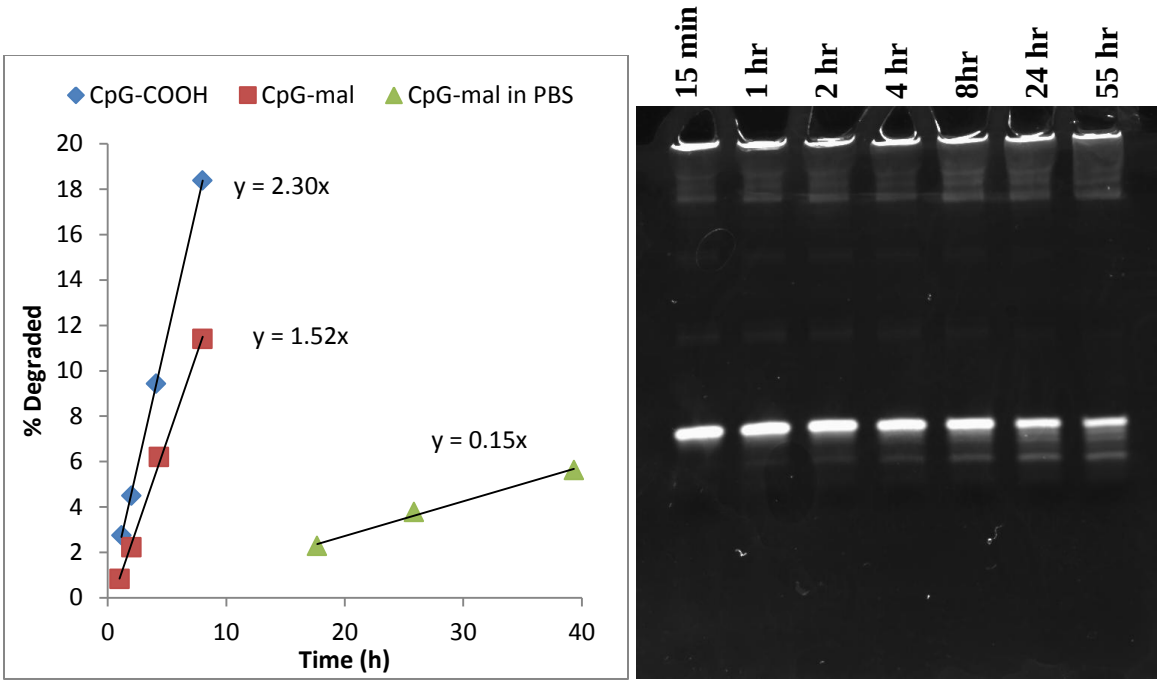

Figure 3.1. *In vitro* plasma stability of PO [^{3}H]-CpG. The difference in rate of degradation in plasma versus PBS buffer indicates enzymatic degradation. Gel electrophoresis show the majority of remaining CpG is intact with the presence of some smaller sequences. Equal size aliquots were loaded onto the gel, the reduction in staining intensity is due to fully degraded nucleotides running off gel.

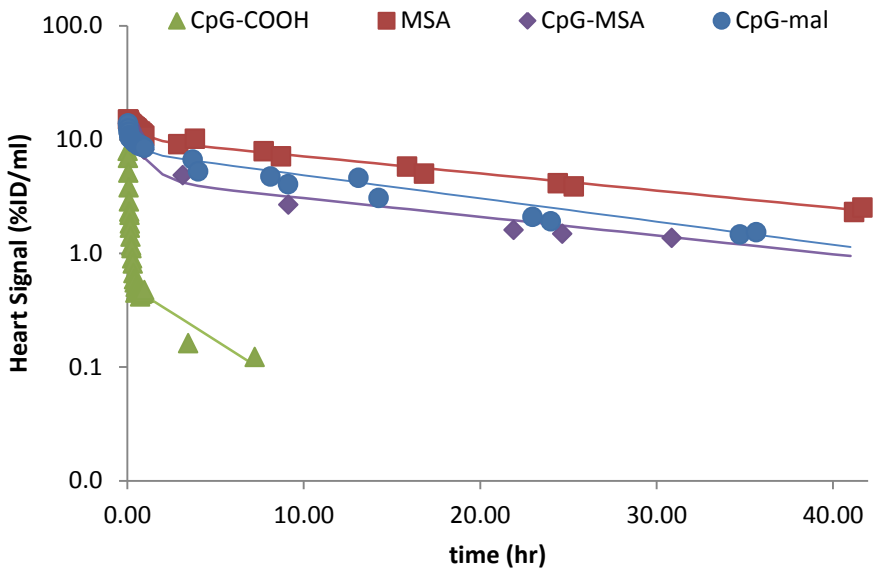

Figure 3.2. Blood concentration of ^{124}I labeled CpG. CpG-COOH is rapidly cleared from the circulation whereas the other treatments exhibit prolonged blood retention. The line represent the 2-compartment model fit parameters found in **Table 3-1**. Each data point is the average of 2 animals imaged simultaneously.

Table 3-1. Plasma and tumor exposure of the [^{124}I]-labeled CpG.

AUC were calculated by non-compartment analysis of the respective time activity curves. Initial volume and compartmental rate constants are calculated from a 2-compartment model.

	Plasma AUC (h %ID/ml)	**Tumor AUC (h %ID/ml)**	**V_1 (mL)**	**k_{10} (h^{-1})**	**k_{12} (h^{-1})**	**k_{21} (h^{-1})**
[^{124}I]-CpG-COOH	3 ± 1	7 ± 1	14.5 ± 1.4	2.4 ± 0.3	8.8 ± 1.0	1.1 ± 0.1
[^{124}I]-CpG-mal	196 ± 19 (69)	200 ± 32 (29)	8.5 ± 0.2	0.07 ± 0.02	0.5 ± 0.1	1.2 ± 0.2
[^{124}I]-CpG-MSA	185 ± 8 (65)	194 ± 99 (29)	8 ± 1.2	0.10 ± 0.01	0.6 ± 0.2	0.4 ± 0.1
[^{124}I]-MSA	305 ± 30 (107)	338 ± 103 (50)	6.8 ± 0.1	0.05 ± 0.01	0.43 ± 0.03	1.0 ± .09

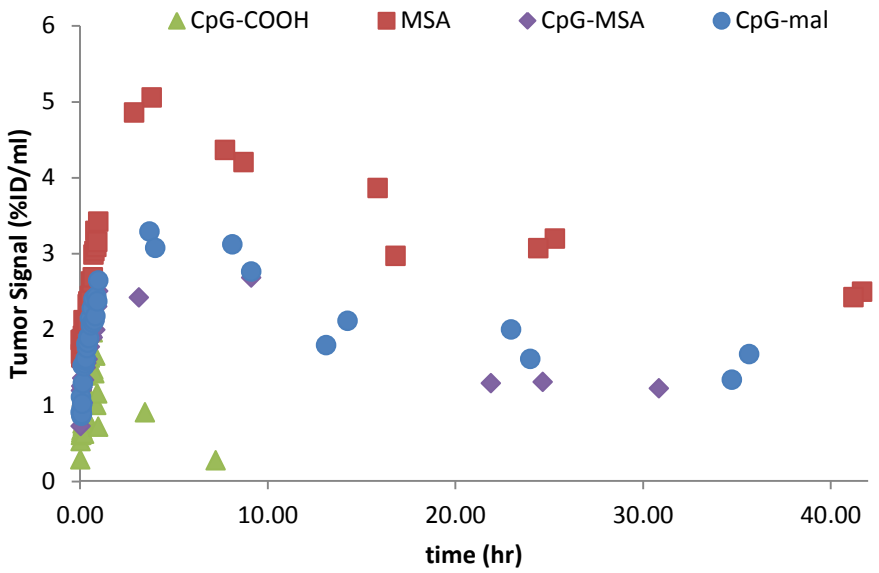

Figure 3.3. Tumor time activity curve showing tumor uptake of ^{124}I labeled CpG. The CpG-COOH quickly rises and falls whereas all other treatments show increased accumulation and retention in the tumor. Each data point is the average of 2 animals imaged simultaneously.

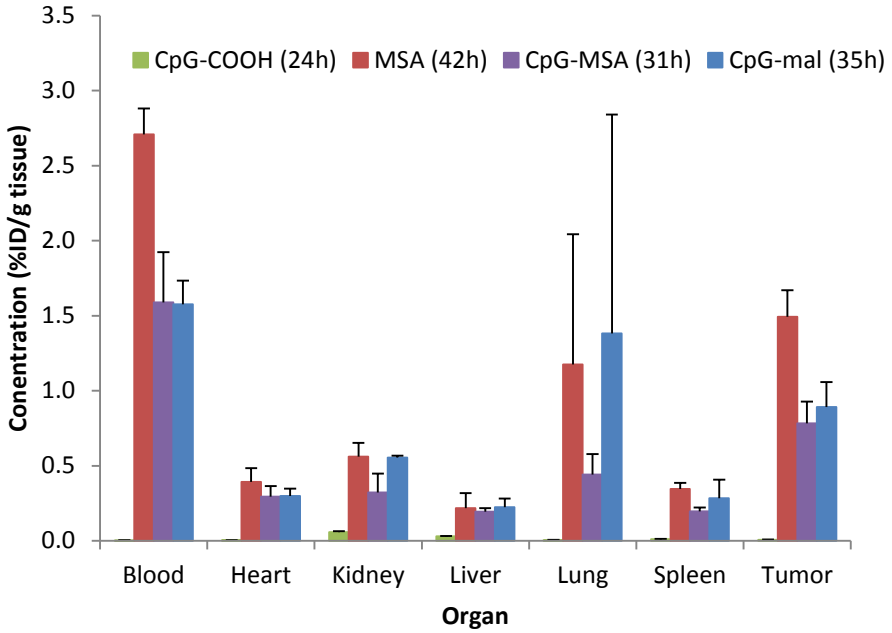

Figure 3.4. Terminal biodistribution of ^{124}I-labeled CpG measured by *ex vivo* gamma counting. The time post injection the samples were extracted from the mice is shown in the legend. For MSA and CpG-mal, N=4; for CpG-COOH and CpG-MSA, N =2. Error bars represent the standard deviation of the measurements. For CpG-mal and MSA, one mouse had large lung uptake which was attributed to the formation of a clot, otherwise the blood had the highest concentration followed by the tumor for all albumin associated formulations.

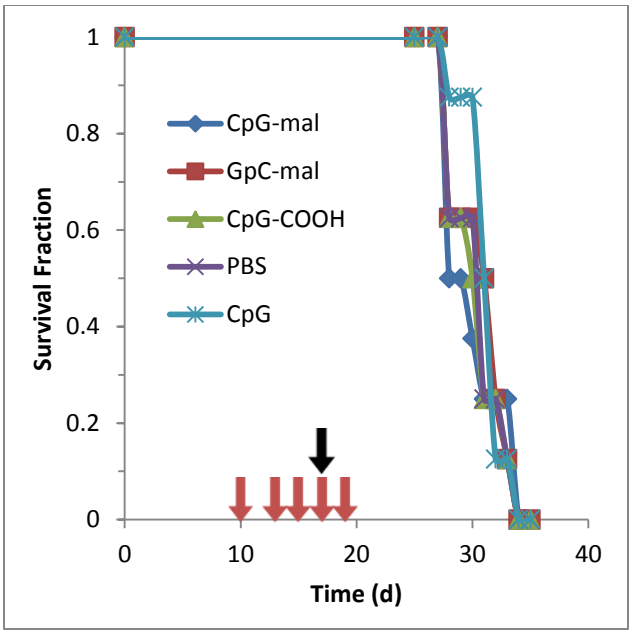

Figure 3.5. Survival after surgical resection of 4T1 primary tumor. Red arrows represent treatment, the black arrow represents surgical resection. In all treatment groups showed uniform lethality by 35 days after tumor inoculation and mice were euthanized prematurely due to skin ulcerations. For all treatment groups N =8.

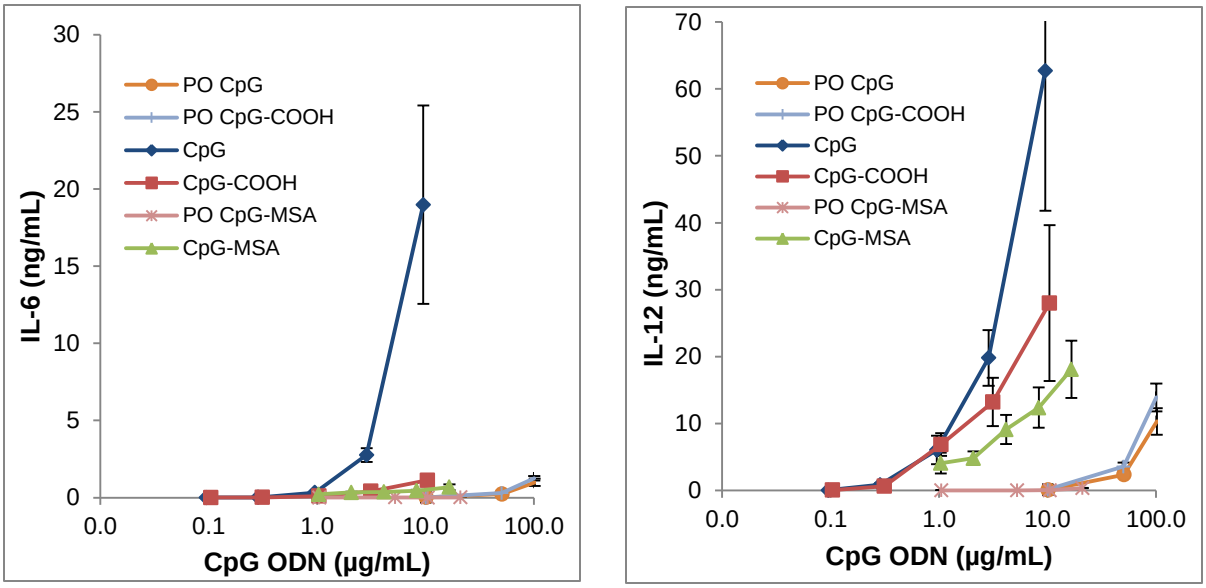

Figure 3.6. *In vitro* IL-12 and IL-6 release from J444 cells. ELISA was performed on cell supernatant after 20 h of incubation.

REFERENCES

Eder, P. S., R. J. DeVine, J. M. Dagle and J. A. Walder (1991). "Substrate specificity and kinetics of degradation of antisense oligonucleotides by a 3' exonuclease in plasma." Antisense Res Dev **1**(2): 141-151.

Elsadek, B. and F. Kratz (2012). "Impact of albumin on drug delivery - New applications on the horizon." J Control Release **157**(1): 4-28.

Graham, M. J., S. M. Freier, R. M. Crooke, D. J. Ecker, R. N. Maslova and E. A. Lesnik (1993). "Tritium labeling of antisense oligonucleotides by exchange with tritiated water." Nucleic Acids Res **21**(16): 3737-3743.

Kandimalla, E. R., L. Bhagat, D. Yu, Y. Cong, J. Tang and S. Agrawal (2002). "Conjugation of ligands at the 5'-end of CpG DNA affects immunostimulatory activity." Bioconjug Chem **13**(5): 966-974.

Kang, Y. S., R. J. Boado and W. M. Pardridge (1995). "Pharmacokinetics and organ clearance of a 3'-biotinylated, internally [32P]-labeled phosphodiester oligodeoxynucleotide coupled to a neutral avidin/monoclonal antibody conjugate." Drug Metab Dispos **23**(1): 55-59.

Kawarada, Y., R. Ganss, N. Garbi, T. Sacher, B. Arnold and G. J. Hammerling (2001). "NK- and CD8(+) T cell-mediated eradication of established tumors by peritumoral injection of CpG-containing oligodeoxynucleotides." J Immunol **167**(9): 5247-5253.

Kratz, F., A. Warnecke, K. Scheuermann, C. Stockmar, J. Schwab, P. Lazar, P. Druckes, N. Esser, J. Drevs, D. Rognan, C. Bissantz, C. Hinderling, G. Folkers, I. Fichtner and C. Unger (2002). "Probing the cysteine-34 position of endogenous serum albumin with thiol-binding doxorubicin derivatives. Improved efficacy of an acid-sensitive doxorubicin derivative with specific albumin-binding properties compared to that of the parent compound." J Med Chem **45**(25): 5523-5533.

Krieg, A. M., S. MATSON and E. FISHER (1996). "Oligodeoxynucleotide modifications determine the magnitude of B cell stimulation by CpG motifs." Antisense and Nucleic Acid Drug Development **6**(2): 133-139.

Kunikata, N., K. Sano, M. Honda, K. Ishii, J. Matsunaga, R. Okuyama, K. Takahashi, H. Watanabe, G. Tamura, H. Tagami and T. Terui (2004). "Peritumoral CpG oligodeoxynucleotide treatment inhibits tumor growth and metastasis of B16F10 melanoma cells." J Invest Dermatol **123**(2): 395-402.

Loening, A. M. and S. S. Gambhir (2003). "AMIDE: a free software tool for multimodality medical image analysis." Mol Imaging **2**(3): 131-137.

Ma, X. J., S. Dahiya, E. Richardson, M. Erlander and D. C. Sgroi (2009). "Gene expression profiling of the tumor microenvironment during breast cancer progression." Breast Cancer Res **11**(1): R7.

Matsumura, Y. and H. Maeda (1986). "A new concept for macromolecular therapeutics in cancer chemotherapy: mechanism of tumoritropic accumulation of proteins and the antitumor agent smancs." Cancer Res **46**(12 Pt 1): 6387-6392.

Palma, E. and M. J. Cho (2007). "Improved systemic pharmacokinetics, biodistribution, and antitumor activity of CpG oligodeoxynucleotides complexed to endogenous antibodies in vivo." J Control Release **120**(1-2): 95-103.

Tlsty, T. D. and L. M. Coussens (2006). "Tumor stroma and regulation of cancer development." Annu Rev Pathol **1**: 119-150.

Verel, I., G. W. Visser, M. J. Vosjan, R. Finn, R. Boellaard and G. A. van Dongen (2004). "High-quality 124I-labelled monoclonal antibodies for use as PET scouting agents prior to 131I-radioimmunotherapy." Eur J Nucl Med Mol Imaging **31**(12): 1645-1652.

CHAPTER IV: PHARMACOKINETICS/BIODISTRIBUTION AND PHARMACODYNAMICS OF MALEIDE-DERIVATIZED OLIGODEOXYNUCLEOTIDES WITH PHOSPHOROTHIOATE BACKBONE IN TUMOR-BEARING MICE

4.1 Overview

In an attempt to increase the efficacy of systemically injected CpG oligodeoxynucleotides with phosphorothioate backbone for cancer immunotherapy, they were modified with a maleimide group (CpG-mal) to promote *in situ* conjugation with Cys_{34} of serum albumin. The CpG-mal had a slower plasma distribution and longer plasma half-life than control CpG (CpG-COOH) that cannot form such a conjugate. The CpG-mal had lower kidney accumulation and increased spleen and liver accumulation compared to CpG-COOH as well as increased tumor concentrations. CpG-mal and CpG-COOH were both able to cause complete tumor regression in 60% of the mice bearing CT26 tumors but no tumor regression was observed for 4T1 tumors. Increasing the length of the maleimide crosslinker or incorporating a reducible disulfide into the crosslinker did not significantly affect the *in vitro* activation of macrophages by CpG-albumin conjugates.

4.2 Introduction

CpG oligodeoxynucleotides (ODN) mimic bacterial DNA and act as toll-like receptor (TLR) 9 agonists to cause activation of the innate and adaptive immune response.(Krieg, Yi

et al., 1995) CpG monotherapy is effective in murine cancer models upon peritumoral injection but never when administered systemically.(Heckelsmiller, Rall et al., 2002; Nierkens, den Brok et al., 2009) The anti-tumor response appears to primarily involve CD8+ T cells, NK cells, and macrophages rather than CD4+ T cells.(Heckelsmiller, Rall et al., 2002; Ballas, 2007; Buhtoiarov, Sondel et al., 2007) The lack of efficacy for systemically-injected CpG is presumably caused by low exposure due to the rapid plasma clearance of CpG. In a previous study in our lab, it was shown that tumor exposure and efficacy of systemically injected CpG could be increased by making *in situ* monomeric IgG complexes of hapten-derivatized CpG injected into mice preimmunized against the hapten.(Palma and Cho, 2007) While the results were quite promising, the clinical use may be limited due to low steady-state titers of specific IgG in humans. In search of an alternative endogenous serum proteins that could be used as a carrier we have shown that maleimide-modified phosphodiester CpG were able to quickly react with serum albumin. The *in situ* conjugation significantly altered the biodistribution increasing both the plasma half-life and tumor accumulation. However, these CpG were not able to activate TLR9 to produce an immune response. The present study was designed to test whether serum albumin could serve as a carrier of phosphorothioate CpG for cancer therapy in a similar fashion to immunoglobulins.

In other studies where albumin has been used as a carrier of cytotoxic anticancer drugs the target has always been the cancer cells themselves. This is in contrast to our study where the CpG-albumin target is the dendritic cells and macrophages within the tumor periphery. Accessing the tumor periphery is a much easier task due to the heterogeneous transport phenomena within tumor tissue.(Chauhan, Stylianopoulos et al., 2011)

Additionally, phagocytic cells are expected to accumulate more albumin than nonphagocytic cells.(Chang, 1969)

4.3 Experimental Procedures

CpG Chemistry

The CpG1826 used in all experiments were purchased from Integrated DNA Technologies (Coralville, IA) with a phosphorothioate backbone as the Na^+ salt. The sequence was TCCATGACGTTCCTGACGTT and contained a commercially available 3' amino modification. CpG1826 with no modifications was also purchased.

HPLC Conditions

All HPLC analysis and purification was performed using Shimadzu SCL-10A system controller with two Shimadzu LC-8A pumps connected to a Rainin Dynamax UV-C detector and a Shimadzu C-R6A Chromatopac recorder. Solvent A was 5% acetonitrile in 100 mM triethylammonium acetate buffer; solvent B was 100% acetonitrile. For analytical work an Agilent Zorbax 300SB-C18 4.6 x 150mm analytical column with 5 μm particle size was used with a total flow rate of 1 ml/min using the following gradient: t = 0-5 min, %B = 0; t = 5-30 min, %B = 0-25; t = 30-33 min, %B = 25-100. For purification work, Solvent A was 5% acetonitrile in 10 mM triethylammonium acetate buffer and the same gradient protocol was used with an Agilent Zorbax 300SB-C18 9.4 x 250mm semi-preparative column and a total flow rate of 4 ml/min. All detection was performed at $\lambda = 260$ nm.

CpG-mal (**Figure 4.1**)

To a microcentrifuge tube containing CpG-NH_2 in 100 mM sodium phosphate buffer pH = 7.4 was added 20 equivalents of EMCS in acetonitrile. After 90 min at 25°C the reaction was judged complete by analytical HPLC. The mixture was concentrated under a stream of N_2 and purified using semi-preparative HPLC. The desired peak was manually collected and concentrated *in vacuo* after acidification to pH = 5.2 by the addition of excess 3 M sodium acetate buffer. The CpG-mal was ethanol precipitated from 0.3 M sodium acetate to give the Na^+ salt.

CpG-COOH (**Figure 4.1**)

To a microcentrifuge tube containing CpG-mal was added 50 mM NaOH solution. After 2 h at 37°C the reaction was judged complete by analytical HPLC. The CpG-COOH was ethanol precipitated from 0.3 M sodium acetate at -20°C to give the Na^+ salt.

CpG-PEG_{24}-mal

To a microcentrifuge tube containing CpG-NH_2 in 100 mM sodium phosphate buffer pH = 7.4 was added 20 equivalents of NHS-PEG_{24}-mal in acetonitrile. After 90 min at 25°C the reaction mixture separated by repeated ultracentrifugation using 5 kDa MWCO filters in 0.3 M sodium acetate buffer pH = 5.2 to remove unreacted crosslinker. The CpG-PEG24-mal was ethanol precipitated from 0.3 M sodium acetate at -20°C to give the Na^+ salt, yield: 60%.

CpG-SS-mal

To a microcentrifuge tube containing CpG-NH_2 in 100 mM sodium phosphate buffer pH = 7.4 was added 20 equivalents of S-SS-4FB (Solulink, San Diego, CA) in

dimethylformamide. After 90 min at 25°C the reaction mixture separated by repeated ultracentrifugation using 5 kDa MWCO filters in 0.3 M sodium acetate pH = 5.2 buffer to remove unreacted crosslinker and 20 equivalents of *N*-β-Maleimidopropionic acid hydrazide (BMPH) was added. After 30 min at 25°C the reaction mixture was ultracentrifuged to remove the unreacted crosslinker. The CpG-SS-mal was ethanol precipitated from 0.3 M sodium acetate at -20°C to give the Na^+ salt; yield: 55%.

[^{3}H] Radiolabeling of CpG

CpG-NH_2 was radiolabeled using the procedure of Graham, et al.(Graham, Freier et al., 1993) Briefly, 6 mg of CpG-NH_2 was lyophilized from 200 µL of 0.1 M sodium phosphate buffer, pH = 7.8, containing 0.2 mM EDTA in microfuge tube. To the dry powder was added 200 µL of T_2O (5 Ci/g, Moravek Biochemicals; Brea, CA) and 8.3 µL of β-mercaptoethanol. After 6h at 90°C the reaction mixture was subjected to repeated ultracentrifugation using 5kDa MWCO filters to remove the bulk of excess T_2O. Exchangeable tritium was removed by several rounds of suspension in 1 mL H_2O, incubation at 25°C for 1 h, and lyophilization. The [^{3}H]-CpG-NH_2 (4.1 mg; 68% yield) was stored as a dry power at -20°C until use. The specific activity (SA) was 3.1 x 10^4 DPM/µg. Analytical HPLC indicated no degradation had occurred during the procedure and the [^{3}H]-CpG-NH_2 was processed with EMCS as above.

4.3.1 *In Vitro* Cytokine Release

J774 cells were obtained from the UNC Tissue Culture Facility, with provenance from ATTC (Manassas, VA), and were cultured with Dubelco modified essential media supplemented with 10% bovine calf serum in 5% CO_2 atmosphere at 37°C. The cells were

grown in T150 flasks and harvested by scraping at 80% confluence. All experiments were performed with cells with a passage number less than twenty. For experiments, the entire contents of a T-150 flask would be transferred to a 24 well plate (ca. 7 x 10^5 cells/well by hemocytometer count) in 1 mL/well of media. After 4 h, the media was removed, and replaced with 900 µL of fresh media and 100 µL of PBS containing the desired treatment. All treatments were sterile filtered using 0.22 µm PVDF membrane filters prior to dilution and addition to the cells. After 20 h, the media was removed and spun at 1000 x *g* for 5 min at 25°C. The supernatant was carefully removed and assayed within 1 h or frozen on dry ice and stored at -20°C until ELISA analysis.

IL-6 and IL-12 (p40) ELISA kits and appropriate buffer sets were purchased from BD Biosciences and 96-well plates were purchased from Nunc. The assays were performed in accordance to manufacturer's instructions with no modifications. When dilutions were necessary the cell culture supernatant was diluted with assay diluent. The absorbance was read at 450 nm and was corrected with 570 nm subtraction using a Mtech plate reader. The concentration of cytokine was then back-calculated using the appropriate standard curve and dilution factors. The results were assayed in duplicate and are expressed as the average ± standard deviation.

CpG-albumin Conjugation

CpG-albumin conjugates were prepared by a method previously reported in **Section 2.3.2**. Briefly, maleimide containing CpG was incubated with 8-fold molar excess murine mercaptalbumin for 2 h at 25°C in PBS. The mixture was directly loaded onto Q strong anion spin columns (Pierce, Rockford, IL) and separated using a stepwise increasing NaCl

gradient in 20 mM sodium phosphate pH = 7.4 buffer. Unreacted albumin was eluted using 500 mM NaCl, CpG-albumin conjugate was eluted using 1 M NaCl, and unreacted CpG was eluted using 2 M NaCl. Repetitive ultracentrifugation using 30 kDa MWCO filters was used to change the buffer to PBS and the conjugate was stored at 4°C not more than 48 h until use.

Mice and Cell Lines

All mice were handled in accordance with an approved protocol by UNC Institutional Animal Care and Use Committee. Female Balb/c mice age, 8-10 weeks, were purchased from the National Cancer Institute (Bethesda, MD). For tumor growth inhibition studies tumor size was measured by calipers three times per week and calculated as $V = \frac{1}{2}ab^2$, where *a* was the longest diameter and *b* was the length of the perpendicular diameter in mm. Mice were allowed to survive until a maximum diameter of 2 cm was reached at which point they were sacrificed by cervical dislocation after CO_2 euthanasia. CT26 and 4T1 cell lines were purchased from ATCC (Manassas, VA) and grown according to the manufacturer's recommendations.

4.3.2 Pharmacokinetic and Biodistribution Study

Fifty mice were inoculated subcutaneously in the right flank with 2.5×10^5 CT26 cells in 50 µL of Hank's balanced buffer solution (HBSS). After 10 days the mice were randomly divided into groups of 3 and were given tail vein injections of 100 µg of either [^{3}H]CpG-mal (SA = 2.1×10^4 DPM/µg) or [^{3}H]CpG-COOH (SA = 2.1×10^4 DPM/µg) in 100 µL of PBS. All treatments were sterile filtered using 0.22 µm PVDF filters prior to injection. For [^{3}H]-CpG-COOH, 3 mice were sacrificed by cardiac puncture at the following time points: 5, 10, 15, 30, 60, 120, 240 min after intraperitoneal injection of 100 µL of 100

mg/mL ketamine hydrochloride. For [^{3}H]-CpG-mal, mice were sacrificed in a similar manner at 10 min, 1, 4, 8, 15, 24, 42 hr. Whole blood was collected into tubes containing EDTA and the heart, liver, spleen, kidneys, lungs, tumor and injection site were rinsed with PBS, blotted dry, and weighed in scintillation vials. Whole organs were processed for radioactivity analysis except for the liver, which was cut into 100 mg pieces. Whole blood was processed in triplicate 100 µL fractions. To each tissue sample was added 1 mL of Solvable® and was incubated overnight at 25°C, and for 2 hr in a 60°C shaking water bath. To decolorize the samples, 100 µL of 0.1M EDTA was added followed by 200 µL of 30% H_2O_2 and the samples incubated for 30 min in a shaking water bath at 60°C. After cooling to 25°C, 10 mL of Ultima Gold scintillation cocktail was added to each vial and the radioactivity was measured using a Packard Tricarb scintillation counter and reported in DPM. Organ-specific quench curves were generated but were found to be unnecessary as no quenching was observed; no correction for organ residual blood volume was performed.

4.3.3 CT26 Tumor Growth Study

Thirty female Balb/c mice, age 8-10 weeks, were subcutaneously inoculated with 2.5 x 10^5 syngeneic CT26 cells in 50 µL HBSS into the right flank. After 10 days the mice were randomly divided into three groups and treatment was initiated. The mice received a total of 4 tail vein iv injections every 3 days. Group A (N = 9) received 100 µl of PBS, group B (N = 10) received 100 µg of CpG-COOH in 100 µl PBS, and group C (N = 10) received 100 µg of CpG-mal in 100 µl of PBS.

4.3.4 4T1 Tumor Growth Study

Forty mice were orthotopically inoculated with 1 x 10^4 4T1 cells in 50 µL PBS into the mammary fat pad. After 10 days, the mice were randomly divided into three groups of 10 and experimental treatments were initiated. A total of three treatments were given every three days. Group A received 100 µg of CpG in 100 µL PBS via tail vein, group B received 50 µg of CpG in 50 µL PBS peritumorally, and group C received 100 µg equivalent of CpG-mal in 100 µL PBS via tail vein. All treatments were sterile filtered through a 0.22 µm PVDF filter immediately prior to injection.

4.4 Results

4.4.1 *In Vitro* Macrophage Activation

It was shown previously that CpG-albumin conjugates display lower IL-12 and IL-6 release from a macrophage cell line than unconjugated control CpG (**Figure 3.6**). In order to test whether steric hindrance was inhibiting the CpG-albumin from interacting with TLR9, CpG was derivatized with a longer crosslinker containing 24 repeating ethylene glycol units, shown in **Figure 4.2.** This chemical manipulation should extend the CpG moiety away from the albumin. As shown in **Figure 4.2** this modification did not increase the activation to any appreciable extent. Additionally, in order to test whether releasing the CpG from albumin in the reductive environment of the endosome could increase the activity, a reversible disulfide crosslinker was employed to create a reducible linkage between CpG and albumin. The disulfide was able to be reductively cleaved by dithiothreitol, indicating its instability in a reductive environment (data not shown). However, the CpG-SS-albumin was still unable to increase the IL-12 or IL-6 secretion.

4.4.2 Pharmacokinetics and Biodistribution

The maleimide modification was able to alter the plasma pharmacokinetics of CpG; as expected the [^{3}H]-CpG-COOH that cannot form an adduct with albumin was rapidly cleared from the circulation and distributed into tissues whereas the [^{3}H]-CpG-mal was more slowly distributed as shown in **Figure 4.3**. Both of the CpG show biphasic plasma profiles indicating distribution into tissue compartments, most likely due to PS ODN have binding to numerous cell membrane proteins.(Beltinger, Saragovi et al., 1995)

The biodistribution of the [^{3}H]-CpG-mal was different than [^{3}H]-CpG-COOH and can be seen in **Figure 4.5**. The major difference was found in the liver and kidney. For [^{3}H]-CpG-COOH the kidney had the highest accumulation of drug, whereas for [^{3}H]-CpG-mal the liver had the highest accumulation. The spleen also had higher accumulation for [^{3}H]-CpG-mal than [^{3}H]-CpG-COOH. The tumor accumulation of [^{3}H]-CpG-mal is presented in **Figure 4.4** and was slightly increased compared to [^{3}H]-CpG-COOH. There is a clear downward trend for [^{3}H]-CpG-COOH tumor concentration from 1-4 h, whereas the [^{3}H]-CpG-mal is increasing during this time.

4.4.3 Tumor Growth Studies

In the CT26 model, a dramatic difference was seen between the groups receiving CpG therapy and the PBS group, and little difference was observed between the CpG-COOH and CpG-mal groups. The mice treated with CpG-COOH and CpG-mal showed a slow increase in tumor size during treatment followed by a complete regression in tumor volume. When the individual mice tumor volumes are examined in **Figure 4.8** it is evident that there are clear-cut responders and non-responders to the CpG monotherapy. There also appears to

be slightly more variability in the response to the CpG-COOH compared to CpG-mal. On the other hand, in **Figure 4.6** the 4T1 model the tumor growth was only slowed during treatment, and when treatment was stopped the tumors quickly began to grow. Additionally, severe toxicity was observed after the second treatment for both of the systemically-injected treatments in this model.

4.5 Discussion

Figure 4.2 demonstrates CpG-albumin conjugates are able to activate the immune system, presumably via TLR9, albeit to a weaker extent than free CpG. The length of the crosslinker did not have a significant effect on the *in vitro* activation of macrophages, suggesting steric hindrance by the conjugated albumin does not interfere with TLR9 signaling. Incorporation of a reversible disulfide bond should generate free CpG if the bond is reduced. This should increase the activation of the macrophages to levels comparable to free CpG. The observation that the reducible disulfide crosslinker was not able to increase the *in vitro* activation is most likely explained by the crosslinker not being biologically reduced during the timeframe of TLR9 signaling. This is in contrast to a study that linked CpG to an antibody using a disulfide linkage and found that a cleavable linker was needed for immune cell activation. It should be noted that study used a 5' conjugated CpG which is known to reduce the activation(Kandimalla, Bhagat et al., 2002), additionally, in their *in vitro* incubation experiments the media was supplemented with β-mercaptoethanol, which could have provided an artificial reductive environment.(Sharma, Dominguez et al., 2008) Whether our observation can be extended to other phagocytic cell types, or if the *in vivo* redox state is faithfully mimicked *in vitro*, remains to be seen. However, if so, it suggests that reduction would need to occur prior to internalization. The difference in activation may

well be due to a difference in the internalization mechanism between the CpG-albumin versus free CpG.

Our results are in agreement with the observation that the maleimide group is compatible with phoshpohthiote ODN.(Sanchez, Pedroso et al., 2012) The plasma half-life of CpG ODN was altered by the conjugation of a maleimide group which allowed the CpG-mal to covalently react with circulating albumin. Since the plasma clearance represents distribution rather than elimination the CpG-mal which has distributed out of the vasculature prior to albumin conjugation may still react with the interstitial albumin. After conjugation, the CpG-albumin displayed a slower plasma distribution, as would be predicted with an increase in hydrodynamic size. Also consistent with this finding is the observation that the kidney accumulation was reduced for the CpG-mal compared to CpG-COOH. The addition of the 3' amino modification and subsequent conjugation with EMCS is not expected to dramatically alter the distribution of CpG. In another study where a PS ODN was modified with a 5' octadecyl-amine moiety, the distribution and clearance was marginally altered.(Crooke, Graham et al., 1996)

Interestingly, the liver accumulation of CpG-mal was significantly increased compared to CpG-COOH. This may be due to the fact that the plasma half-life was increased, promoting more interaction with richly-perfused liver tissue. Since the liver accumulation was not rapid, it does not appear to involve high-affinity scavenger receptors that are thought to specifically bind degraded albumin.(Schnitzer and Bravo, 1993) The liver uptake is not expected to be saturated at the doses of CpG that were administered in this study.(Graham, Crooke et al., 1998) Also, the large amount of liver uptake appears to be inherent to phosphorothioate ODN as it is not seen with phosphodiester ODN.(Sands, Gorey-

Feret et al., 1994) The slight increased spleen uptake could lead to an increase in efficacy due to the high amount of antigen presenting cells in this organ. Alternatively, the increased uptake by the spleen and liver could lead to non-specific systemic immune response which may have caused the increase in toxicity observed in the 4T1 study.(Martin-Armas, Simon-Santamaria et al., 2006)

The difference in tumor accumulation was less striking than would be predicted based on the difference in plasma concentration. Again, we attribute this to the high liver clearance of the CpG-mal. Additionally, CpG-mal had a slightly increased tumor accumulation compared to CpG-COOH and it appears the tumor retention was also increased. This increase in exposure may account for the less variable response of the CpG-mal compared to CpG-COOH in the CT26 tumor model.

The efficacy of CpG therapy was found to be dependent on the tumor model. In the CT26 model tumor regression was observed, whereas no regression was seen in the 4T1 model. Since CpG is not inherently cytotoxic, the only way for there to be delayed regression in tumor volume would be if an adaptive immune response involving mostly CD8+ cytotoxic lymphocytes against the tumor was generated. The fact that there was observed regression in the CT26 model suggests a specific immune response was generated. This is supported by the finding that the CT26 model is known to be moderately immunogenic(Belnap, Cleveland et al., 1979), whereas the 4T1 model is non-immunogenic.(Pulaski and Ostrand-Rosenberg, 1998) Only studies which tested a combination of CpG with an apoptosis-inducing component were found to be successful in the 4T1 model.(Mroz, Castano et al., 2009; Shirota and Klinman, 2011) Clearly the need for

tumor-associated antigens is critical for CpG therapy, as well as for all adjuvant immunotherapies in general.

It has been reported that tumor burden when CpG therapy is initiated determines the efficacy, with small tumors showing a better response.(Heckelsmiller, Rall et al., 2002; Sharma, Karakousis et al., 2004) The tumor size in the current study was intermediate compared to these previous studies but there was no correlation in the current study between the initial size at treatment and the non-responders. Unexpectedly, CpG-COOH was also found to be efficacious when administered systemically. This may be explained by the dosing schedule used in the current study, administering the maximally-tolerated dose. Alternatively, this may be due to the differences in the activation of immune cells by CpG-COOH versus CpG. It is also interesting to note the difference in individual tumor growth patterns. For the CpG-COOH, it appears the tumors had more variability in growth during treatment, whereas the CpG-mal had reliably more controlled growth. This suggests there is a difference in the immediate cytokine release and NK cell activation. Minimizing the tumor growth during treatment is clinically important especially if the comorbidities are associated with the tumor size.

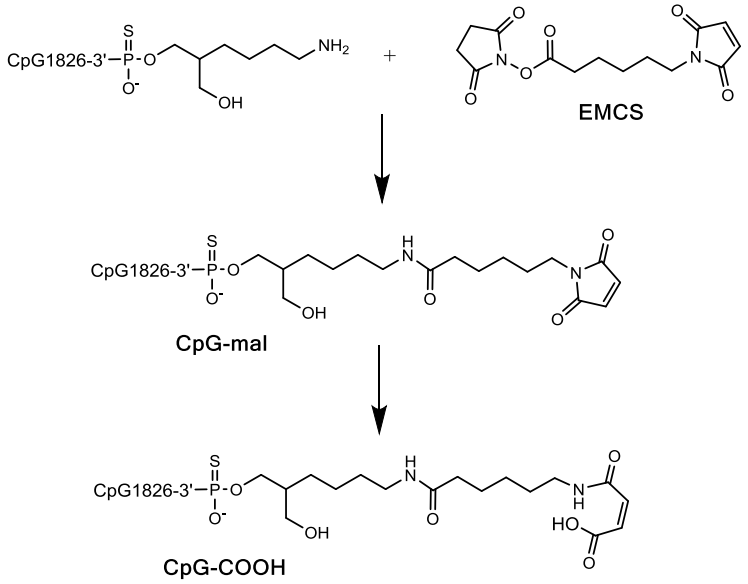

Figure 4.1. Chemical structures and synthetic scheme for the synthesis of CpG-mal and CpG-COOH.

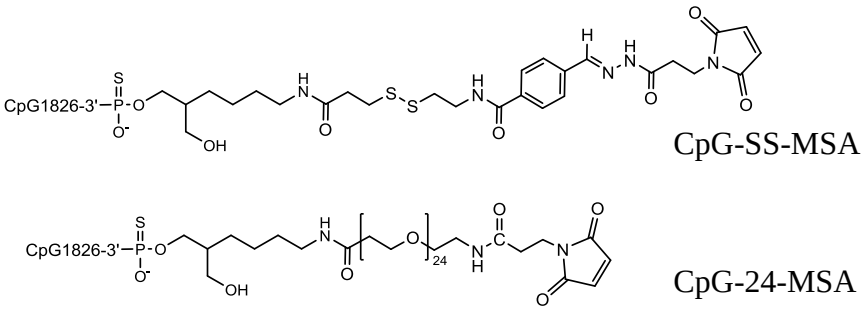

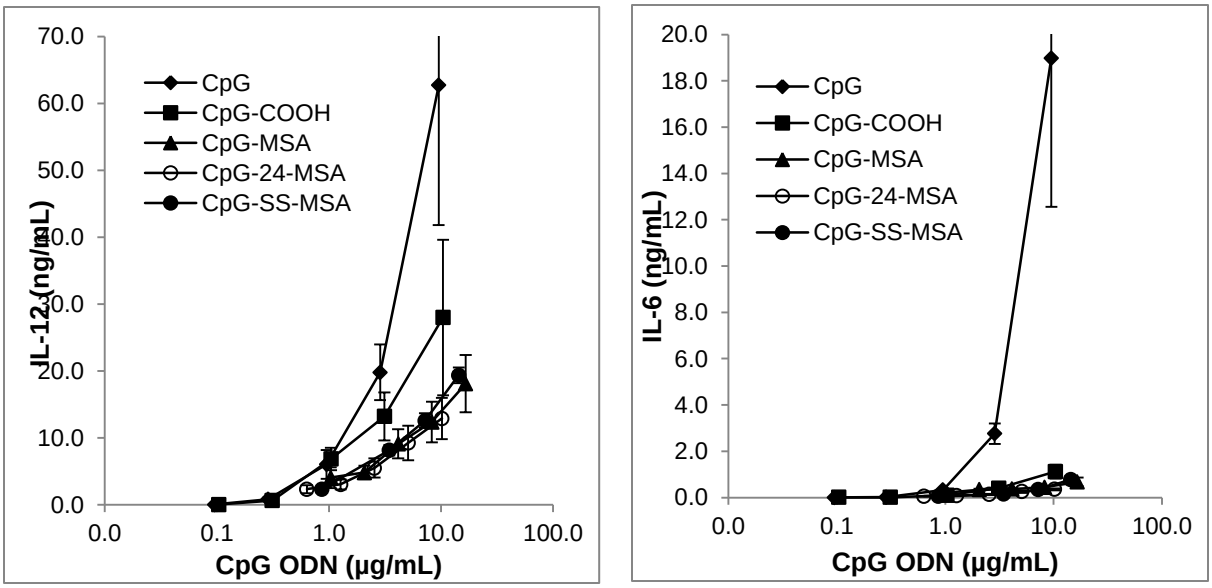

Figure 4.2. *In vitro* IL-12 and IL-6 release from CpG-albumin conjugates.The chemical structures of the different CpG-mal to prepare CpG-albumin conjugates are shown. It does not appear that the activtion of the macrophages is sensitive to the crosslinker.

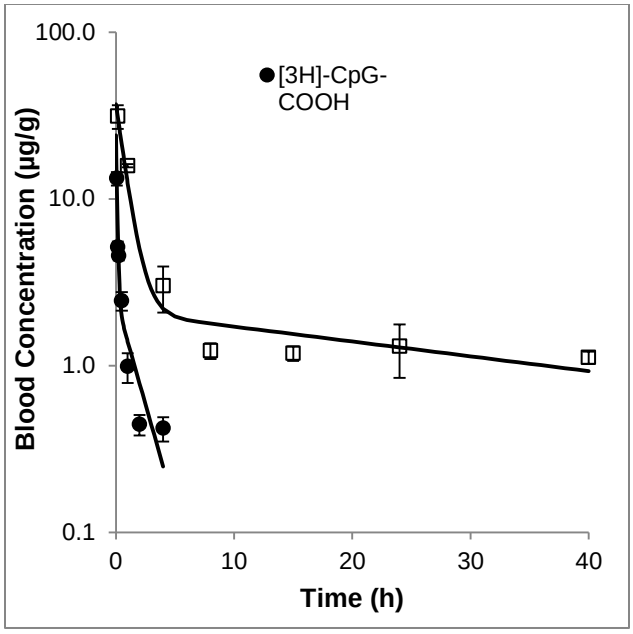

Figure 4.3. Blood concentration of [^{3}H]-CpG. The CpG-mal exhibits much less initial distribution than CpG-COOH. The lines represent the 2-compartment model parameters in **Table 4-1** fit to the data. For each timepoint 3 mice were sacrificed. The error bars represent the standard deviation.

Table 4-1. Two-compartment model parameters for [^{3}H]-labeled CpG.

	V_1 (mL)	k_{10} (h^{-1})	k_{12} (h^{-1})	k_{21} (h^{-1})
[^{3}H]-CpG-COOH	3.8 ± 1.4	4.0 ± 1.5	5.6 ± 1.0	1.5 ± 0.8
[^{3}H]-CpG-mal	2.7 ± 0.3	0.3 ± 0.02	0.9 ± 0.2	0.08 ± 0.04

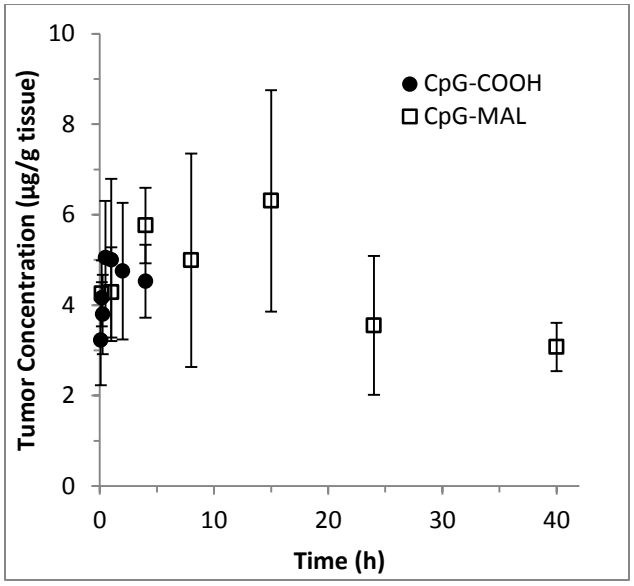

Figure 4.4. Tumor accumulation of PS [^{3}H]-CpG. The tumor accumulation appears to quickly saturate for both treatments. There is a clear downward trend for CpG-COOH between 1-4 h whereas, the CpG-mal is increasing during this time. . For each timepoint 3 mice were sacrificed. The error bars represent the standard deviation.

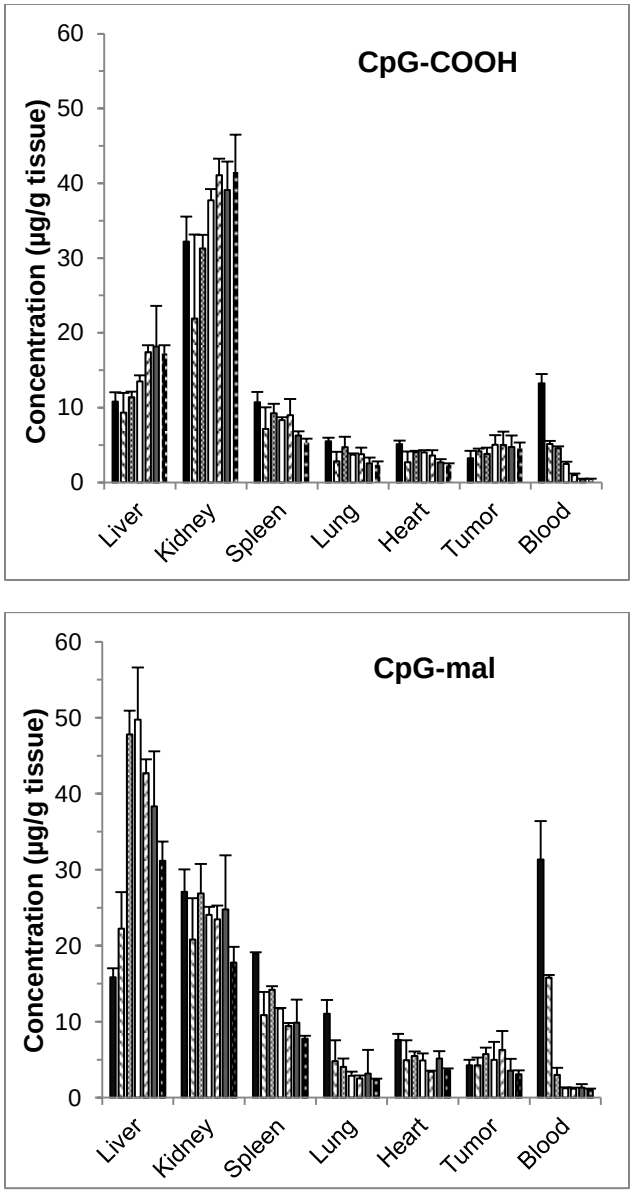

Figure 4.5. Biodistribution of [^{3}H]-labeled CpG. For the CpG-COOH, each bar represents data from each of the following timepoints: 5, 10, 15, 30, 60, 120, 240 min. For CpG-mal, each bar represents data for the following timepoints: 10 min, 1, 4, 8, 15, 24, 40 h. Each timepoint is the average concentration calculated from 3 mice and the error bars represent the standard deviation.

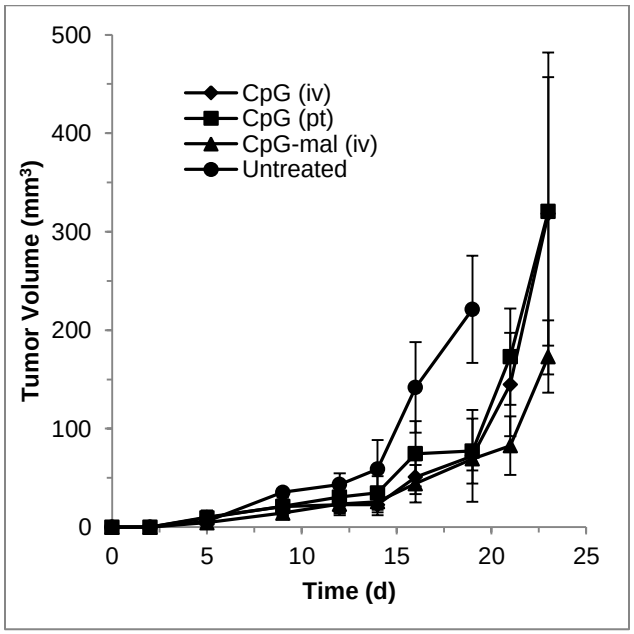

Figure 4.6. Tumor growth inhibition of 4T1 tumors. The growth appears to be slowed during treatment but promptly resumes after the last dose. N=4 for CpG (iv); N=10 for CpG (pt); N=3 for CpG-mal (iv); and N = 7 for untreated. Severe toxicity was observed in this model for both systemically injected treatments.

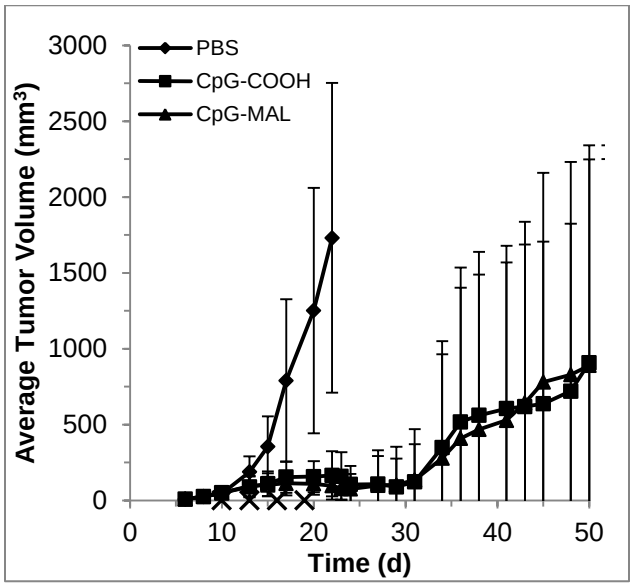

Figure 4.7. CT26 tumor growth curves. Both CpG-COOH and CpG-mal caused marked tumor growth reduction compared to PBS. Four total treatments were given starting day 10 every 3 days.

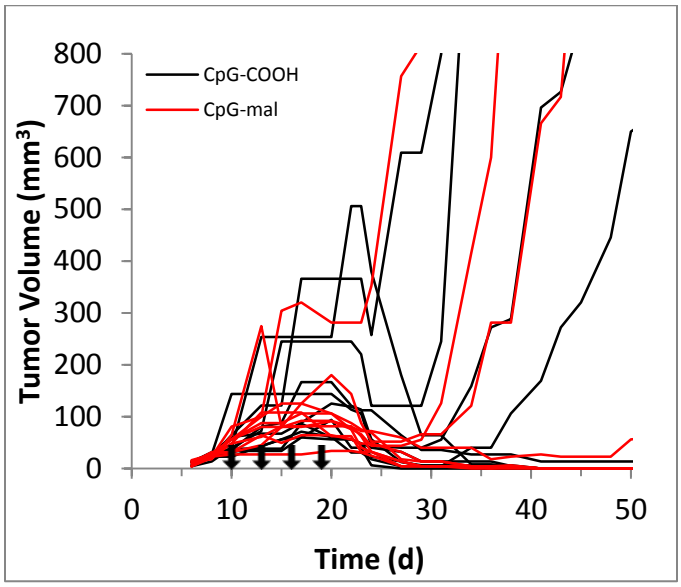

Figure 4.8. Individual growth curves for CT26 tumors. There were clear responders and non-responders to both treatments. The CpG-mal has less variability in growth during treatment. The arrows represent treatments.

REFERENCES

Ballas, Z. K. (2007). "Modulation of NK cell activity by CpG oligodeoxynucleotides." Immunol Res **39**(1-3): 15-21.

Belnap, L. P., P. H. Cleveland, M. E. Colmerauer, R. M. Barone and Y. H. Pilch (1979). "Immunogenicity of chemically induced murine colon cancers." Cancer Res **39**(4): 1174-1179.

Beltinger, C., H. Saragovi, R. Smith, L. LeSauteur, N. Shah, L. DeDionisio, L. Christensen, A. Raible, L. Jarett and A. Gewirtz (1995). "Binding, uptake, and intracellular trafficking of phosphorothioate-modified oligodeoxynucleotides." Journal of Clinical Investigation **95**(4): 1814.

Buhtoiarov, I. N., P. M. Sondel, J. C. Eickhoff and A. L. Rakhmilevich (2007). "Macrophages are essential for antitumour effects against weakly immunogenic murine tumours induced by class B CpG-oligodeoxynucleotides." Immunology **120**(3): 412-423.

Chang, Y.-H. (1969). "Studies on phagocytosis: I. Uptake of radio-iodinated (131I) human serum albumin as a measure of the degree of phagocytosis in vitro." Exp Cell Res **54**(1): 42-48.

Chauhan, V. P., T. Stylianopoulos, Y. Boucher and R. K. Jain (2011). "Delivery of molecular and nanoscale medicine to tumors: transport barriers and strategies." Annu Rev Chem Biomol Eng **2**: 281-298.

Crooke, S. T., M. J. Graham, J. E. Zuckerman, D. Brooks, B. S. Conklin, L. L. Cummins, M. J. Greig, C. J. Guinosso, D. Kornbrust, M. Manoharan, H. M. Sasmor, T. Schleich, K. L. Tivel and R. H. Griffey (1996). "Pharmacokinetic properties of several novel oligonucleotide analogs in mice." Journal of Pharmacology and Experimental Therapeutics **277**(2): 923-937.

Graham, M. J., S. T. Crooke, D. K. Monteith, S. R. Cooper, K. M. Lemonidis, K. K. Stecker, M. J. Martin and R. M. Crooke (1998). "In vivo distribution and metabolism of a phosphorothioate oligonucleotide within rat liver after intravenous administration." Journal of Pharmacology and Experimental Therapeutics **286**(1): 447-458.

Graham, M. J., S. M. Freier, R. M. Crooke, D. J. Ecker, R. N. Maslova and E. A. Lesnik (1993). "Tritium labeling of antisense oligonucleotides by exchange with tritiated water." Nucleic Acids Res **21**(16): 3737-3743.

Heckelsmiller, K., K. Rall, S. Beck, A. Schlamp, J. Seiderer, B. Jahrsdorfer, A. Krug, S. Rothenfusser, S. Endres and G. Hartmann (2002). "Peritumoral CpG DNA elicits a coordinated response of CD8 T cells and innate effectors to cure established tumors in a murine colon carcinoma model." J Immunol **169**(7): 3892-3899.

Kandimalla, E. R., L. Bhagat, D. Yu, Y. Cong, J. Tang and S. Agrawal (2002). "Conjugation of ligands at the 5'-end of CpG DNA affects immunostimulatory activity." Bioconjug Chem **13**(5): 966-974.

Krieg, A. M., A. K. Yi, S. Matson, T. J. Waldschmidt, G. A. Bishop, R. Teasdale, G. A. Koretzky and D. M. Klinman (1995). "CpG motifs in bacterial DNA trigger direct B-cell activation." Nature **374**(6522): 546-549.

Martin-Armas, M., J. Simon-Santamaria, I. Pettersen, U. Moens, B. Smedsrod and B. Sveinbjornsson (2006). "Toll-like receptor 9 (TLR9) is present in murine liver sinusoidal endothelial cells (LSECs) and mediates the effect of CpG-oligonucleotides." J Hepatol **44**(5): 939-946.

Mroz, P., A. P. Castano and M. R. Hamblin (2009). "Stimulation of dendritic cells enhances immune response after photodynamic therapy." 717803-717803.

Nierkens, S., M. H. den Brok, T. Roelofsen, J. A. Wagenaars, C. G. Figdor, T. J. Ruers and G. J. Adema (2009). "Route of administration of the TLR9 agonist CpG critically determines the efficacy of cancer immunotherapy in mice." PLoS One **4**(12): e8368.

Palma, E. and M. J. Cho (2007). "Improved systemic pharmacokinetics, biodistribution, and antitumor activity of CpG oligodeoxynucleotides complexed to endogenous antibodies in vivo." J Control Release **120**(1-2): 95-103.

Pulaski, B. A. and S. Ostrand-Rosenberg (1998). "Reduction of established spontaneous mammary carcinoma metastases following immunotherapy with major histocompatibility complex class II and B7.1 cell-based tumor vaccines." Cancer Res **58**(7): 1486-1493.

Sanchez, A., E. Pedroso and A. Grandas (2012). "Conjugation reactions involving maleimides and phosphorothioate oligonucleotides." Bioconjug Chem **23**(2): 300-307.

Sands, H., L. J. Gorey-Feret, A. J. Cocuzza, F. W. Hobbs, D. Chidester and G. L. Trainor (1994). "Biodistribution and metabolism of internally 3H-labeled oligonucleotides. I. Comparison of a phosphodiester and a phosphorothioate." Mol Pharmacol **45**(5): 932-943.

Schnitzer, J. E. and J. Bravo (1993). "High affinity binding, endocytosis, and degradation of conformationally modified albumins. Potential role of gp30 and gp18 as novel scavenger receptors." J Biol Chem **268**(10): 7562-7570.

Sharma, S., A. L. Dominguez, S. Z. Manrique, F. Cavallo, S. Sakaguchi and J. Lustgarten (2008). "Systemic targeting of CpG-ODN to the tumor microenvironment with anti-neu-CpG hybrid molecule and T regulatory cell depletion induces memory responses in BALB-neuT tolerant mice." Cancer Res **68**(18): 7530-7540.

Sharma, S., C. P. Karakousis, H. Takita, K. Shin and S. P. Brooks (2004). "Cytokines and chemokines are expressed at different levels in small and large murine colon-26 tumors following intratumoral injections of CpG ODN." Neoplasia **6**(5): 523-528.

Shirota, H. and D. M. Klinman (2011). "CpG-conjugated apoptotic tumor cells elicit potent tumor-specific immunity." Cancer Immunol Immunother **60**(5): 659-669.

CHAPTER V: CONCLUSIONS & FUTURE DIRECTION

The goal of this dissertation was to determine if serum albumin had potential utility as a carrier of CpG for cancer therapy. The collective results support the notion that albumin may have a utility, albeit limited, in this narrowly-defined scope.

CpG oligodeoxynucleotide (ODN) was modified with maleimide groups to allow an *in situ* reaction with Cys_{34} of serum albumin. For phosphodiester (PO) CpG, PET/CT imaging was used to determine the pharmacokinetics and biodistribution (PK/BD) of ^{124}I-labeled CpG-mal. The *in situ* reaction with albumin was determined to be complete within minutes and was sufficient to compete with the rapid plasma clearance *in vivo*. The plasma half-life and tumor accumulation were increased compared to control CpG-COOH that is unable to react with albumin. Despite this increase in tumor exposure, the PO CpG-mal was not efficacious in the 4T1 cancer model at inhibiting tumor growth, increasing survival, or decreasing the number of lung metastasis. Subsequent *in vitro* activation of macrophages indicated that PO CpG is not a potent agonist of TLR9 which was attributed instability to endogenous nucleases. Since the amount of cellular uptake was not directly measured in the *in vitro* experiments it is unknown if a difference in uptake could account for the reduction in cytokine release. Further experiments should be done to elucidate if any differences in *in vitro* uptake is observed.

In contrast to PO CpG, the PS CpG was able to significantly increase the TLR9 activation and subsequent release of IL-6 and IL-12 *in vitro*. Conjugation of the PS CpG to albumin reduced, but did not abolish, the activation. The reduction in activation is not believed to be caused by steric hindrance of albumin because increasing the crosslinker length did not increase the activation. Additionally, adding a reducible disulfide linker did not increase the activation, which suggests biological reduction did not happen within the timeframe of TLR9 signaling. This may support the notion that endosomes are not sufficiently reductive environments for reducing disulfide bonds.

Tumor growth inhibition studies using the 4T1 model and PS CpG showed a slowing of tumor growth during treatment, but after treatment was stopped the tumor growth resumed. Additionally, severe toxicity was seen in this aggressive model which was attributed to an additive effect of the metastatic spread and the induced inflammatory response. The lack of efficacy in this model was attributed to the lack of shedding of tumor antigens as the 4T1 is known to be inherently non-immunogenic.(Pulaski and Ostrand-Rosenberg, 1998)

The physicochemical properties of PS CpG are different than PO CpG and extrapolation of the PK/BD results for the PO CpG to PS CpG is tenuous. Attempts to radiolabel the PS CpG with ^{124}I were not successful, therefore a tritium label was used to monitor the PK/BD of PS [^{3}H]-CpG-mal. The plasma half-life of the PS CpG-mal was increased compared to control CpG, but the increase was not as striking as for PO CpG. This is due to the high liver accumulation of PS CpG-mal which was not observed for PO CpG-mal. The accumulation in the liver was not immediate, but sustained, and reached approximately 50 µg/g tissue at 4 h. This rules out high-affinity scavenger receptors which

quickly remove highly modified albumin, but it may indicate low-affinity scavenger receptors that can remove partially-modified albumin.(Stehle, Sinn et al., 1997) In support of this is the fact that highly anionic substrates are usually taken up by scavenger receptors located on macrophages and liver sinusoidal endothelial cells.(Yamasaki, Hisazumi et al., 2003) Conjugation of the CpG to albumin is expected to roughly double the amount of negative charge, rendering the conjugate a better substrate for these receptors. Although, conjugation of PO CpG is expected to also increase the negative charge.

Unfortunately, this high liver accumulation reduces the tumor exposure. Future studies should investigate the nature of this uptake. Is it due to receptors specific for PS ODN, or is it due to albumin scavenger receptors recognizing the PS CpG-albumin conjugate as degraded albumin? This could be tested by adding a competitor of these receptors and seeing if the uptake is reduced. However, both receptors share an overlap in inhibitors, so a specific inhibitor without a monoclonal antibody would be difficult to employ. Even so, knowing the mechanism of liver uptake does not materially change the fact that it happens and it is a significant limitation for the therapeutic potential of PS CpG. If the uptake is determined to be caused by receptors recognizing the PS CpG, then reducing the length of the CpG may reduce the affinity towards these receptors, although this may also reduce the TLR9 affinity as well. Another option is to use chimeric CpG which contains both PS and PO backbone which should reduce the non-specific interactions caused by the PS. But this also may have nuclease instability due to the presence of endonucleases that can cleave the PO bonds.(Boado, Kang et al., 1995) It may also be possible for future CpG chimeras that have other backbone modifications to be used as well.

Interestingly, the tumor appears to quickly accumulate PS CpG, which may be due to some type of binding process to cellular targets.(Beltinger, Saragovi et al., 1995) The tumor concentration for CpG-mal also quickly reaches close to maximal level, but still shows an increase in tumor accumulation with time. This increase stems from the increased half-life of the CpG-albumin conjugate in the circulation. In both biodistribution experiments the tumor concentration reached a maximal value of approximately 3-6 %ID/g tissue. Since the average mice body weight used in the studies was approximately 18-20 g, it appears that on a per-weight basis selective accumulation in the tumor was minimal.

The antitumor effects of CpG-mal and CpG-COOH were clearly observed in the CT26 colon cancer model. Both treatments showed a remarkable reduction in growth rate during treatment, and between 6-10 days after the first treatment the tumors began to regress. This timeline is consistent with the expected activation and infiltration of CD8+ T cells. Examination of the individual tumor growth curves suggest 6/10 mice had full regression of the tumors while the others had stasis or partial regression following by rapid regrowth of the tumors suggesting a lack of an adaptive immune response. These results are typical of nearly all immunotherapies and were even observed in Dr. Coley's initial experiments.

The increased retention by the tumor of CpG-mal compared to CpG-COOH suggests that decreasing the dose or dosing frequency may magnify the difference in the efficacy between the two treatments. This could be tested in future dose-response studies, where a clinical response may still be observed with less frequent or lower dose injections for CpG-mal but not CpG-COOH.

The immune response in the tumor microenvironment is delicate and sometimes activation of the immune system can increase the growth rate of tumors and increase the chance of metastasis.(DeNardo, Barreto et al., 2009) Therefore, the manner in which the immune system is manipulated in the tumor microevironment is critically important. The fact that we noticed different cytokine release patterns for CpG-albumin compared to free CpG could have a dramatic effect on the nature of the local immune response. This is indicated by the more controlled growth observed in **Figure 4.8**. In future studies, a wider variety of cytokines could be measured to determine the differences in activation between the CpG-albumin and free CpG.

The tumor growth inhibition assay, while clinically important, is a crude measure of efficacy. Cellular mechanistic studies should be investigated in future experiments. The most important measure of efficacy is the infiltration of tumor-specific CD8+ T cells. Flow cytometry could be performed on single cells suspensions of excised tumors to determine the percentage of CD8+ T cells in the tumor. Additionally, dendritic cells from the tumor-draining lymph nodes could be cultured and stimulated with tumor homogenates and the expression of activation markers could be quantified by flow cytometry.

Long-term toxicity was not assayed during the current studies, but it does not appear that conjugation of the CpG to albumin caused a catastrophic immune response to albumin. The fact that CpG-albumin is present in the circulation for longer times in an active form is not inherently a problem. It is known that circulating monocytes and dendritic cells have a reduced phagocytic rate compared to peripheral tissue phagocytic cells. This should reduce their uptake of the active CpG-albumin conjugate.

CpG has been conjugated to antigens in order to increase accumulation of the CpG and the antigen in the same antigen presenting cell in order to encourage cross-presentation.(Maurer, Heit et al., 2002) In our case though, albumin is not an antigen and an immune response to albumin would be highly undesirable. Many studies have synthesized albumin fusion proteins with various cytokines and have not seen deleterious immune responses against albumin in preclinical settings; their clinical safety is under investigation.(Chang, Gupta et al., 2009) Conceptually, it is more probable that if an immune response were to be generated it would be against the crosslinker or the CpG rather than native albumin. Since the PK experiments were only determined for the first dose, the results would not be expected to be influenced by a generated immune response. In order to test this, PK after multiple dosing should be performed. If an immune response is generated against the CpG-albumin conjugate, then the clearance should be expected to be increased.

Since maleimide is not selective to which thiols they react with, any exposed thiols are subject to reaction. N-ethylmaleimide (NEM) has been used to study enzyme inhibition and has been shown to be toxic.(Schoonen, De Roos et al., 2005) However, NEM is considerably smaller and more hydrophobic so it readily diffuses into cell membranes and has access intracellular proteins and enzymes with catalytic thiol residues. The CpG-mal is not expected to readily diffuse through plasma membranes and will not have access to these intracellular thiols. This restricted distribution should dramatically reduce the maleimide-related toxicity.

One potential drawback of using endogenous albumin as a carrier for anticancer drugs is that cancer patients have reduced concentrations of serum albumin. This limits the amount of carrier protein present at any given time. Additionally, during an acute immune response,

the transcription of albumin is known to be transiently reduced.(Liao, Jefferson et al., 1986) This may limit the amount of albumin available for future dosing. Nevertheless, albumin should be in a 10 fold excess compared to CpG-mal at the administered concentration.

Conjugation to albumin does not appear to abolish interaction with extracellular or endosomal targets based off the observations that CpG-albumin was degraded by plasma nucleases and able to activate macrophages by TLR9 signaling. This suggests that albumin could be used as a carrier for any therapeutic whose target is accessible to native albumin, which includes any surface, extracellular, or endosomal targets but would not include any intracellular or nuclear targets. This no doubt limits the therapeutic opportunities but still leaves significant number of targets which could be improved by albumin conjugation. In summary, the use of albumin as a carrier for CpG may be limited, but that does not rule out other potential therapeutics that could benefit from albumin conjugation.

REFERENCES

Beltinger, C., H. U. Saragovi, R. M. Smith, L. LeSauteur, N. Shah, L. DeDionisio, L. Christensen, A. Raible, L. Jarett and A. M. Gewirtz (1995). "Binding, uptake, and intracellular trafficking of phosphorothioate-modified oligodeoxynucleotides." J Clin Invest **95**(4): 1814-1823.

Boado, R. J., Y. S. Kang, D. Wu and W. M. Pardridge (1995). "Rapid plasma clearance and metabolism in vivo of a phosphorothioate oligodeoxynucleotide with a single, internal phosphodiester bond." Drug Metab Dispos **23**(11): 1297-1300.

Chang, C.-H., P. Gupta and D. M. Goldenberg (2009). "Advances and challenges in developing cytokine fusion proteins as improved therapeutics."

DeNardo, D. G., J. B. Barreto, P. Andreu, L. Vasquez, D. Tawfik, N. Kolhatkar and L. M. Coussens (2009). "CD4(+) T cells regulate pulmonary metastasis of mammary carcinomas by enhancing protumor properties of macrophages." Cancer Cell **16**(2): 91-102.

Liao, W. S., L. S. Jefferson and J. M. Taylor (1986). "Changes in plasma albumin concentration, synthesis rate, and mRNA level during acute inflammation." Am J Physiol **251**(6 Pt 1): C928-934.

Maurer, T., A. Heit, H. Hochrein, F. Ampenberger, M. O'Keeffe, S. Bauer, G. B. Lipford, R. M. Vabulas and H. Wagner (2002). "CpG-DNA aided cross-presentation of soluble antigens by dendritic cells." Eur J Immunol **32**(8): 2356-2364.

Pulaski, B. A. and S. Ostrand-Rosenberg (1998). "Reduction of established spontaneous mammary carcinoma metastases following immunotherapy with major histocompatibility complex class II and B7.1 cell-based tumor vaccines." Cancer Res **58**(7): 1486-1493.

Schoonen, W. G., J. A. De Roos, W. Westerink and E. Débiton (2005). "Cytotoxic effects of 110 reference compounds on HepG2 cells and for 60 compounds on HeLa, ECC-1 and CHO cells.: II Mechanistic assays on NAD (P) H, ATP and DNA contents." Toxicology in vitro **19**(4): 491-503.

Stehle, G., H. Sinn, A. Wunder, H. H. Schrenk, S. Schutt, W. Maier-Borst and D. L. Heene (1997). "The loading rate determines tumor targeting properties of methotrexate-albumin conjugates in rats." Anticancer Drugs **8**(7): 677-685.

Yamasaki, Y., J. Hisazumi, K. Yamaoka and Y. Takakura (2003). "Efficient scavenger receptor-mediated hepatic targeting of proteins by introduction of negative charges on the proteins by aconitylation: the influence of charge density and size of the proteins molecules." European Journal of Pharmaceutical Sciences **18**(5): 305-312.

APPENDIX A

Included in the appendix are the NMR spectra and m/s analysis for the crosslinker synthesized in Chapter II.

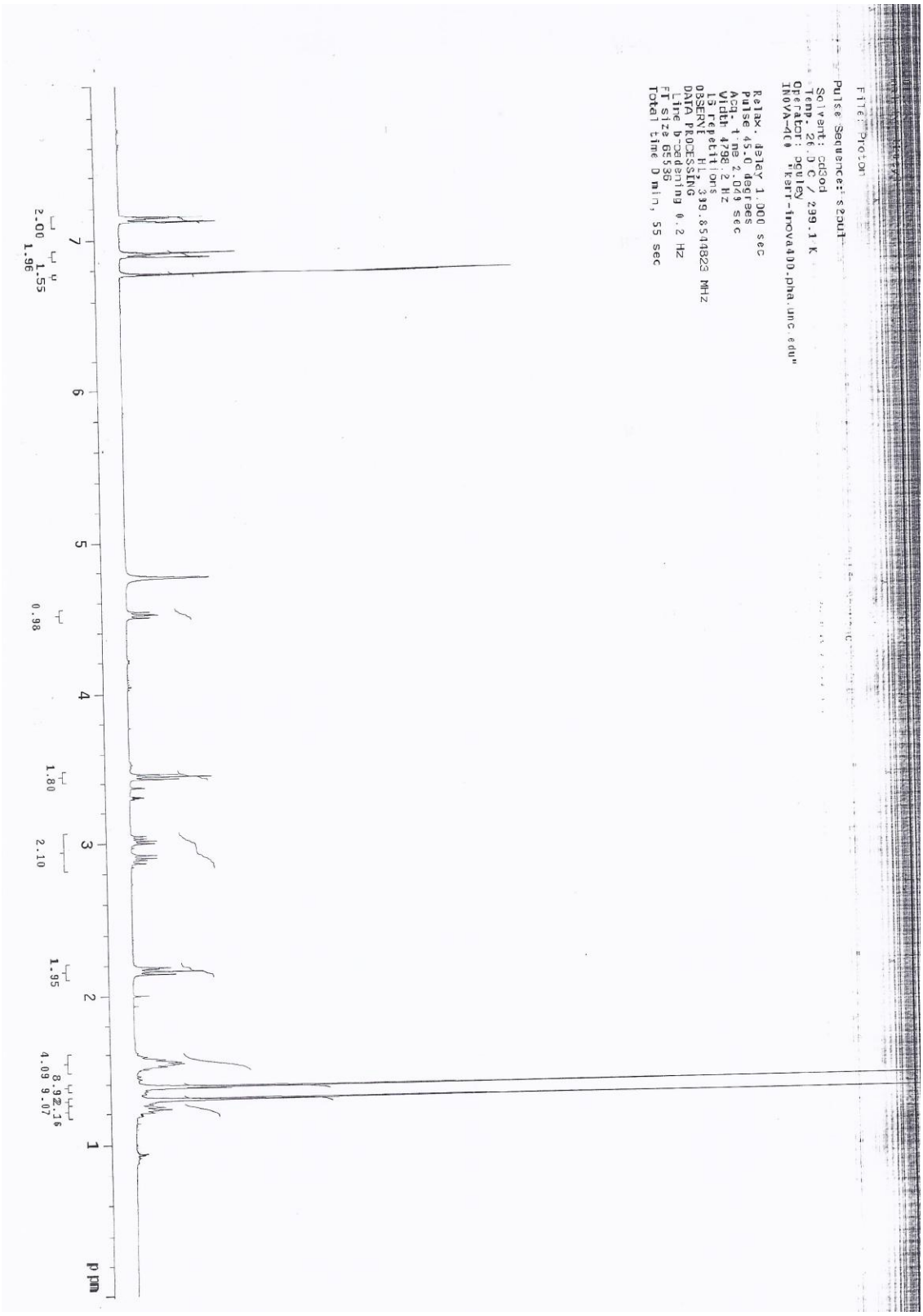

Figure A.1. ^{1}H NMR spectrum of Mal-Tyr(tBu)-OtBu (**1**)

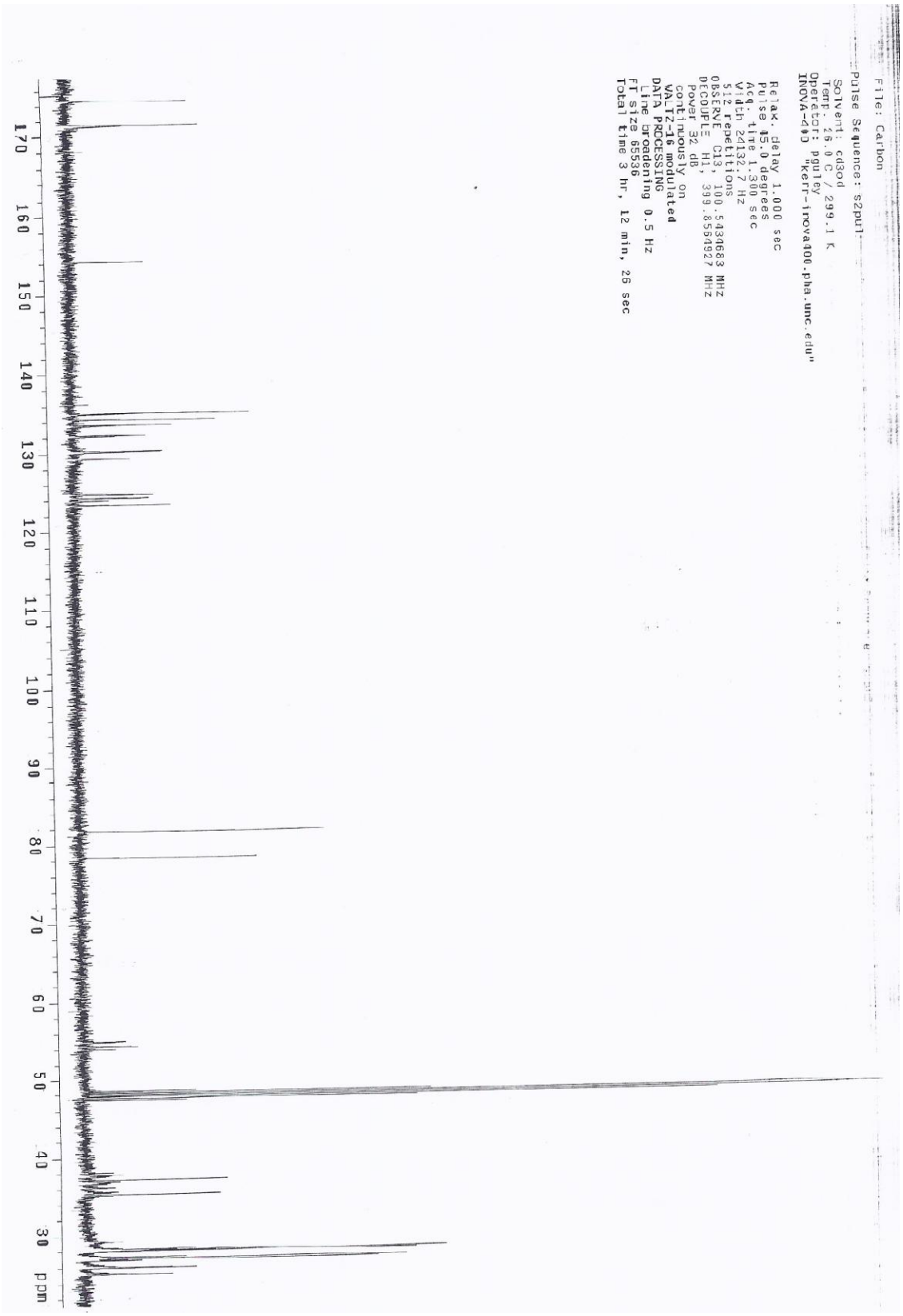

Figure A.2. ^{13}C NMR of Mal-Tyr(tBu)-OtBu **(1)**

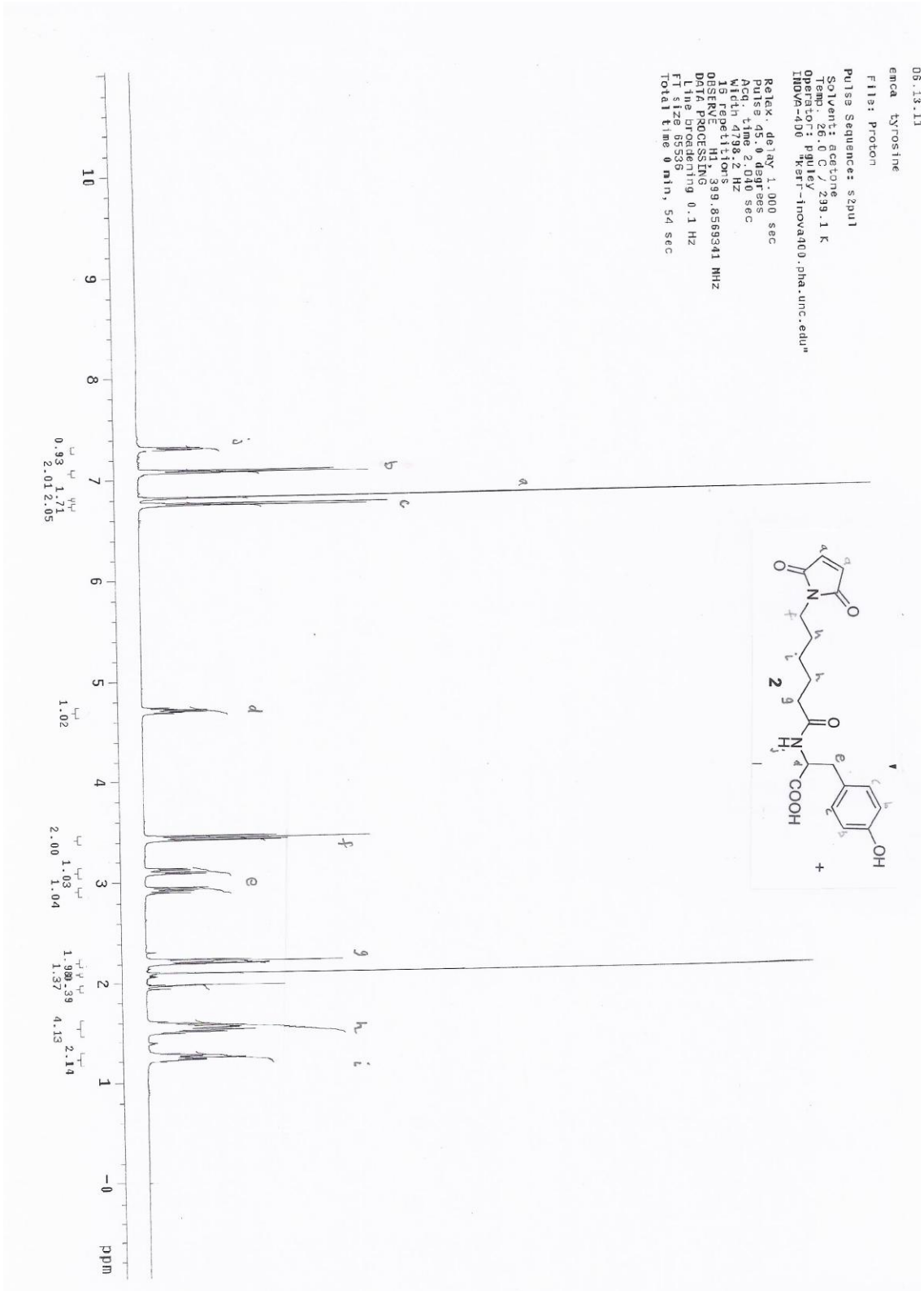

Figure A.3. ^{1}H NMR of Mal-Tyr **(2)**

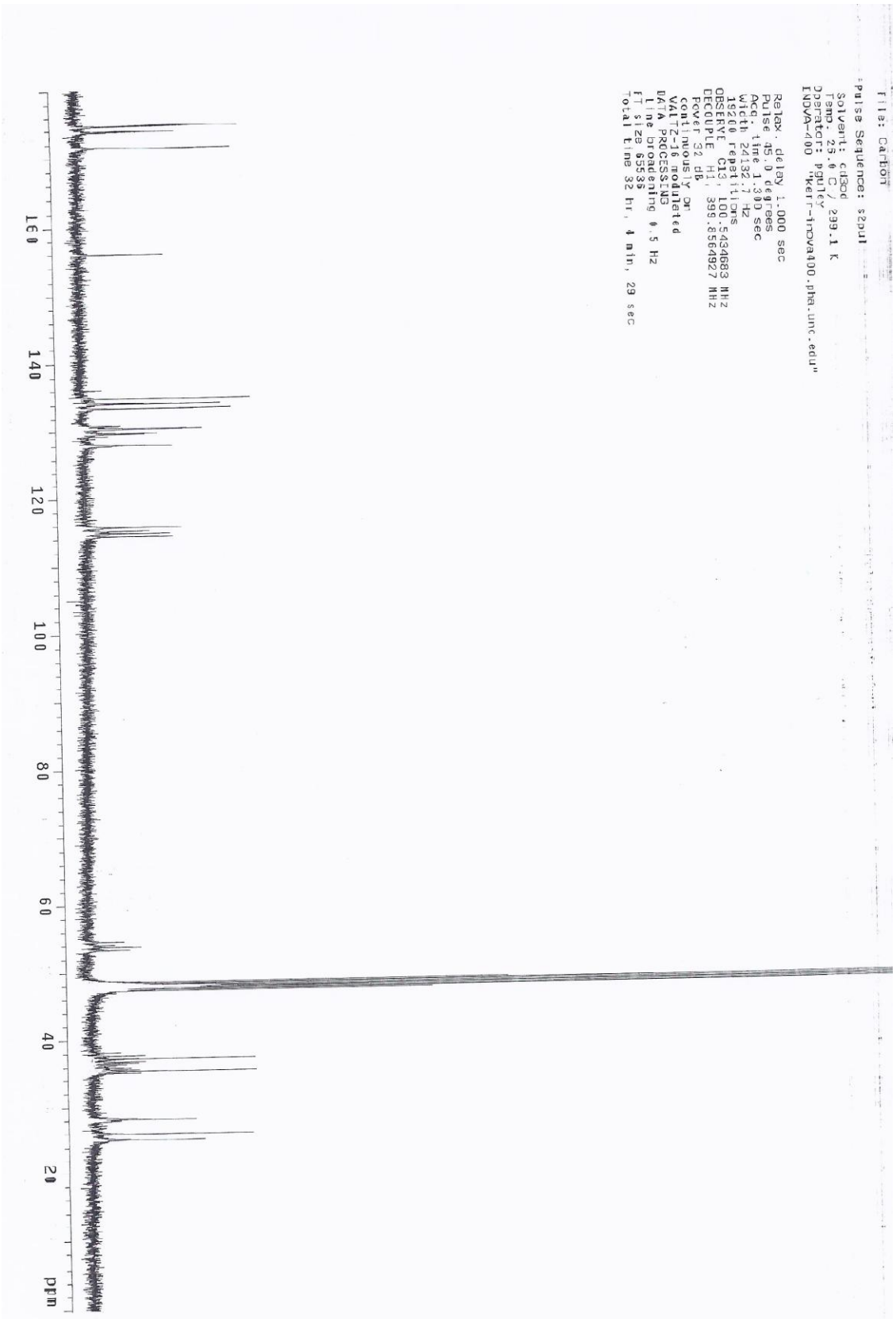

Figure A.4. ^{13}C NMR of Mal-Tyr **(2)**

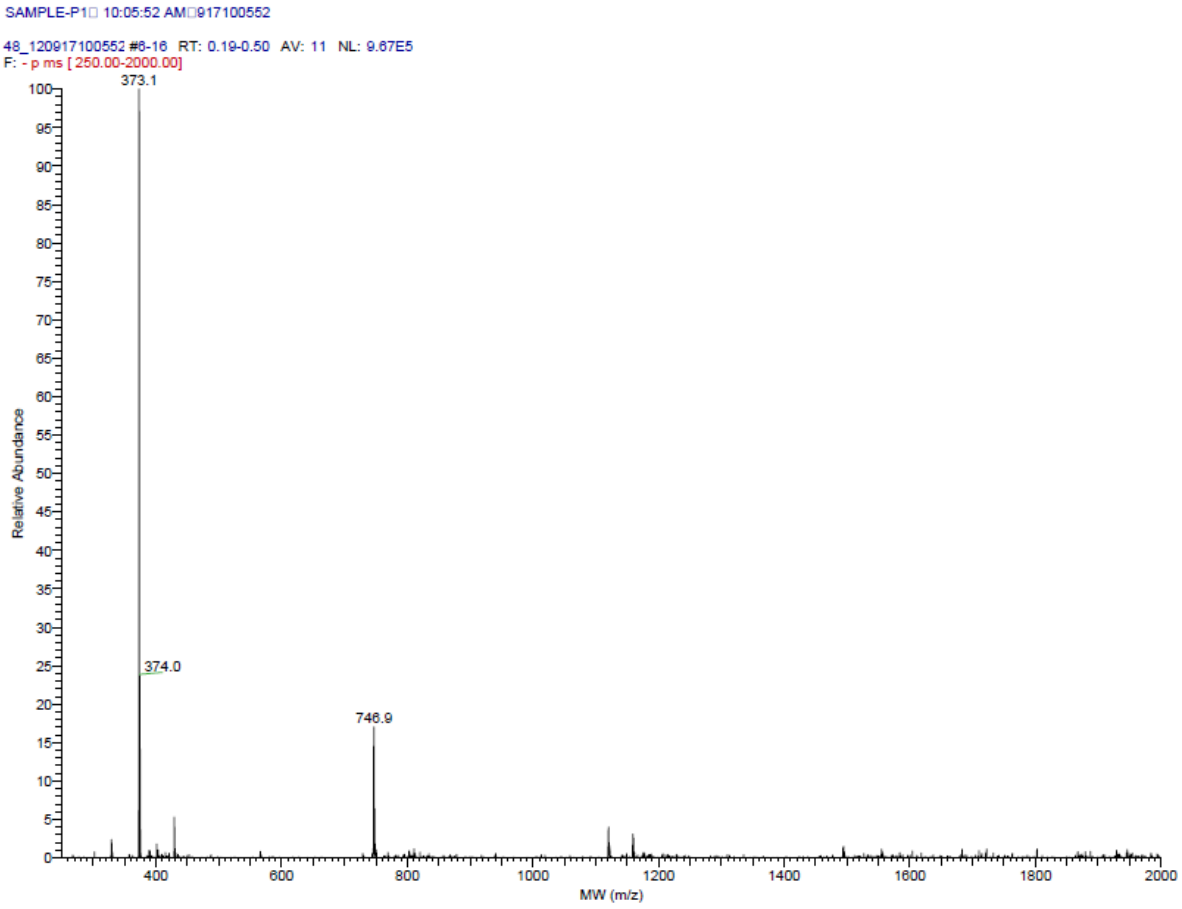

Figure A.5. Mass Spectrum of Mal-Tyr **(2)**

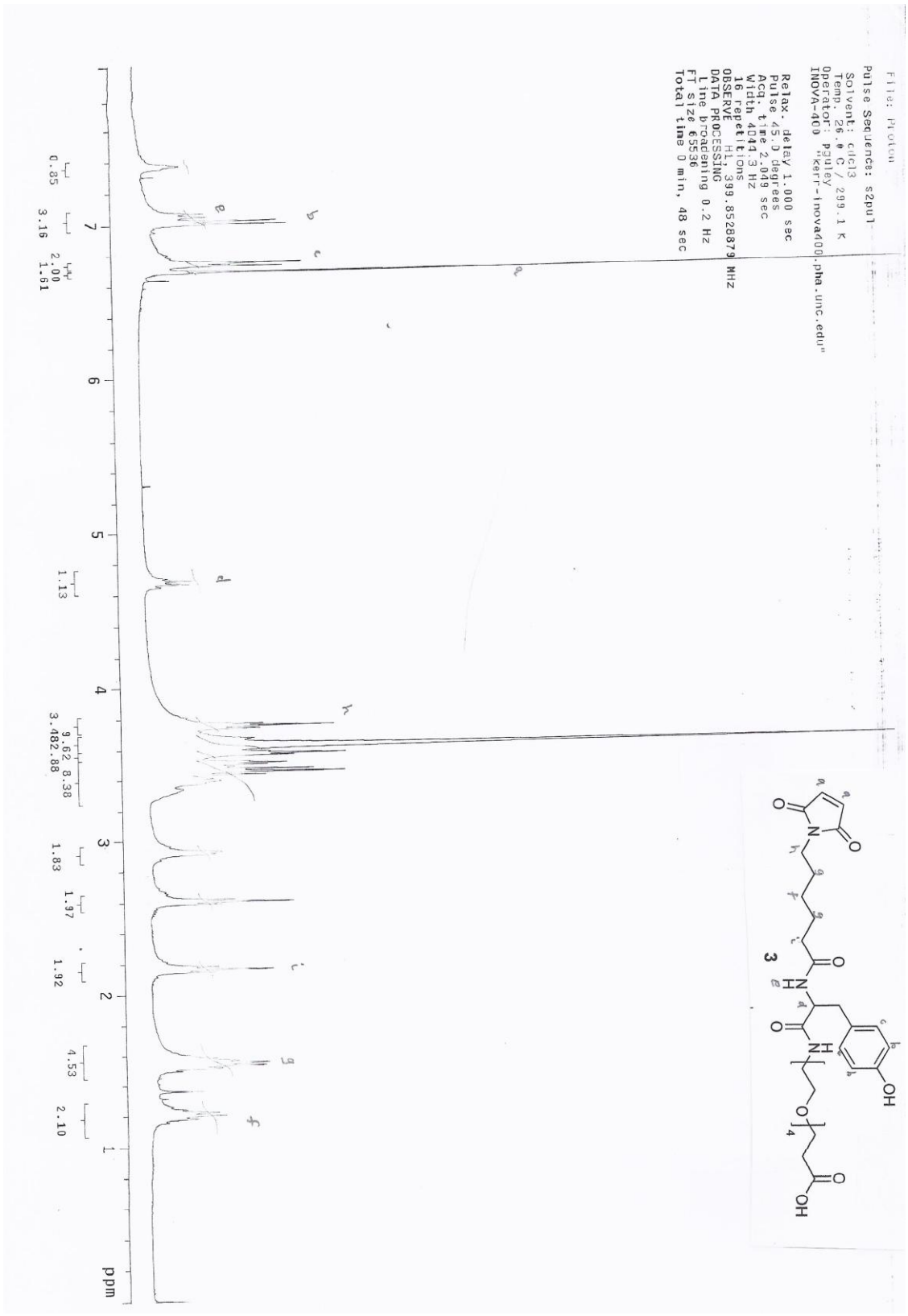

Figure A.6. ^{1}H NMR spectrum of Mal-Tyr-TEG-COOH **(3)**

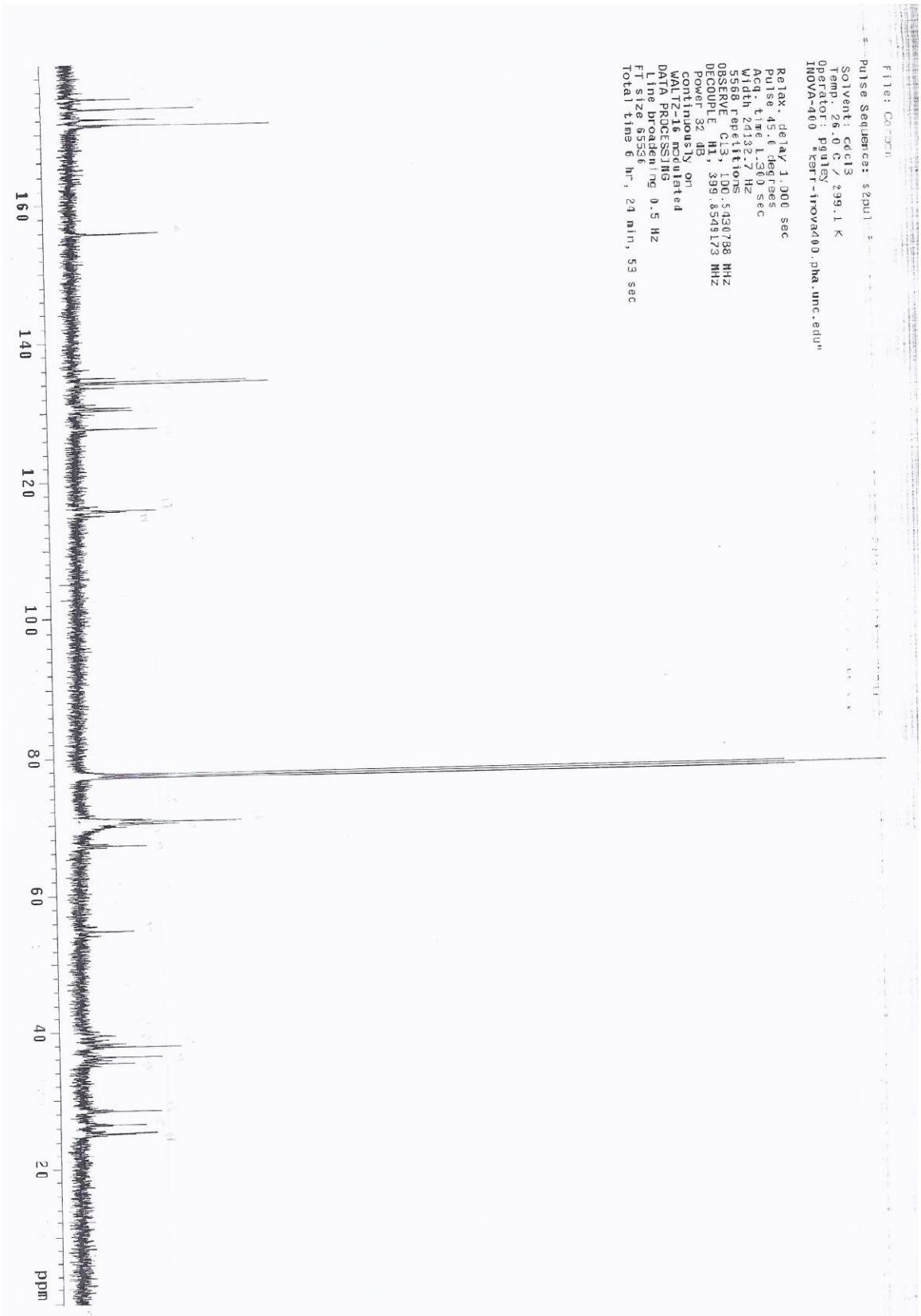

Figure A.7. ^{13}C NMR spectrum of Mal-Tyr-TEG-COOH **(3)**

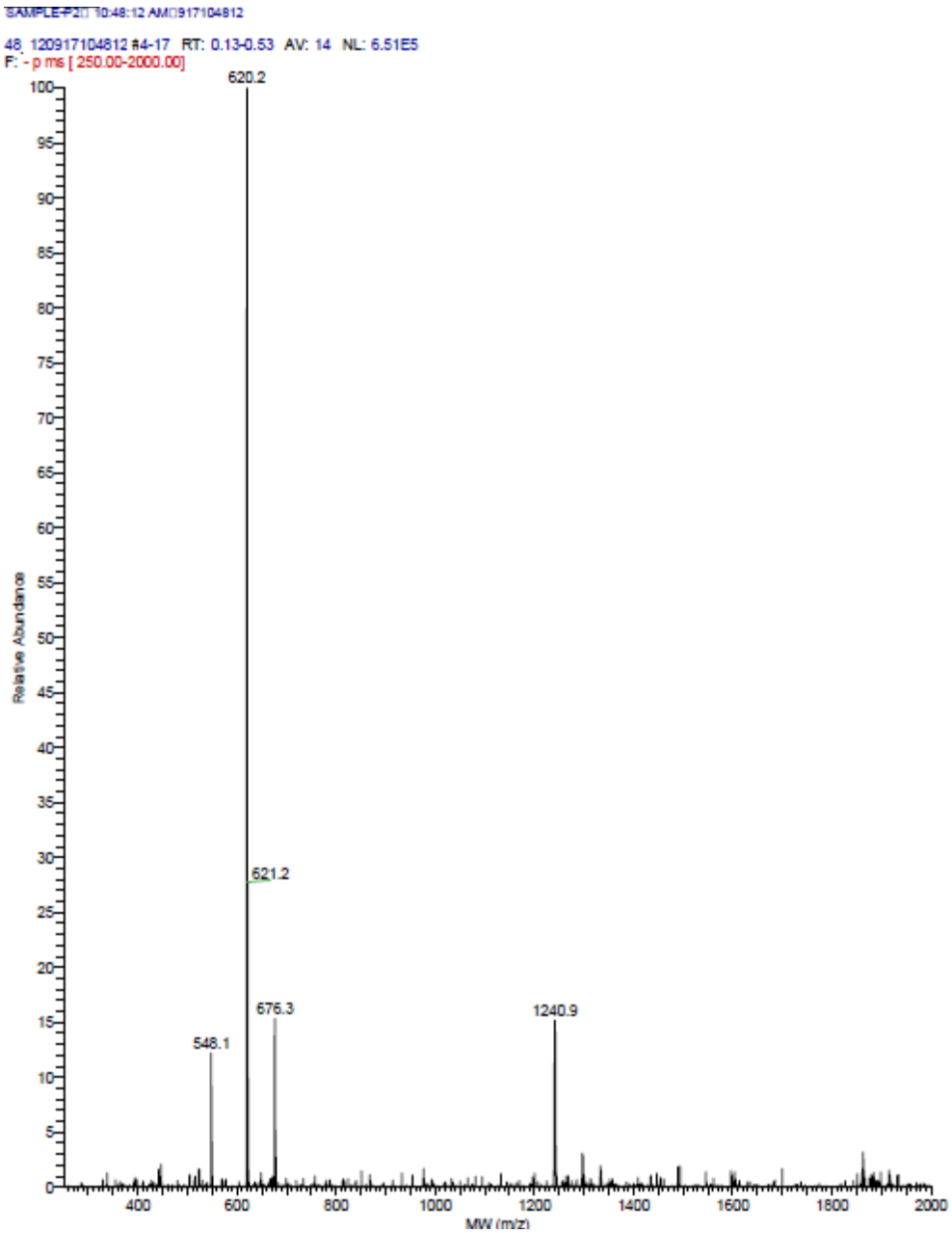

Figure A.8. Mass spectrum of Mal-Tyr-TEG-COOH **(3)**

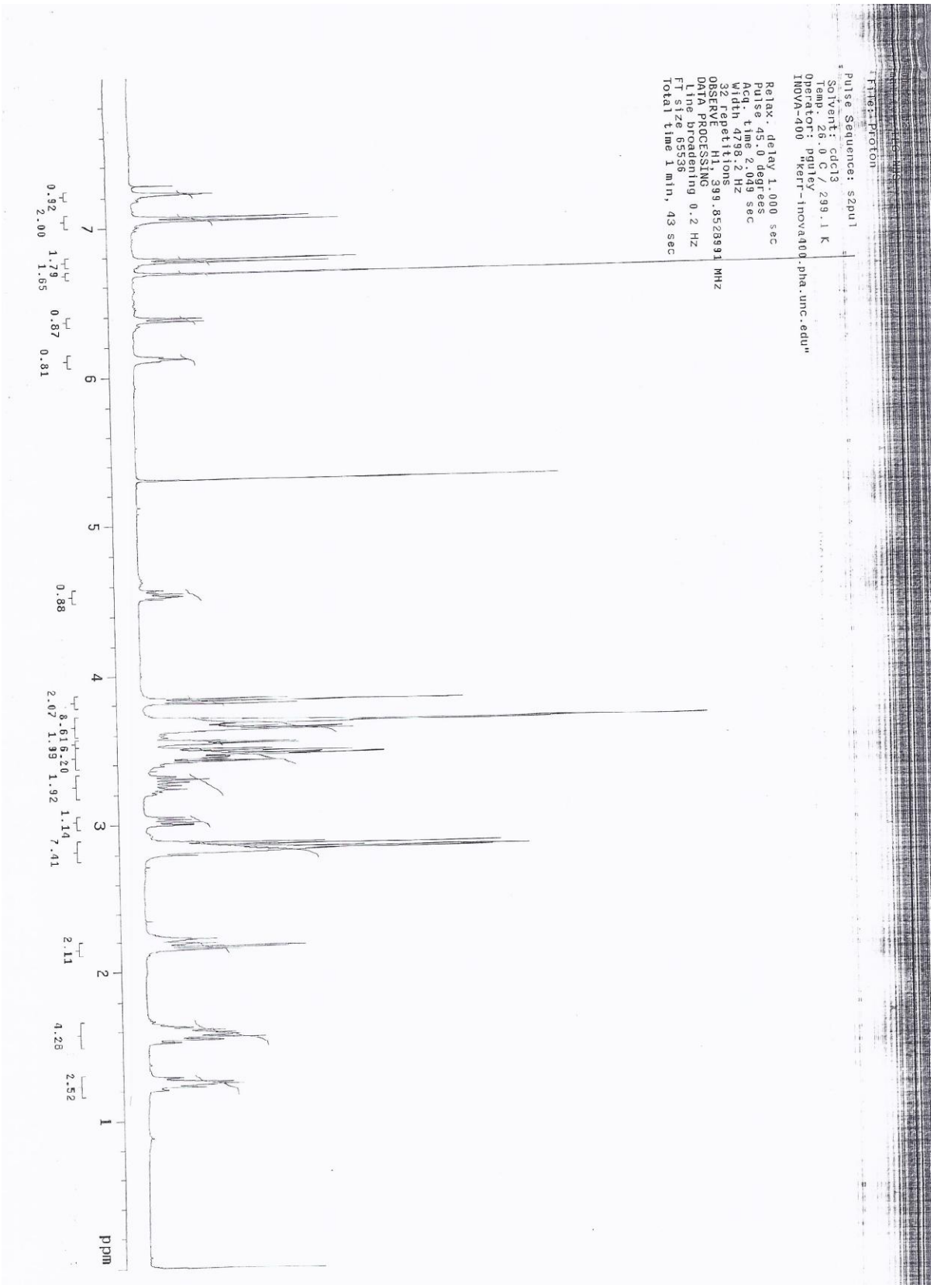

Figure A.9. ^{1}H NMR of Mal-Tyr-TEG-NHS **(4)**

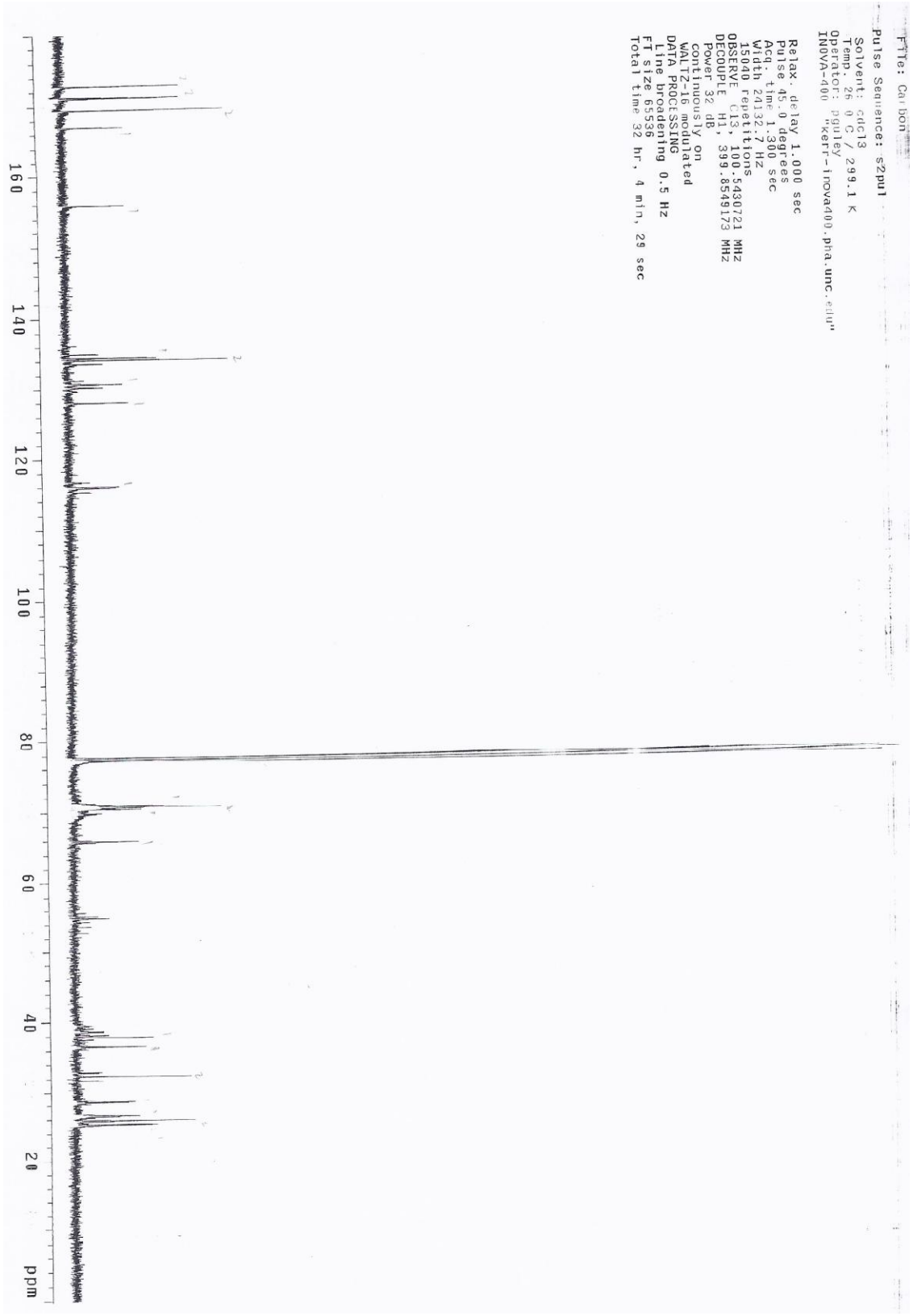

Figure A.10. ^{13}C NMR of Mal-Tyr-TEG-NHS **(4)**

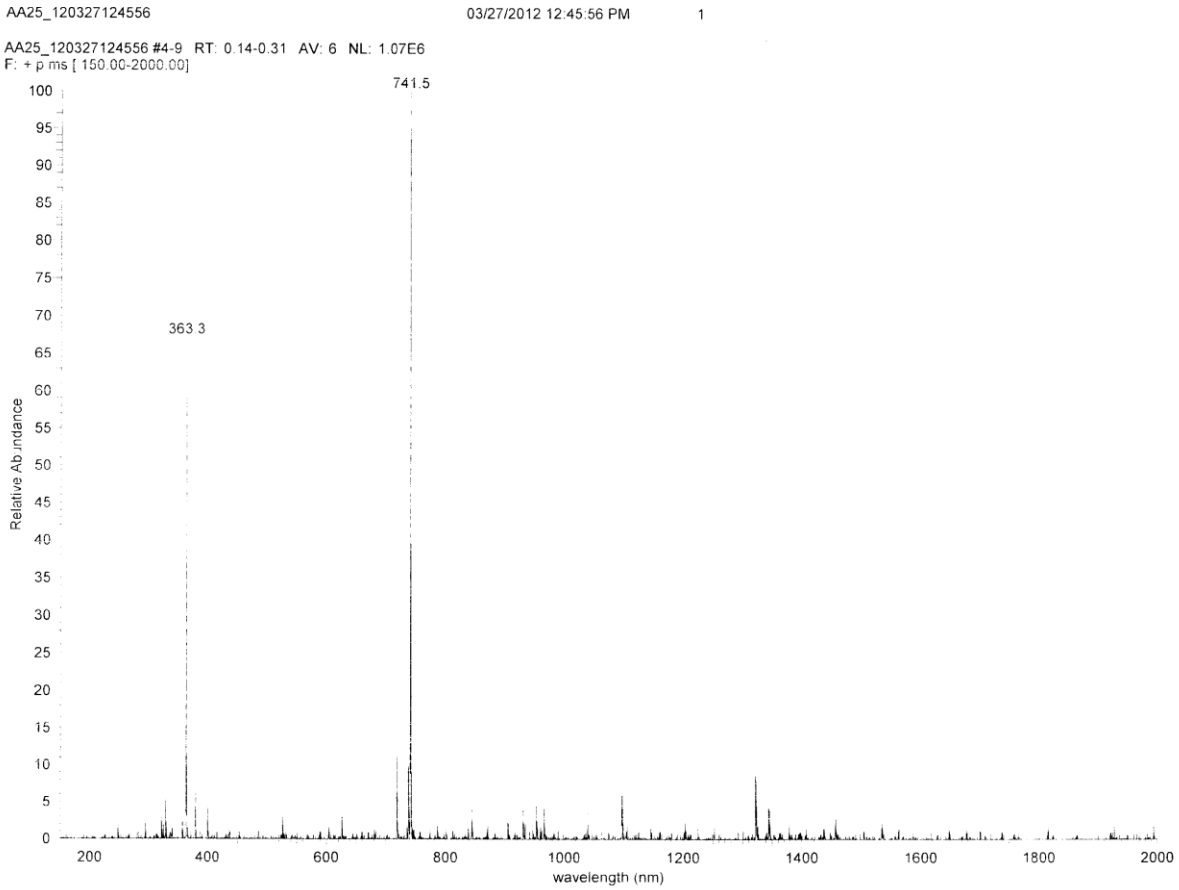

Figure A.11. Mass spectrum of Mal-Tyr-TEG-NHS **(4)**

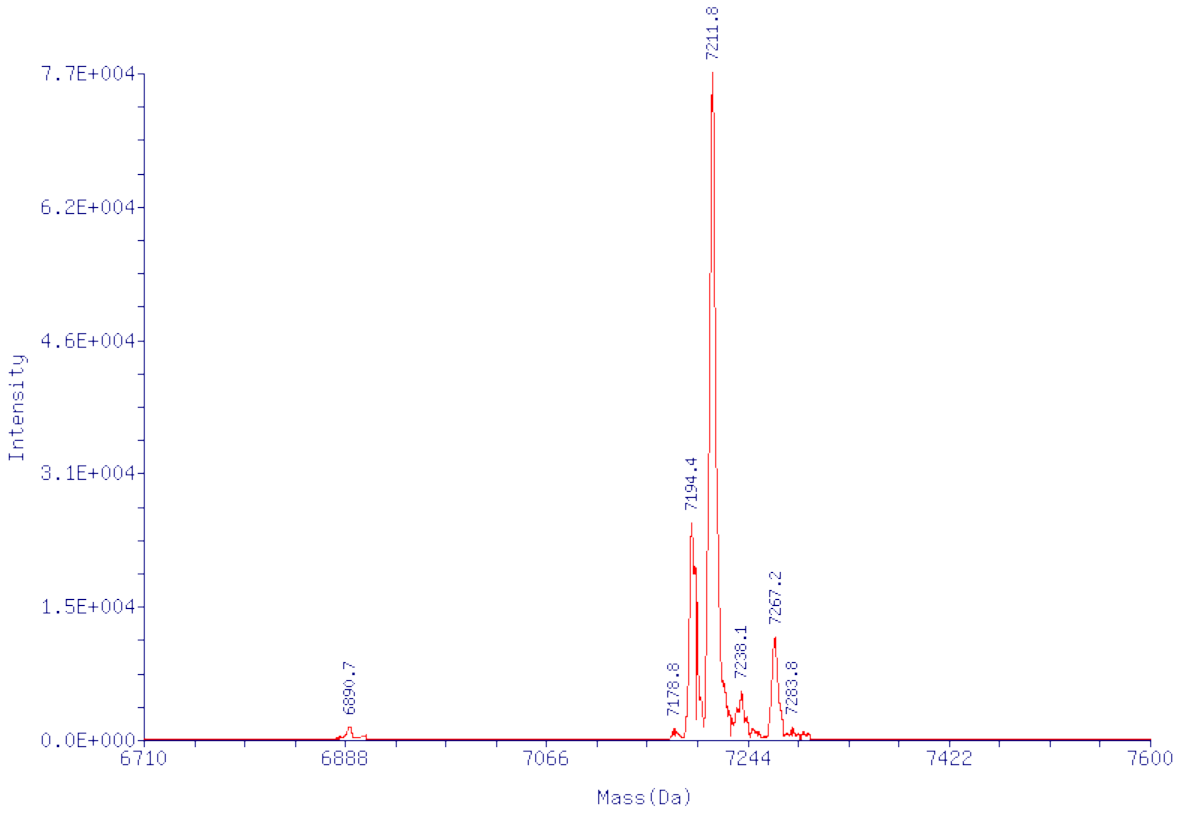

Figure A.12. Deconvoluted mass spectrum of ODN-mal.

REFERENCES

Akilesh, S., G. J. Christianson, D. C. Roopenian and A. S. Shaw (2007). "Neonatal FcR expression in bone marrow-derived cells functions to protect serum IgG from catabolism." J Immunol **179**(7): 4580-4588.

Allison, A. C. (1960). "Turnovers of erythrocytes and plasma proteins in mammals." Nature **188**: 37-40.

Andersen, J. T. and I. Sandlie (2009). "The versatile MHC class I-related FcRn protects IgG and albumin from degradation: implications for development of new diagnostics and therapeutics." Drug Metab Pharmacokinet **24**(4): 318-332.

Andersen, J. T., J. Dee Qian and I. Sandlie (2006). "The conserved histidine 166 residue of the human neonatal Fc receptor heavy chain is critical for the pH-dependent binding to albumin." Eur J Immunol **36**(11): 3044-3051.

Bading, J. R., M. Horling, L. E. Williams, D. Colcher, A. Raubitschek and S. E. Strand (2008). "Quantitative serial imaging of an 124I anti-CEA monoclonal antibody in tumor-bearing mice." Cancer Biother Radiopharm **23**(4): 399-409.

Bae, Y. H. and K. Park (2011). "Targeted drug delivery to tumors: myths, reality and possibility." J Control Release **153**(3): 198-205.

Ballas, Z. K. (2007). "Modulation of NK cell activity by CpG oligodeoxynucleotides." Immunol Res **39**(1-3): 15-21.

Belnap, L. P., P. H. Cleveland, M. E. Colmerauer, R. M. Barone and Y. H. Pilch (1979). "Immunogenicity of chemically induced murine colon cancers." Cancer Res **39**(4): 1174-1179.

Beltinger, C., H. U. Saragovi, R. M. Smith, L. LeSauteur, N. Shah, L. DeDionisio, L. Christensen, A. Raible, L. Jarett and A. M. Gewirtz (1995). "Binding, uptake, and intracellular trafficking of phosphorothioate-modified oligodeoxynucleotides." J Clin Invest **95**(4): 1814-1823.

Bird, A. P. (1986). "CpG-rich islands and the function of DNA methylation." Nature **321**(6067): 209-213.

Boado, R. J., Y. S. Kang, D. Wu and W. M. Pardridge (1995). "Rapid plasma clearance and metabolism in vivo of a phosphorothioate oligodeoxynucleotide with a single, internal phosphodiester bond." Drug Metab Dispos **23**(11): 1297-1300.

Buhtoiarov, I. N., P. M. Sondel, J. C. Eickhoff and A. L. Rakhmilevich (2007). "Macrophages are essential for antitumour effects against weakly immunogenic murine tumours induced by class B CpG-oligodeoxynucleotides." Immunology **120**(3): 412-423.

Chang, C.-H., P. Gupta and D. M. Goldenberg (2009). "Advances and challenges in developing cytokine fusion proteins as improved therapeutics."

Chang, Y.-H. (1969). "Studies on phagocytosis: I. Uptake of radio-iodinated (131I) human serum albumin as a measure of the degree of phagocytosis in vitro." Exp Cell Res **54**(1): 42-48.

Chaudhury, C., S. Mehnaz, J. M. Robinson, W. L. Hayton, D. K. Pearl, D. C. Roopenian and C. L. Anderson (2003). "The major histocompatibility complex-related Fc receptor for IgG (FcRn) binds albumin and prolongs its lifespan." J Exp Med **197**(3): 315-322.

Chauhan, V. P., T. Stylianopoulos, Y. Boucher and R. K. Jain (2011). "Delivery of molecular and nanoscale medicine to tumors: transport barriers and strategies." Annu Rev Chem Biomol Eng **2**: 281-298.

Cheung, R. and M. Cho (2010). "Importance of avidity for an endogenous drug carrier: an antibody carrier for CpG oligonucleotides." Mol Pharm **7**(4): 1338-1341.

Chung, D. E. and F. Kratz (2006). "Development of a novel albumin-binding prodrug that is cleaved by urokinase-type-plasminogen activator (uPA)." Bioorg Med Chem Lett **16**(19): 5157-5163.

Crooke, S. T. (1992). "therapeutic applications of oligonucleotides."

Crooke, S. T., M. J. Graham, J. E. Zuckerman, D. Brooks, B. S. Conklin, L. L. Cummins, M. J. Greig, C. J. Guinosso, D. Kornbrust, M. Manoharan, H. M. Sasmor, T. Schleich, K. L. Tivel and R. H. Griffey (1996). "Pharmacokinetic properties of several novel oligonucleotide analogs in mice." Journal of Pharmacology and Experimental Therapeutics **277**(2): 923-937.

DeNardo, D. G., J. B. Barreto, P. Andreu, L. Vasquez, D. Tawfik, N. Kolhatkar and L. M. Coussens (2009). "CD4(+) T cells regulate pulmonary metastasis of mammary carcinomas by enhancing protumor properties of macrophages." Cancer Cell **16**(2): 91-102.

Dunn, G. P., L. J. Old and R. D. Schreiber (2004). "The three Es of cancer immunoediting." Annu Rev Immunol **22**: 329-360.

Eder, P. S., R. J. DeVine, J. M. Dagle and J. A. Walder (1991). "Substrate specificity and kinetics of degradation of antisense oligonucleotides by a 3' exonuclease in plasma." Antisense Res Dev **1**(2): 141-151.

Elsadek, B. and F. Kratz (2012). "Impact of albumin on drug delivery - New applications on the horizon." J Control Release **157**(1): 4-28.

El-Sagheer, A. H., V. V. Cheong and T. Brown (2011). "Rapid chemical ligation of oligonucleotides by the Diels-Alder reaction." Org Biomol Chem **9**(1): 232-235.

Enzler, T., S. Gillessen, J. P. Manis, D. Ferguson, J. Fleming, F. W. Alt, M. Mihm and G. Dranoff (2003). "Deficiencies of GM-CSF and interferon gamma link inflammation and cancer." J Exp Med **197**(9): 1213-1219.

Folkman, J. (1990). "What is the evidence that tumors are angiogenesis dependent?" J Natl Cancer Inst **82**(1): 4-6.

Funk, W. E., H. Li, A. T. Iavarone, E. R. Williams, J. Riby and S. M. Rappaport (2010). "Enrichment of cysteinyl adducts of human serum albumin." Anal Biochem **400**(1): 61-68.

Graham, M. J., S. M. Freier, R. M. Crooke, D. J. Ecker, R. N. Maslova and E. A. Lesnik (1993). "Tritium labeling of antisense oligonucleotides by exchange with tritiated water." Nucleic Acids Res **21**(16): 3737-3743.

Graham, M. J., S. T. Crooke, D. K. Monteith, S. R. Cooper, K. M. Lemonidis, K. K. Stecker, M. J. Martin and R. M. Crooke (1998). "In vivo distribution and metabolism of a phosphorothioate oligonucleotide within rat liver after intravenous administration." Journal of Pharmacology and Experimental Therapeutics **286**(1): 447-458.

Grulich, A. E., M. T. van Leeuwen, M. O. Falster and C. M. Vajdic (2007). "Incidence of cancers in people with HIV/AIDS compared with immunosuppressed transplant recipients: a meta-analysis." The Lancet **370**(9581): 59-67.

Gupta, G. K. and D. K. Agrawal (2010). "CpG oligodeoxynucleotides as TLR9 agonists: therapeutic application in allergy and asthma." BioDrugs **24**(4): 225-235.

Hashizume, H., P. Baluk, S. Morikawa, J. W. McLean, G. Thurston, S. Roberge, R. K. Jain and D. M. McDonald (2000). "Openings between defective endothelial cells explain tumor vessel leakiness." Am J Pathol **156**(4): 1363-1380.

Heckelsmiller, K., K. Rall, S. Beck, A. Schlamp, J. Seiderer, B. Jahrsdorfer, A. Krug, S. Rothenfusser, S. Endres and G. Hartmann (2002). "Peritumoral CpG DNA elicits a coordinated response of CD8 T cells and innate effectors to cure established tumors in a murine colon carcinoma model." J Immunol **169**(7): 3892-3899.

Hermanson, G. T. (1996). Bioconjugate techniques. San Diego, Academic Press.

Jain, R. K. and T. Stylianopoulos (2010). "Delivering nanomedicine to solid tumors." Nat Rev Clin Oncol **7**(11): 653-664.

Janatova, J., J. K. Fuller and M. J. Hunter (1968). "The heterogeneity of bovine albumin with respect to sulfhydryl and dimer content." J Biol Chem **243**(13): 3612-3622.

Kandimalla, E. R., L. Bhagat, D. Yu, Y. Cong, J. Tang and S. Agrawal (2002). "Conjugation of ligands at the 5'-end of CpG DNA affects immunostimulatory activity." Bioconjug Chem **13**(5): 966-974.

Kang, Y. S., R. J. Boado and W. M. Pardridge (1995). "Pharmacokinetics and organ clearance of a 3'-biotinylated, internally [32P]-labeled phosphodiester oligodeoxynucleotide coupled to a neutral avidin/monoclonal antibody conjugate." Drug Metab Dispos **23**(1): 55-59.

Kawai, T. and S. Akira (2010). "The role of pattern-recognition receptors in innate immunity: update on Toll-like receptors." Nat Immunol **11**(5): 373-384.

Kawarada, Y., R. Ganss, N. Garbi, T. Sacher, B. Arnold and G. J. Hammerling (2001). "NK- and CD8(+) T cell-mediated eradication of established tumors by peritumoral injection of CpG-containing oligodeoxynucleotides." J Immunol **167**(9): 5247-5253.

Kratz, F. (2007). "DOXO-EMCH (INNO-206): the first albumin-binding prodrug of doxorubicin to enter clinical trials." Expert Opin Investig Drugs **16**(6): 855-866.

Kratz, F., A. Warnecke, K. Scheuermann, C. Stockmar, J. Schwab, P. Lazar, P. Druckes, N. Esser, J. Drevs, D. Rognan, C. Bissantz, C. Hinderling, G. Folkers, I. Fichtner and C. Unger (2002). "Probing the cysteine-34 position of endogenous serum albumin with thiol-binding doxorubicin derivatives. Improved efficacy of an acid-sensitive doxorubicin derivative with specific albumin-binding properties compared to that of the parent compound." J Med Chem **45**(25): 5523-5533.

Kratz, F., A. Warnecke, K. Scheuermann, C. Stockmar, J. Schwab, P. Lazar, P. Druckes, N. Esser, J. Drevs, D. Rognan, C. Bissantz, C. Hinderling, G. Folkers, I. Fichtner and C. Unger (2002). "Probing the cysteine-34 position of endogenous serum albumin with thiol-binding doxorubicin derivatives. Improved efficacy of an acid-sensitive doxorubicin derivative with specific albumin-binding properties compared to that of the parent compound." J Med Chem **45**(25): 5523-5533.

Krieg, A. M. (2003). "CpG motifs: the active ingredient in bacterial extracts?" Nat Med **9**(7): 831-835.

Krieg, A. M., A. K. Yi, S. Matson, T. J. Waldschmidt, G. A. Bishop, R. Teasdale, G. A. Koretzky and D. M. Klinman (1995). "CpG motifs in bacterial DNA trigger direct B-cell activation." Nature **374**(6522): 546-549.

Krieg, A. M., S. MATSON and E. FISHER (1996). "Oligodeoxynucleotide modifications determine the magnitude of B cell stimulation by CpG motifs." Antisense and Nucleic Acid Drug Development **6**(2): 133-139.

Krieg, A. M., T. Wu, R. Weeratna, S. M. Efler, L. Love-Homan, L. Yang, A. K. Yi, D. Short and H. L. Davis (1998). "Sequence motifs in adenoviral DNA block immune activation by stimulatory CpG motifs." Proc Natl Acad Sci U S A **95**(21): 12631-12636.

Kunikata, N., K. Sano, M. Honda, K. Ishii, J. Matsunaga, R. Okuyama, K. Takahashi, H. Watanabe, G. Tamura, H. Tagami and T. Terui (2004). "Peritumoral CpG oligodeoxynucleotide treatment inhibits tumor growth and metastasis of B16F10 melanoma cells." J Invest Dermatol **123**(2): 395-402.

Latz, E., A. Schoenemeyer, A. Visintin, K. A. Fitzgerald, B. G. Monks, C. F. Knetter, E. Lien, N. J. Nilsen, T. Espevik and D. T. Golenbock (2004). "TLR9 signals after translocating from the ER to CpG DNA in the lysosome." Nat Immunol **5**(2): 190-198.

Latz, E., A. Verma, A. Visintin, M. Gong, C. M. Sirois, D. C. Klein, B. G. Monks, C. J. McKnight, M. S. Lamphier, W. P. Duprex, T. Espevik and D. T. Golenbock (2007). "Ligand-induced conformational changes allosterically activate Toll-like receptor 9." Nat Immunol **8**(7): 772-779.

Lau, S., B. Graham, N. Cao, B. J. Boyd, C. W. Pouton and P. J. White (2012). "Enhanced extravasation, stability and in vivo cardiac gene silencing via in situ siRNA-albumin conjugation." Mol Pharm **9**(1): 71-80.

Leger, R., K. Thibaudeau, M. Robitaille, O. Quraishi, P. van Wyk, N. Bousquet-Gagnon, J. Carette, J. P. Castaigne and D. P. Bridon (2004). "Identification of CJC-1131-albumin bioconjugate as a stable and bioactive GLP-1(7-36) analog." Bioorg Med Chem Lett **14**(17): 4395-4398.

Liao, W. S., L. S. Jefferson and J. M. Taylor (1986). "Changes in plasma albumin concentration, synthesis rate, and mRNA level during acute inflammation." Am J Physiol **251**(6 Pt 1): C928-934.

Lin, E. Y. and J. W. Pollard (2004). "Role of infiltrated leucocytes in tumour growth and spread." Br J Cancer **90**(11): 2053-2058.

Loening, A. M. and S. S. Gambhir (2003). "AMIDE: a free software tool for multimodality medical image analysis." Mol Imaging **2**(3): 131-137.

Ma, X. J., S. Dahiya, E. Richardson, M. Erlander and D. C. Sgroi (2009). "Gene expression profiling of the tumor microenvironment during breast cancer progression." Breast Cancer Res **11**(1): R7.

Martin-Armas, M., J. Simon-Santamaria, I. Pettersen, U. Moens, B. Smedsrod and B. Sveinbjornsson (2006). "Toll-like receptor 9 (TLR9) is present in murine liver sinusoidal endothelial cells (LSECs) and mediates the effect of CpG-oligonucleotides." J Hepatol **44**(5): 939-946.

Matsumura, Y. and H. Maeda (1986). "A new concept for macromolecular therapeutics in cancer chemotherapy: mechanism of tumoritropic accumulation of proteins and the antitumor agent smancs." Cancer Res **46**(12 Pt 1): 6387-6392.

Maurer, T., A. Heit, H. Hochrein, F. Ampenberger, M. O'Keeffe, S. Bauer, G. B. Lipford, R. M. Vabulas and H. Wagner (2002). "CpG-DNA aided cross-presentation of soluble antigens by dendritic cells." Eur J Immunol **32**(8): 2356-2364.

Mroz, P., A. P. Castano and M. R. Hamblin (2009). "Stimulation of dendritic cells enhances immune response after photodynamic therapy." 717803-717803.

Nierkens, S., M. H. den Brok, T. Roelofsen, J. A. Wagenaars, C. G. Figdor, T. J. Ruers and G. J. Adema (2009). "Route of administration of the TLR9 agonist CpG critically determines the efficacy of cancer immunotherapy in mice." PLoS One **4**(12): e8368.

Norbury, C. J. and I. D. Hickson (2001). "Cellular responses to DNA damage." Annu Rev Pharmacol Toxicol **41**: 367-401.

Palma, E. and M. J. Cho (2007). "Improved systemic pharmacokinetics, biodistribution, and antitumor activity of CpG oligodeoxynucleotides complexed to endogenous antibodies in vivo." J Control Release **120**(1-2): 95-103.

Park, B., M. M. Brinkmann, E. Spooner, C. C. Lee, Y. M. Kim and H. L. Ploegh (2008). "Proteolytic cleavage in an endolysosomal compartment is required for activation of Toll-like receptor 9." Nat Immunol **9**(12): 1407-1414.

Pentlow, K. S., M. C. Graham, R. M. Lambrecht, F. Daghighian, S. L. Bacharach, B. Bendriem, R. D. Finn, K. Jordan, H. Kalaigian, J. S. Karp, W. R. Robeson and S. M. Larson (1996). "Quantitative imaging of iodine-124 with PET." J Nucl Med **37**(9): 1557-1562.

Peters, T. (1996). All about albumin : biochemistry, genetics, and medical applications. San Diego, Academic Press.

Piatyszek, M. A., A. Jarmolowski and J. Augustyniak (1988). "Iodo-Gen-mediated radioiodination of nucleic acids." Anal Biochem **172**(2): 356-359.

Pulaski, B. A. and S. Ostrand-Rosenberg (1998). "Reduction of established spontaneous mammary carcinoma metastases following immunotherapy with major histocompatibility complex class II and B7.1 cell-based tumor vaccines." Cancer Res **58**(7): 1486-1493.

Rabkin, C. S., R. J. Biggar and J. W. Horm (1991). "Increasing incidence of cancers associated with the human immunodeficiency virus epidemic." Int J Cancer **47**(5): 692-696.

Rankin, R., R. Pontarollo, X. Ioannou, A. M. Krieg, R. Hecker, L. A. Babiuk, S. van Drunen and L. V. van den Hurk (2001). "CpG motif identification for veterinary and laboratory species demonstrates that sequence recognition is highly conserved." Antisense Nucleic Acid Drug Dev **11**(5): 333-340.

Rippe, B., B. I. Rosengren, O. Carlsson and D. Venturoli (2002). "Transendothelial transport: the vesicle controversy." J Vasc Res **39**(5): 375-390.

Rygh, C. B., S. Qin, J. W. Seo, L. M. Mahakian, H. Zhang, R. Adamson, J. Q. Chen, A. D. Borowsky, R. D. Cardiff, R. K. Reed, F. R. Curry and K. W. Ferrara (2011). "Longitudinal investigation of permeability and distribution of macromolecules in mouse malignant transformation using PET." Clin Cancer Res **17**(3): 550-559.

Sanchez, A., E. Pedroso and A. Grandas (2012). "Conjugation reactions involving maleimides and phosphorothioate oligonucleotides." Bioconjug Chem **23**(2): 300-307.

Sands, H., L. J. Gorey-Feret, A. J. Cocuzza, F. W. Hobbs, D. Chidester and G. L. Trainor (1994). "Biodistribution and metabolism of internally 3H-labeled oligonucleotides. I. Comparison of a phosphodiester and a phosphorothioate." Mol Pharmacol **45**(5): 932-943.

Schnitzer, J. E. and J. Bravo (1993). "High affinity binding, endocytosis, and degradation of conformationally modified albumins. Potential role of gp30 and gp18 as novel scavenger receptors." J Biol Chem **268**(10): 7562-7570.

Schnitzer, J. E. and P. Oh (1994). "Albondin-mediated capillary permeability to albumin. Differential role of receptors in endothelial transcytosis and endocytosis of native and modified albumins." J Biol Chem **269**(8): 6072-6082.

Schnitzer, J. E., A. Sung, R. Horvat and J. Bravo (1992). "Preferential interaction of albumin-binding proteins, gp30 and gp18, with conformationally modified albumins. Presence in many cells and tissues with a possible role in catabolism." J Biol Chem **267**(34): 24544-24553.

Schoonen, W. G., J. A. De Roos, W. Westerink and E. Débiton (2005). "Cytotoxic effects of 110 reference compounds on HepG2 cells and for 60 compounds on HeLa, ECC-1 and CHO cells.: II Mechanistic assays on NAD (P) H, ATP and DNA contents." Toxicology in vitro **19**(4): 491-503.

Shankaran, V., H. Ikeda, A. T. Bruce, J. M. White, P. E. Swanson, L. J. Old and R. D. Schreiber (2001). "IFNgamma and lymphocytes prevent primary tumour development and shape tumour immunogenicity." Nature **410**(6832): 1107-1111.

Sharma, S., A. L. Dominguez, S. Z. Manrique, F. Cavallo, S. Sakaguchi and J. Lustgarten (2008). "Systemic targeting of CpG-ODN to the tumor microenvironment with anti-neu-CpG hybrid molecule and T regulatory cell depletion induces memory responses in BALB-neuT tolerant mice." Cancer Res **68**(18): 7530-7540.

Sharma, S., C. P. Karakousis, H. Takita, K. Shin and S. P. Brooks (2004). "Cytokines and chemokines are expressed at different levels in small and large murine colon-26 tumors following intratumoral injections of CpG ODN." Neoplasia **6**(5): 523-528.

Shirota, H. and D. M. Klinman (2011). "CpG-conjugated apoptotic tumor cells elicit potent tumor-specific immunity." Cancer Immunol Immunother **60**(5): 659-669.

Siegel, R., D. Naishadham and A. Jemal (2013). "Cancer statistics, 2013." CA Cancer J Clin **63**(1): 11-30.

Singh, K. V., J. Kaur, G. C. Varshney, M. Raje and C. R. Suri (2004). "Synthesis and characterization of hapten-protein conjugates for antibody production against small molecules." Bioconjug Chem **15**(1): 168-173.

Society, A. C. (2013). "Cancer Facts & Figures 2013." Atlanta: American Cancer Society.

Srinivasan, S. K., H. K. Tewary and P. L. Iversen (1995). "Characterization of binding sites, extent of binding, and drug interactions of oligonucleotides with albumin." Antisense Res Dev **5**(2): 131-139.

Stehle, G., H. Sinn, A. Wunder, H. H. Schrenk, J. C. M. Stewart, G. Hartung, W. MaierBorst and D. L. Heene (1997). "Plasma protein (albumin) catabolism by the tumor itself - implications for tumor metabolism and the genesis of cachexia." Critical Reviews in Oncology/Hematology **26**(2): 77-100.

Stehle, G., H. Sinn, A. Wunder, H. H. Schrenk, S. Schutt, W. Maier-Borst and D. L. Heene (1997). "The loading rate determines tumor targeting properties of methotrexate-albumin conjugates in rats." Anticancer Drugs **8**(7): 677-685.

Street, S. E., Y. Hayakawa, Y. Zhan, A. M. Lew, D. MacGregor, A. M. Jamieson, A. Diefenbach, H. Yagita, D. I. Godfrey and M. J. Smyth (2004). "Innate immune surveillance of spontaneous B cell lymphomas by natural killer cells and gammadelta T cells." J Exp Med **199**(6): 879-884.

Thibaudeau, K., R. Leger, X. Huang, M. Robitaille, O. Quraishi, C. Soucy, N. Bousquet-Gagnon, P. van Wyk, V. Paradis, J. P. Castaigne and D. Bridon (2005). "Synthesis and evaluation of insulin-human serum albumin conjugates." Bioconjug Chem **16**(4): 1000-1008.

Tlsty, T. D. and L. M. Coussens (2006). "Tumor stroma and regulation of cancer development." Annu Rev Pathol **1**: 119-150.

Vaidyanathan, G. and M. R. Zalutsky (1990). "Protein radiohalogenation: observations on the design of N-succinimidyl ester acylation agents." Bioconjug Chem **1**(4): 269-273.

Verel, I., G. W. Visser, M. J. Vosjan, R. Finn, R. Boellaard and G. A. van Dongen (2004). "High-quality 124I-labelled monoclonal antibodies for use as PET scouting agents prior to 131I-radioimmunotherapy." Eur J Nucl Med Mol Imaging **31**(12): 1645-1652.

Williams, D. L., T. Ha, C. Li, J. H. Kalbfleisch, J. J. Laffan and D. A. Ferguson (1999). "Inhibiting early activation of tissue nuclear factor-κB and nuclear factor interleukin 6 with (1→ 3)-β-d-glucan increases long-term survival in polymicrobial sepsis." Surgery **126**(1): 54-65.

Wolf, A. M., D. Wolf, M. Steurer, G. Gastl, E. Gunsilius and B. Grubeck-Loebenstein (2003). "Increase of regulatory T cells in the peripheral blood of cancer patients." Clin Cancer Res **9**(2): 606-612.

Xie, D., C. Yao, L. Wang, W. Min, J. Xu, J. Xiao, M. Huang, B. Chen, B. Liu, X. Li and H. Jiang (2010). "An albumin-conjugated peptide exhibits potent anti-HIV activity and long in vivo half-life." Antimicrob Agents Chemother **54**(1): 191-196.

Xie, X., J. Liang, T. Pu, F. Xu, F. Yao, Y. Yang, Y. L. Zhao, D. You, X. Zhou, Z. Deng and Z. Wang (2012). "Phosphorothioate DNA as an antioxidant in bacteria." Nucleic Acids Res **40**(18): 9115-9124.

Yamasaki, Y., J. Hisazumi, K. Yamaoka and Y. Takakura (2003). "Efficient scavenger receptor-mediated hepatic targeting of proteins by introduction of negative charges on the proteins by aconitylation: the influence of charge density and size of the proteins molecules." European Journal of Pharmaceutical Sciences **18**(5): 305-312.

Yuan, F., M. Dellian, D. Fukumura, M. Leunig, D. A. Berk, V. P. Torchilin and R. K. Jain (1995). "Vascular permeability in a human tumor xenograft: molecular size dependence and cutoff size." Cancer Res **55**(17): 3752-3756.

Zhang, Q., K. Itagaki and C. J. Hauser (2010). "Mitochondrial DNA is released by shock and activates neutrophils via p38 map kinase." Shock **34**(1): 55-59.